Simple Functions Spreadsheet tool: Phosphates update and Temperature assessment

Final Report

Mireia Grivé

David García

Isaac Campos

Andrés Idiart

Lara Duro

October , 2013

Written:	Revised:	Validated:
David García Isaac Campos Mireia Grivé	Mireia Grivé	Lara Duro

R-2225.2

Table of contents

1. BACKGROUND AND INTRODUCTION 1

2. OBJECTIVES 3

3. METHODOLOGY 4

4. TASK 1: INFLUENCE OF PHOSPHATE ON THE CHEMISTRY OF RADIONUCLIDES .. 6

4.1 RANGE OF PHOSPHATE AQUEOUS CONCENTRATIONS IN GROUNDWATERS 6
4.2 THERMODYNAMIC DATA SELECTION 9
4.2.1 Dissociation of phosphoric acid 9
4.2.2 Calcium 11
4.2.3 Iron 14
4.2.4 Strontium 15
4.2.5 Radium 17
4.2.6 Nickel 18
4.2.7 Zirconium 20
4.2.8 Niobium 23
4.2.9 Technetium 23
4.2.10 Palladium 23
4.2.11 Silver 24
4.2.12 Tin 24
4.2.13 Lead 28
4.2.14 Selenium 31
4.2.15 Lanthanides (Sm, Ho) 31
4.2.16 Actinides (Th, Pa, U, Np, Pu, Am, Cm) 34
4.3 SIMPLE FUNCTIONS SPREADSHEET TOOL UPDATE 48
4.3.1 DON'T TOUCH sheet 48
4.3.2 INPUT DATA sheet 49
4.3.3 Radionuclides sheets 51
4.3.4 Simple Functions Spreadsheet Validation 52
4.4 PHOSPHATES EFFECT OVER RADIONUCLIDE SOLUBILITY LIMITS 57

5. TASK 2: INFLUENCE OF TEMEPRATURE ON RADIONUCLIDE SOLUBILITY LIMITS59

5.1 APPROACHES TO DEAL WITH TEMPERATURE CORRECTIONS 59
5.2 SOLUBILITY LIMITS VARIATION WITH TEMPERATURE 61

5.2.1 Geochemical conditions of the study *61*
5.2.2 Radium *61*
5.2.3 Nickel *63*
5.2.4 Selenium *64*
5.2.5 Lanthanides (Sm and Ho) *66*
5.2.6 Actinides (U, Np, Pu, Am and Cm) *68*

6. CONCLUSIONS **76**

7. REFERENCES **78**

APPENDIX I: SKB GROUNDWATER COMPOSITIONS **88**

APPENDIX II: ENTHALPY DATA USED IN THE CALCULATIONS **89**

1. Background and Introduction

Within the framework of the SR-Can safety assessment of SKB, the team of Amphos 21 conducted the solubility assessment of some key radionuclides (the reader is referred to Duro et al., 2006a, Duro et al., 2006b, Grivé et al., 2010a for more information). One of the outcomes of these studies was the development and implementation of an Excel© spread sheet, named Simple Functions Spreadsheet, to easily perform simple solubility calculations, which were implemented for several elements (Grivé et al., 2010b). The calculations included in the Excel Spreadsheet considered only those solid phases that are likely to form under the surrounding conditions of interest for the waste disposal for SKB and the corresponding aqueous species accounting for, at least, 1% of the total aqueous concentration of the element under study.

The Simple Functions Spreadsheet is a tool that calculates the solubility of radionuclides under different conditions for a variety of groundwater compositions. It has been especially tailored to the needs of Performance Assessment (PA) exercises. The development of this tool was motivated by the need of having a confident and easy-to-handle tool to calculate solubility limits in an agile and fast manner. Thus, only a simplified set of solid phases and aqueous species considered to be the most relevant in the environments of interest have been included. The Spreadsheet also includes an estimation of the uncertainty of the calculated solubility that arises from the uncertainty in the thermodynamic data used in the calculations, through an error propagation algorithm.

As part of the review of the SR-Site Safety Assessment, SSM has requested SKB to provide additional information about (1) the handling of phosphate in the solubility assessment, and (2) the effect of temperature on solubility limit calculations.

It is well known that phosphate can form strong complexes with some radionuclides (see for example Ekberg et al., 2011; Mathur, 1991; Xia et al., 2009) and thus its effect on the solubility limit of those radionuclides may not be completely neglected. One of the concerns within the solubility limit calculations for PA exercises is the temperature effect (Duro et al., 2011; Ekberg et al., 1995). Although temperatures above 25ºC are only relevant for potential early canister failures, an assessment of its effect on radionuclide solubility is required in PA exercises.

The present document is the final report that includes the study of both, the phosphate effects on radionuclides complexation and solubility, as well as the temperature influence on radionuclides solubility limits. Additionally, the implementation of selected phosphate thermodynamic data in the Simple Functions Spreadsheet tool is documented in the present document.

The report is organized as follows:

- Chapter 2 describes the main objectives of this work,
- in The methodology that has been followed is presented in chapter 3,
- Chapter 4 is devoted to the discussion and thermodynamic data selection of phosphate basic chemistry and radionuclide complexation, including a brief review and discussion on phosphate concentrations together with some details about the implementation of phosphate thermodynamic data in the Simple Functions Spreadsheet tool,
- Chapter 5 deals with the effect of temperature over radionuclides solubility limits, and
- Chapter 6 summarizes the main conclusions from this work.

2. Objectives

The objectives of this work are twofold:

- to address the effect of phosphates on the radionuclide solubility limits calculated with the Simple Functions Spreadsheet tool, and
- to study the effect of temperature over the following radionuclides: Ra, Se, Ni, Sm, Ho, Am, Cm, Pu, U, and Np

To this aim, a literature review on the phosphate chemistry (i.e. hydrolysis reactions, major elements complexation and radionuclide phosphate complexes stability) based on the open literature data and on the specific data generated in tailored national and international programs has been conducted.

In a second stage, the solubility limits of the selected radionuclides at temperatures different than 25ºC have been calculated by means of the simplified Van't Hoff equation.

3. Methodology

The work within this project has been divided in two different and independent tasks:

- Task 1 – Phosphates chemistry and its role on radionuclides solubility limits
- Task 2 – Temperature influence on radionuclide solubility limits

For the first task, a three-step approach has been followed (Figure 3-1):

1) The range of phosphate concentrations in groundwaters of interest to SKB (Grivé et al., 2010a) have been investigated and discussed,
2) A literature research has been conducted with emphasis on the affinity of phosphate towards the radionuclides of interest and by considering its major elements chemistry (hydrolysis, Ca, and Fe interactions),
3) An assessment on the relevance of the complexation on the groundwater conditions obtained in 1) has been performed in order to select a final thermodynamic data set.

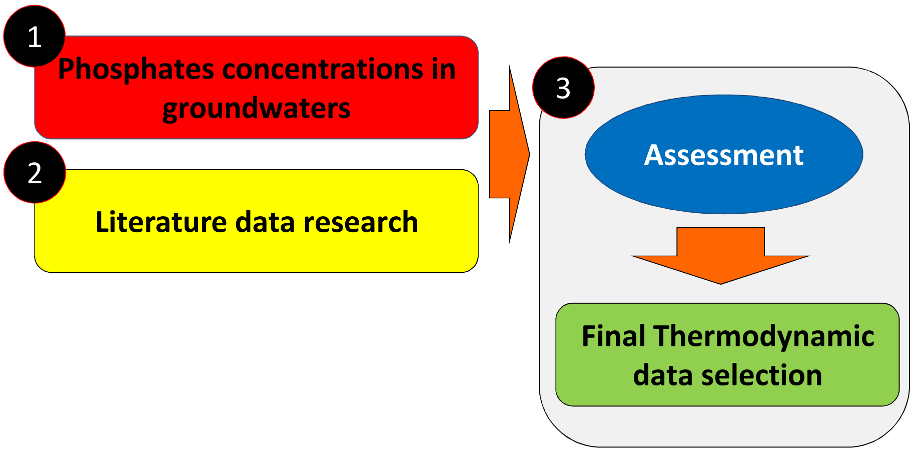
1
Phosphates concentrations in groundwaters
2
Literature data research
3
Assessment
Final Thermodynamic data selection

Figure 3-1. Sketch showing the methodology followed in this work.

Task 2 methodology consisted of:

1) The selection of the most appropriate approach for doing temperature corrections,
2) The selection of enthalpy values from SKB database (Grivé et al., 2008; Duro et al., 2006a),

3) The definition of the main geochemical constraints for performing the calculations, and

4) The assessment of the temperature effect on radionuclides solubilities under the studied conditions.

4. Task 1: Influence of phosphate on the chemistry of radionuclides

4.1 Range of phosphate aqueous concentrations in groundwaters

Phosphate concentrations in natural groundwaters have been reported by a number of authors. In the study conducted on aqueous neptunium, Kaszuba and Runde (1999) reported phosphate concentrations ranging from 0.01 – 0.5 ppm (10^{-7} – $5·10^{-6}$ M) and rarely exceeding 1 ppm (10^{-5} M) in groundwater, surface water and seawater conditions. The authors also reported that, in the specific case of Np (IV and V), phosphate concentrations higher than 10^{-4} M are required in order to compete with carbonate and hydroxide complexation. Wanner (1996), reported phosphate concentrations of 10^{-6}M in the reference granitic groundwater used during the Swiss Safety Case of 1985. In an early work, Langmuir (1978) reported natural groundwaters from the Wind River formation (USA), with phosphate aqueous concentration about 0.1 ppm (10^{-6} M). Yanase et al. (1995) reported Koongarra ore deposit groundwater geochemistry with phosphate concentrations ranging between 0.03-0.09 ppm ($3 - 9·10^{-7}$ M) at pH of 5.7 - 6.8. Phosphate aqueous concentrations in the natural fission reactor at Bangombé (Gabon) were reported by Stille et al. (2003) ranging from 0.02 - 0.83 ppm ($2·10^{-7}$ – $8·10^{-6}$ M) at pH 4.5 – 6.0, respectively. Groundwater phosphate aqueous concentrations have also been reported in some SKB reports (Laaksoharju et al., 1995, 2008, 2009; Salas et al., 2010). Laaksoharju et al. (1995) chemically characterised a Laxemar deep borehole (KLX02) groundwater, reporting phosphate aqueous concentrations ranging from 10^{-7} to 10^{-5} M at 315m and 1420m depth, respectively. More recently, Laaksoharju et al. (2008, 2009) and Salas et al. (2010) reported phosphate aqueous concentrations ranging from 10^{-5} to 10^{-7} and from 10^{-5} to 10^{-8}M in Forsmark and Laxemar conditions. Figure 4-1 summarises the range of phosphate aqueous concentrations reported in the above mentioned studies.

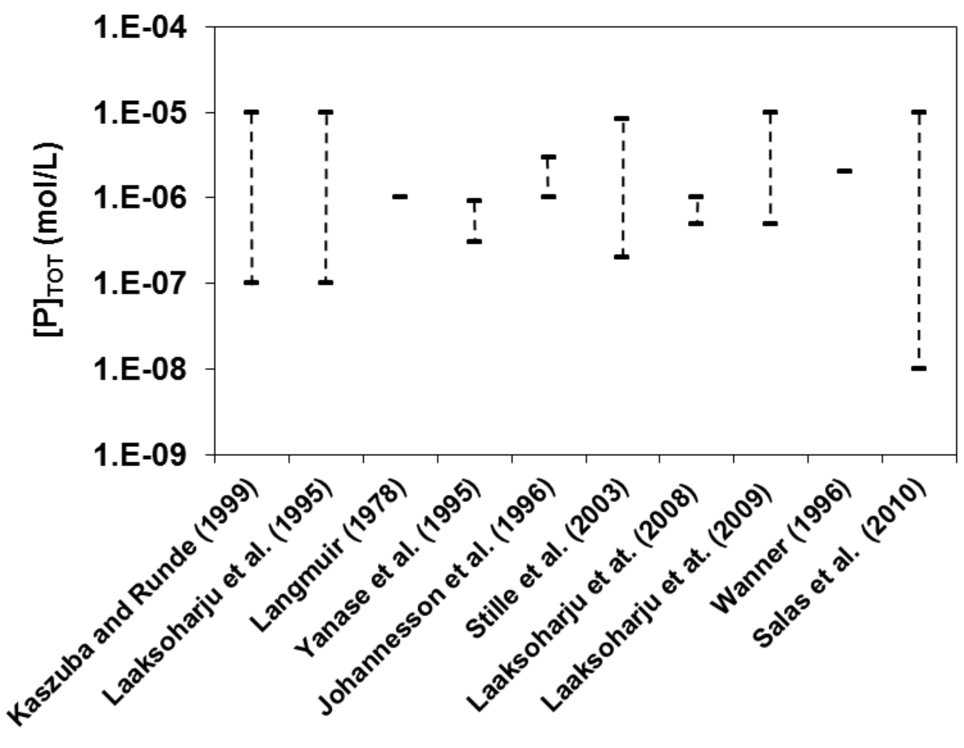

Figure 4-1. Range of phosphate aqueous concentrations in natural waters reported in the reviewed literature.

From these studies, the ones from Laaksoharju et al. (1995, 2008, 2009) (reported for the Laxemar and Forsmark sites), Salas et al. (2010) (reported for Forsmark), Wanner (1996) (reported for Swiss granitic conditions), and Kaszuba and Runde (1999) (which report a range of concentrations valid for seawater environments) are directly linked and applicable to the groundwater conditions of interest for SKB (see Appendix I). The rest of studies were performed in sedimentary rock conditions.

It is noteworthy that due to the scarcity of trusted phosphate aqueous concentrations data for most natural systems, modellers have usually assumed that the presence major phosphate minerals, such as hydroxyapatite ($Ca_5(PO_4)_3(OH)(s)$), exerts the control of phosphate concentrations (Bruno et al., 2001). Based on this assumption and using thermodynamic data for the calcium-phosphate system as described in section 4.2.1, the aqueous phosphate concentrations in equilibrium with hydroxyapatite (Figure 4-2) have been calculated according to the groundwater conditions detailed in Grivé et al. (2010a) (see Appendix I). As can be seen, the calculated phosphate aqueous concentrations are in the range 10^{-8} to 10^{-10} M, except for the cement groundwater where values might decrease down to ~10^{-11} M. This range of concentrations is lower than the values reported in the literature at different conditions (Figure 4-2).

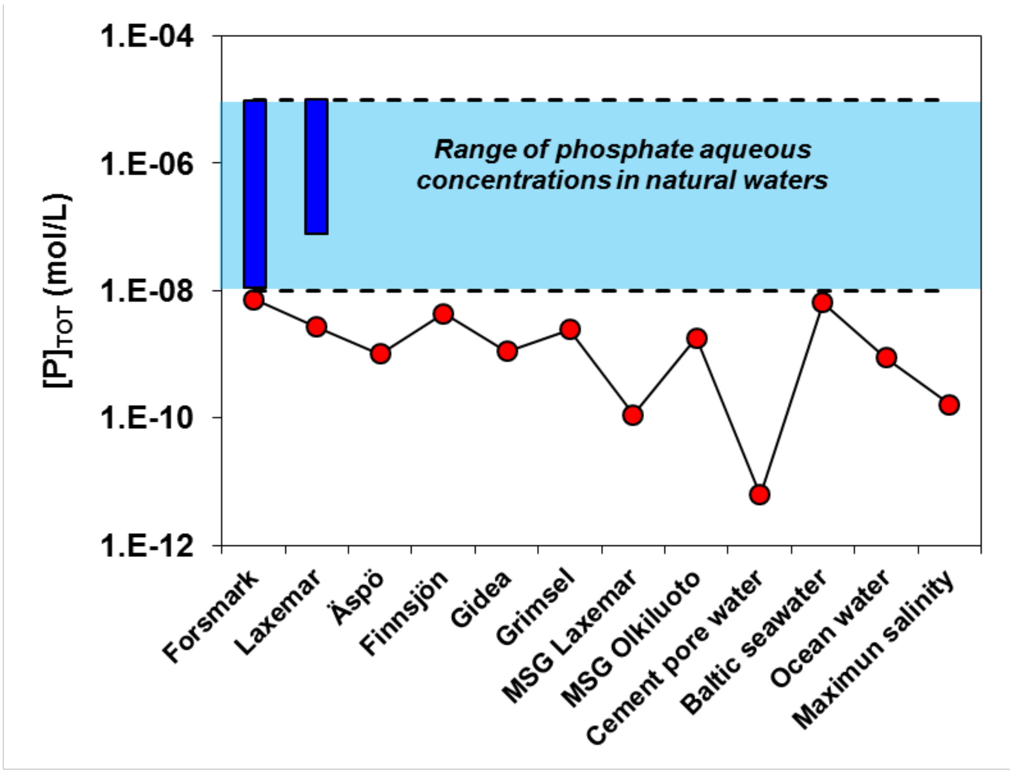

Figure 4-2. Phosphate aqueous concentrations calculated in equilibrium with hydroxyapatite at different groundwater conditions (red dots, see Appendix I). Light blue rectangle: range of experimentally determined phosphate aqueous concentrations reported in the reviewed literature for groundwaters of SKB interest.. Dark blue rectangles: range of experimentally determined phosphate aqueous concentrations reported in for the Forsmark and Laxemar sites (Laaksoharju et al., 1995, 2008, 2009; Salas et al., 2010).

Phosphate concentrations in the pore water of the buffer and backfill materials have not been reported. However, only small amounts of accessory minerals containing phosphate have been measured. For instance, the amount of P_2O_5 in MX-80 bentonite has been measured to be 0.25 wt.% in Montes-Hernández (2002). In turn, Vuorinen and Snellman (1998) reported a 0.1 wt.% of phosphate in MX-80 bentonite. In other bentonite materials such as the Kunipia-F Japanese bentonite, values smaller than

0.01 wt.% have been reported (Nessa et al. 2008). In (Vuorinen and Snellman 1998), the phosphate is assumed to occur at least partly as hydroxyapatite. Therefore, the assumption of a phosphate concentration in equilibrium with hydroxyapatite, as in (Salas et al. 2010) seems to be reasonable.

Due to the low amounts of phosphate minerals present in the near-field, it is not expected that phosphate originating from the buffer or backfill can have impact on the phosphate concentration in groundwater. However, more data would be needed to confirm this statement.

In the present work, a range of phosphate concentrations between 10^{-5} M (upper phosphate aqueous concentration reported for Laxemar and Forsmark groundwater in Laaksoharju et al. (1995, 2008, 2009) and Salas et al. (2010)) and 10^{-9} M (the average of lower phosphate aqueous concentration in equilibrium with hydroxyapatite at the different groundwater conditions) has been selected. This range is expected to provide a general picture of the role of phosphates on the solubility of different radionuclides in the groundwater conditions of interest for SKB.

4.2 Thermodynamic data selection

The starting point for the data review and selection has been the SKB-TDB reported in (Duro et al., 2006a and updates), although the review for the available thermodynamic data presented in this chapter includes the open literature data and specific data generated in tailored national and international programs, as well. Uncertainties to the log K^0 errors have been set up according with the Simple Functions criteria (Grivé et al., 2010b):

- If no error was reported in the original source, the range of variation between different bibliographic sources was taken as the uncertainty.
- If there was only one reference without an associated error, a default value of ± 0.3 log units has been taken as the uncertainty in $logK_i$.

4.2.1 Dissociation of phosphoric acid

Under natural groundwater conditions, phosphorous occurs in the P(V) state as phosphate (PO_4^{3-}). There are four dissociation products of phosphoric acid (PO_4^{3-},

HPO_4^{2-}, $H_2PO_4^-$ and $H_3PO_4(aq)$) dominating its chemistry in a wide pH range (Figure 4-3).

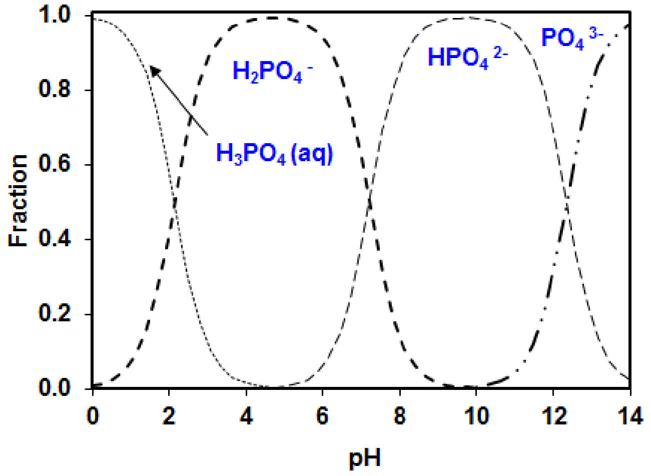

Figure 4-3. Diagram showing phosphoric acid dissociation products stability as a function of pH ($[P]_{TOT}=1\cdot10^{-7}$M).

The selected thermodynamic data (Table 4-1) for this system is the one adopted by NEA (Gamsjäger et al., 2012), originally coming from CODATA key values (Cox et al., 1989). $H_2PO_4^-$ has been set up as phosphate master species and thus all reactions have been rewritten accordingly. Data are in agreement with the ones already included in SKB-TDB (Duro et al., 2006a and updates).

Table 4-1. Selected phosphate hydrolysis species and their corresponding log K^o_{eq} values.

Species	**Reaction**	**Log K^o_{eq}**	**Reference**
PO_4^{3-}	$H_2PO_4^- \leftrightarrow 2H^+ + PO_4^{3-}$	-19.56 ± 0.03	Gamsjäger et al. (2012)
HPO_4^{2-}	$H_2PO_4^- \leftrightarrow H^+ + HPO_4^{2-}$	-7.21 ± 0.02	Gamsjäger et al. (2012)
H_3PO_4	$H_2PO_4^- + H^+ \leftrightarrow H_3PO_4$	9.35 ± 0.03	Gamsjäger et al. (2012)

4.2.2 Calcium

Calcium presents high affinity to phosphate (Nriagu and Moore, 1984), as shown in Figure 4-4. According to previous thermodynamic data compilations (i.e. Martell and Smith, 2004), there are several datasets including Ca-P aqueous species.

For example, llnl.dat database (delivered within the PhreeqC code (Parkhurst and Appelo, 2013)) include data for three different aqueous species: $Ca(H_2PO_4)^+$, $Ca(HPO_4)(aq)$, and $CaPO_4^-$. These data are in good agreement with thermodynamic data (Table 4-2) in the sit.dat (also delivered within the PhreeqC code) originally coming from potentiometric measurements performed to determine the association constants for the formation of those complexes (Chughtai et al., 1968). A Japanese thermodynamic database reported in (Kitamura and Yoshida, 2010) is also in fair agreement with that selection (Table 4-2).

A review of recent published literature data has not provided any new or additional hints for the stability constants of these complexes, different from the ones reported by Chughtai et al. (1968). Thus, the thermodynamic data for the calcium-phosphate aqueous species from this reference (Table 4-3) have been retained in this work.

Table 4-2. Comparison among Ca-P aqueous species thermodynamic data included in other databases.

Species	**Reaction**	**Log K^o_{eq}**		
		llnl.dat	**sit.dat**	**JAEA**
$Ca(H_2PO_4)^+$	$Ca^{2+} + H_2PO_4^- \leftrightarrow Ca(H_2PO_4)^+$	1.40	1.41	1.40
$Ca(HPO_4)(aq)$	$Ca^{2+} + H_2PO_4^- \leftrightarrow H^+ + Ca(HPO_4)(aq)$	-4.47	-4.47	-4.48
$CaPO_4^-$	$Ca^{2+} + H_2PO_4^- \leftrightarrow CaPO_4^- + 2H^+$	-13.07	-13.10	-13.11

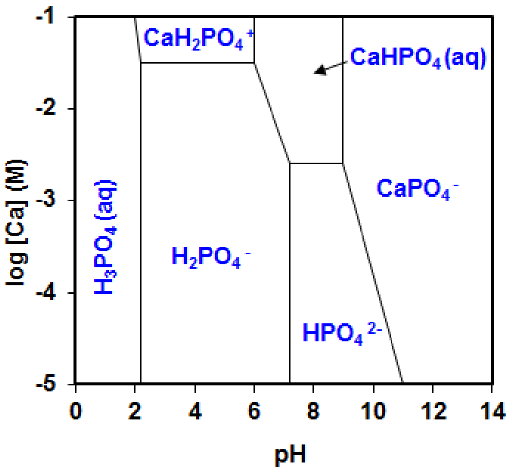

Figure 4-4. Predominance diagram log [Ca] vs pH showing the stability of Ca-P aqueous species ($[P]_{TOT}=1\cdot10^{-7}$ M).

Concentrations of phosphate in groundwaters are in many cases likely to be controlled by equilibrium with major Ca-bearing phases, usually hydroxyapatite ($Ca_5(PO_4)_3(OH)$) (Duro et al., 2010). Thermodynamic data for this solid phase have been selected from solubility data reported in Nancollas (1984), originally from McDowell et al. (1977) (Table 4-4). Figure 4-5 shows the calculated hydroxyapatite solubility as a function of the pH at different Ca concentrations, 10^{-1} M and 10^{-3} M, which are representative of: a) saline groundwaters (10^{-1} M) (i.e. Laxemar and Olkiluoto most saline groundwaters), and b) non-saline groundwater (10^{-3} M) (i.e. Laxemar groundwater, Finnsjön groundwater, and Baltic seawater) (see appendix I for a detailed description of groundwaters composition). With the selected range (10^{-1} M to 10^{-3} M), we ensure to include different types of pore water, among them cement pore waters with a Ca concentration ~ 10^{-2} M (see appendix I).

Table 4-3. Selected Ca-phosphate aqueous species and their corresponding log K^o_{eq} values.

Species	**Reaction**	**Log K^o_{eq}**	**Reference**
$Ca(H_2PO_4)^+$	$Ca^{2+} + H_2PO_4^- \leftrightarrow Ca(H_2PO_4)^+$	1.41 ± 0.3	Chughtai et al. (1968)
$Ca(HPO_4)(aq)$	$Ca^{2+} + H_2PO_4^- \leftrightarrow H^+ + Ca(HPO_4)(aq)$	-4.47 ± 0.3	Chughtai et al. (1968)
$CaPO_4^-$	$Ca^{2+} + H_2PO_4^- \leftrightarrow CaPO_4^- + 2H^+$	-13.10 ± 0.3	Chughtai et al. (1968)

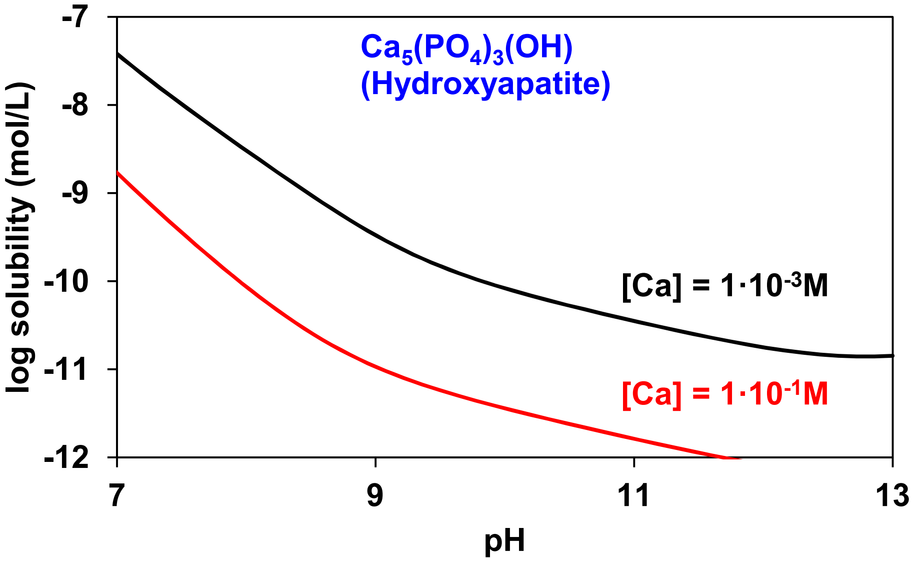

Figure 4-5. Hydroxyapatite ($Ca_5(PO_4)_3(OH)$) solubility as a function of pH: a) assuming $[Ca] = 1 \cdot 10^{-3}$ M (black line) and, b) assuming $[Ca] = 1 \cdot 10^{-1}$ M (red line). In both cases $[CO_3]_{TOT}$ in equilibrium with calcite ($CaCO_3$).

Table 4-4. Selected Ca-phosphate solids and their corresponding log K^o_{eq} values.

Solid phase	**Reaction**	**Log K^o_{eq}**	**Reference**
Hydroxyapatite $Ca_5(PO_4)_3(OH)$	$5Ca^{2+} + 3H_2PO_4^- + H_2O \leftrightarrow Ca_5(PO_4)_3(OH)(s) + 7H^+$	-14.35 ± 0.04	Nancollas (1984)

4.2.3 Iron

Several authors reported the formation of a variety of species for the iron-phosphate system (Wilhelmy et al., 1985). However, few of these studies reported reliable thermodynamic data for the iron-phosphate species.

The CHEMVAL database (Falck et al., 1996) summarized thermodynamic data for four different Fe-P aqueous species (Table 4-5).

Table 4-5. Thermodynamic data for Fe-P aqueous species in CHEMVAL database.

Species	Reaction	Log K$^o_{eq}$
$FeHPO_4(aq)$	$H_2PO_4^- + Fe^{2+} \leftrightarrow FeHPO_4(aq) + H^+$	-3.56
$FeH_2PO_4^+$	$H_2PO_4^- + Fe^{2+} \leftrightarrow FeH_2PO_4^+$	2.64
$FeHPO_4^+$	$H_2PO_4^- + Fe^{2+} \leftrightarrow FeHPO_4^+ + 1e^- + H^+$	-10.26
$FeH_2PO_4^{2+}$	$H_2PO_4^- + Fe^{2+} \leftrightarrow FeH_2PO_4^{2+} + 1e$	-8.76

Figure 4-6 shows the predominance diagrams obtained for the Fe-P system by using Table 4-5 thermodynamic data. As can be seen, $FeHPO_4^+$ would be the only phosphate species that could be relevant under oxidising conditions (Eh>0.5V) and pH conditions (pH<6) out of the range of interest for SKB (see appendix I).

Based on those results, it is recommended to exclude the formation of Fe-P species from the Simple Functions Spreadsheet tool. Thus, no thermodynamic data for that system has been selected in the present work.

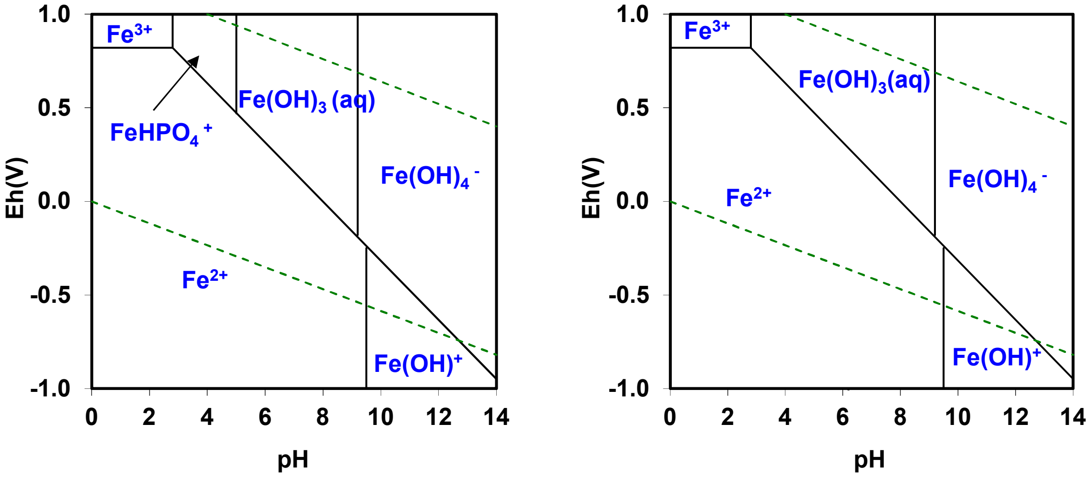

Figure 4-6. Predominance diagrams Eh(V) vs pH showing the stability of Fe-P aqueous species. Left plot $[P]_{TOT}=1\cdot10^{-5}$ M, right plot $[P]_{TOT}=1\cdot10^{-7}$ M. $[Fe]_{TOT} = 1\cdot10^{-5}$ M in both cases, corresponding to the higher Fe concentration reported in groundwater compositions of SKB interest (see Appendix I).

4.2.4 Strontium

Thermodynamic data for this system are scarce. The NIST compilation of stability constants (Martell and Smith, 2004), reported thermodynamic data for two Sr-PO_4 aqueous species ($Sr(HPO_4)(aq)$ and $Sr(H_2PO_4)^+$) at I (*Ionic Strength*) = 0.1M. By using the extended Debye-Hückel equation we have extrapolated these constants to infinite dilution (Table 4-6).

Table 4-6. Thermodynamic data for Sr-P aqueous species in NIST database.

Species	**Reaction**	**Log K^o_{eq}**
$Sr(HPO_4)(aq)$	$Sr^{2+} + H_2(PO_4)^- \leftrightarrow H^+ + Sr(HPO_4)(aq)$	-4.70
$Sr(H_2PO_4)^+$	$Sr^{2+} + H_2(PO_4)^- \leftrightarrow Sr(H_2PO_4)^+$	0.83
Solid phase	**Reaction**	**Log K^o_{eq}**
$SrHPO_4(s)$	$Sr^{2+} + H_2PO_4^- \leftrightarrow SrHPO_4(s) + H^+$	-0.29

Figure 4-7 shows the stability of the Sr-P species reported by NIST as a function of pH and phosphate concentration. As can be seen, the formation of these species would require aqueous phosphate concentrations above ~10^{-2} M, which are far from the upper phosphate aqueous concentrations expected in the studied system. The low affinity of phosphate towards Sr compared to the one for Ca is in agreement with the chemical trends of the alkaline earth elements. Down the same chemical family group in the periodic table, with increasing atomic number, the ionic radii of the elements increase for the same oxidation state. The heavier elements of the group have larger radii for the same charge, thus polarize less the ligands and have lower affinity towards ligand complexation.

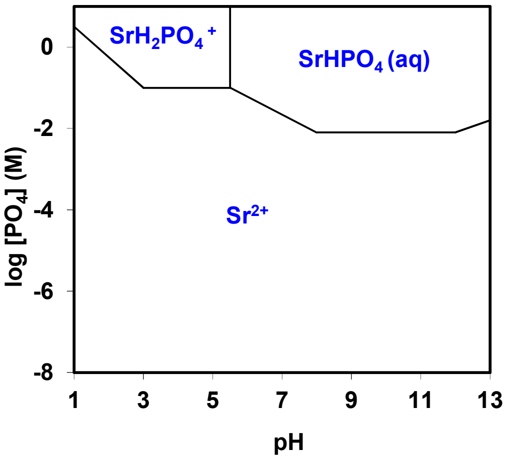

Figure 4-7. Predominance diagram log [PO_4] vs pH showing the stability of Sr-P aqueous species. $[Sr]_{TOT}=1\cdot10^{-4}$ M.

Martell and Smith (2004) also reported thermodynamic data for the solid phase $Sr(HPO_4)(s)$ (Table 4-6). The solubility of this solid phase is shown in Figure 4-8 as a function of pH. From this figure, it can be observed that with phosphate concentrations about 10^{-5} M, the solubility of this solid phase is about 10^{-3} M in the pH range 7-12. These Sr concentrations are within the range expected in natural groundwaters (from 10^{-6} to 10^{-3}M in Salas et al. (2010)). It is worth mentioning that in agreement with Figure 4-7 results, phosphate aqueous species reported by NIST do not appear in the underlying speciation of $Sr(HPO_4)(s)$ shown in Figure 4-8.

Based on these results, we would recommend to include the solid phase $Sr(HPO_4)(s)$, with thermodynamic data from Martell and Smith (2004), in the Simple Functions Spreadsheet tool as possible Sr solubility limiting phase (Table 4-7). Additionally we also do not recommend including Sr-PO_4 aqueous species given their low relevance.

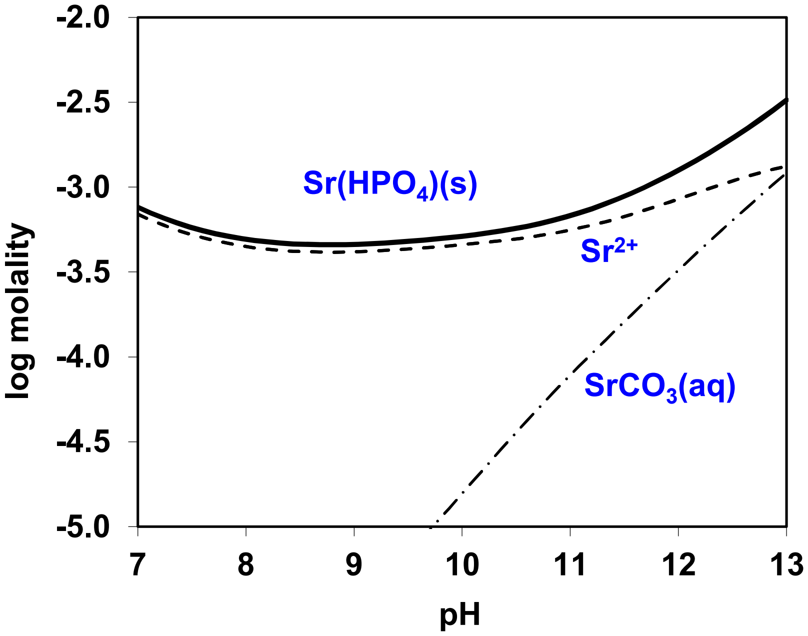

Figure 4-8. $Sr(HPO_4)(s)$ solubility and underlying speciation as a function of pH at a constant phosphate concentration (10^{-5} M). [Ca]= $1 \cdot 10^{-4}$ M and carbonate in equilibrium with calcite.

Table 4-7. Thermodynamic data for Sr-P selected in this work.

Solid phase	Reaction	Log K^o_{eq}	Reference
$SrHPO_4(s)$	$Sr^{2+} + H_2PO_4^- \leftrightarrow SrHPO_4(s) + H^+$	-0.29 ± 0.3	Martell and Smith (2004)

4.2.5 Radium

Few studies dealt with radium complexation by phosphate. As part of the alkaline earth metal group, Ra should behave similarly to its counterparts Sr and Ca. As previously mentioned, down the same chemical family group in the periodic table, with increasing atomic number, the ionic radii of the elements increase for the same oxidation state. The heavier elements of the group have larger radii for the same charge. Thus, they polarize less the ligands and have lower affinity towards ligand complexation.

Therefore aqueous Ra phosphate complexes formation can be neglected in the conditions studied in the present work and no thermodynamic data are selected.

4.2.6 Nickel

As reported by the NEA team (Gamsjäger et al., 2005) the formation of complexes between phosphate and Ni(II) ions in solution is nearly non-existing.

Gamsjäger et al. (2005) selected thermodynamic data for the species $NiHPO_4(aq)$ based on the results of several potentiometric studies. Additionally, the NEA team reviewed and discussed the work by Ziemniak et al. (1989), which studied Ni(II) oxide solubilities at two different temperatures (290 K and 560 K) in phosphate media. In agreement with Lemire (1995) arguments, Gamsjäger et al. (2005) reported that the the species $Ni(OH)_2HPO_4^{2-}$ may exist and its existence is in agreement with the work from Ziemniak et al. (1989). Gamsjäger et al., 2005 decided to not include the selection of thermodynamic data for this species given the difficulties for the wide range of ionic strength.

The NEA review on Ni thermodynamics reported the formation of several Ni phosphate solid phases. Nevertheless, thermodynamic data are almost non-existent for these solid phases and thus NEA did not select data for nickel phosphate solid phases. Tardy and Vieillard (1977) studied the relationships among Gibbs free energies and enthalpies of phosphates solid phases. The authors reported thermodynamic data for a solid phase ($Ni_3(PO_4)_2(s)$) from which a stability constant can be derived.

Figure 4-9 shows the solubility of $Ni_3(PO_4)_2(s)$, with thermodynamic data from Tardy and Vieillard (1977), and the underlying Ni aqueous speciation. As can be seen, at the highest phosphate concentrations studied in the present work (10^{-5} M), Ni phosphate complexation is only relevant at high pH (>11). Solubility values of $Ni_3(PO_4)_2(s)$ seem to be in the range of solubility limits reported by Grivé et al. (2010a) for a pH between 7 and 10.

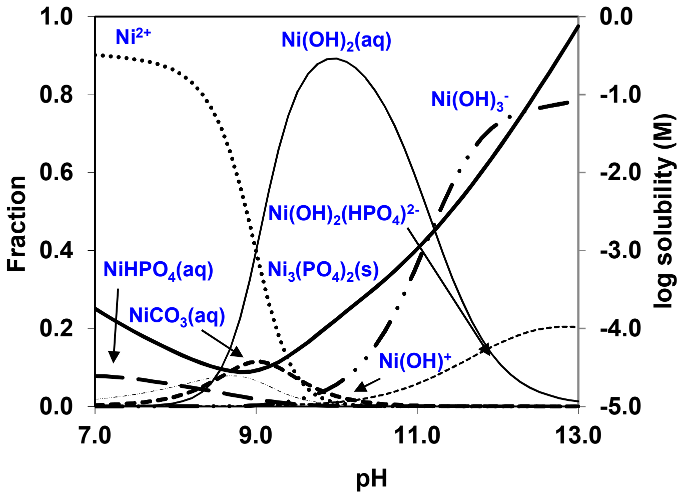

Figure 4-9. $Ni_3(PO_4)_2(s)$ solubility and underlying Ni speciation as a function of pH at a constant phosphate concentration (10^{-5} M). [Ca]= $1 \cdot 10^{-4}$ M and carbonate in equilibrium with calcite.

Based on these results, it is recommended to include thermodynamic data detailed in Table 4-8 for both, the aqueous Ni phosphate species and solid phases in the Simple Functions Spreadsheet tool.

Table 4-8. Thermodynamic data for Ni-P aqueous species and solid phases selected in the present work.

Species	**Reaction**	**Log K°$_{eq}$**	**Reference**
$Ni(HPO_4)(aq)$	$Ni^{2+} + H_2(PO_4)^- \leftrightarrow H^+ + Ni(HPO_4)(aq)$	-4.16 ± 0.4	Gamsjäger et al. (2005)
$Ni(OH)_2HPO_4^{2-}$	$Ni^{2+} + H_2(PO_4)^- + 2H_2O \leftrightarrow Ni(OH)_2HPO_4^{2-} + 3H^+$	-23.24 ± 0.3	Lemire (1995)
Solid phase	**Reaction**	**Log K°$_{eq}$**	**Reference**
$Ni_3(PO_4)_2(s)$	$3Ni^{2+} + 2H_2PO_4^- \leftrightarrow Ni_3(PO_4)_2(s) + 4H^+$	-10.25 ± 0.3	Tardy and Vieillard (1977)

4.2.7 Zirconium

No relevant data for the formation of aqueous Zr phosphates species have been reported. The NEA review on Zr chemical thermodynamics (Brown et al., 2005) selected thermodynamic data for two Zr-PO_4 solid phases with different crystallinity: $Zr(HPO_4)_2 \cdot H_2O(cr)$ and $Zr(HPO_4)_2(alfa)$.

Calorimetric measurements from different sources together with solubility measurements in hydrochloric acid media were used by Brown et al. (2005) for selecting thermodynamic data or $Zr(HPO_4)_2 \cdot H_2O(cr)$. In the case of $Zr(HPO_4)_2(alfa)$ solid phase, Brown et al. (2005) only used calorimetric data for selecting their thermodynamic data.

Figure 4-10 shows the solubility of $Zr(HPO_4)_2 \cdot H_2O(cr)$ and $Zr(HPO_4)_2(alfa)$ solid phases, together with Zr underlying speciation. As can be seen, at high phosphate concentrations (10^{-5}M) $Zr(HPO_4)_2 \cdot H_2O(cr)$ presented low solubilities in a wide pH range (7-13) while the more amorphous $Zr(HPO_4)_2(alfa)$ is ~7-8 times more soluble. In any case, $Zr(OH)_4(aq)$ is the main Zr species under the studied conditions.

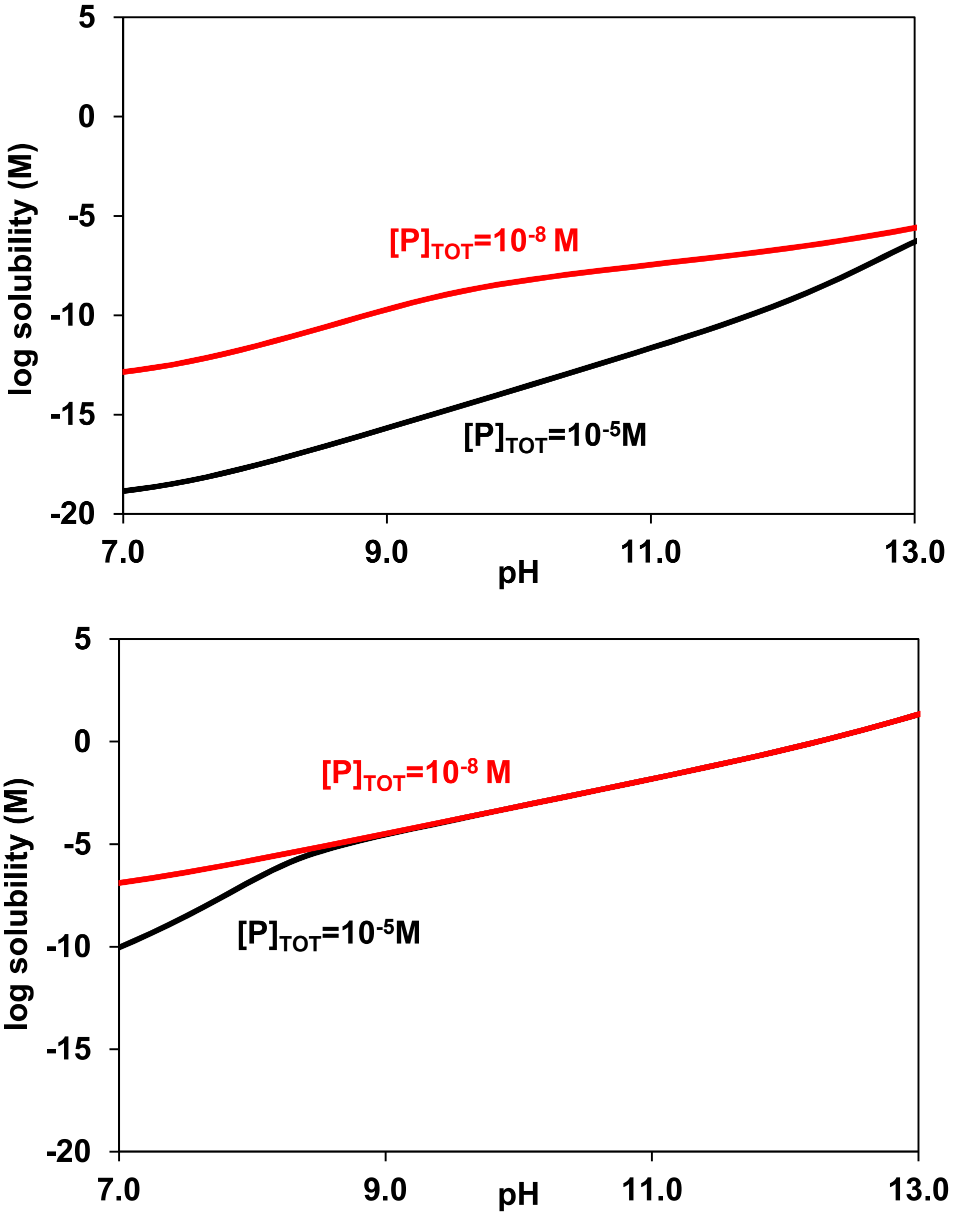

Figure 4-10. Solubility (black and red lines) of: a) $Zr(HPO_4)_2 \cdot H_2O(cr)$ (top plot), and b) $Zr(HPO_4)_2$(alfa) (bottom plot). In both cases the aqueous speciation is completely dominated by $Zr(OH)_4(aq)$ species (100%). Red lines calculated at $[P]_{TOT}=10^{-8}$ M and black lines at $[P]_{TOT}=10^{-5}$ M.

In the presence of a competing cation as Ca^{2+}, and a complementary anionic ligand as CO_3^{2-} (controlled through calcite equilibrium), it can be seen in Figure 4-11 that Zr-PO_4 solid phases solubilities slightly increases at constant phosphate concentration due to the higher affinity of Ca towards phosphate.

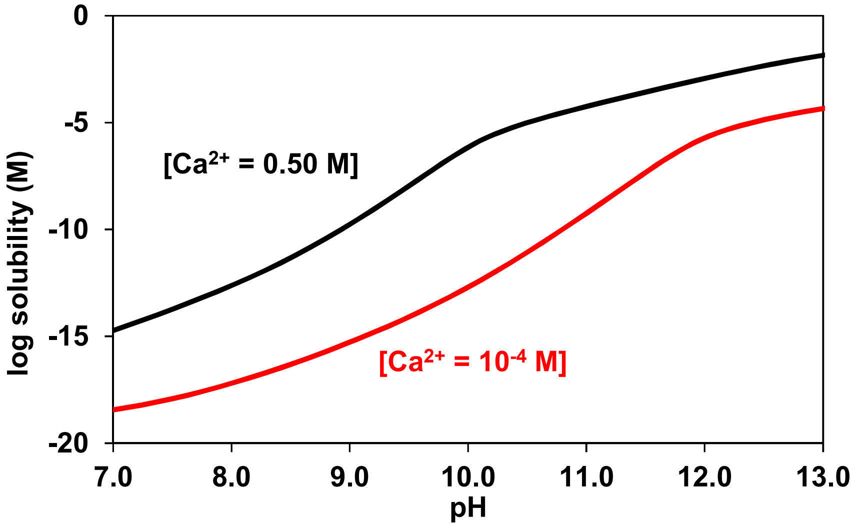

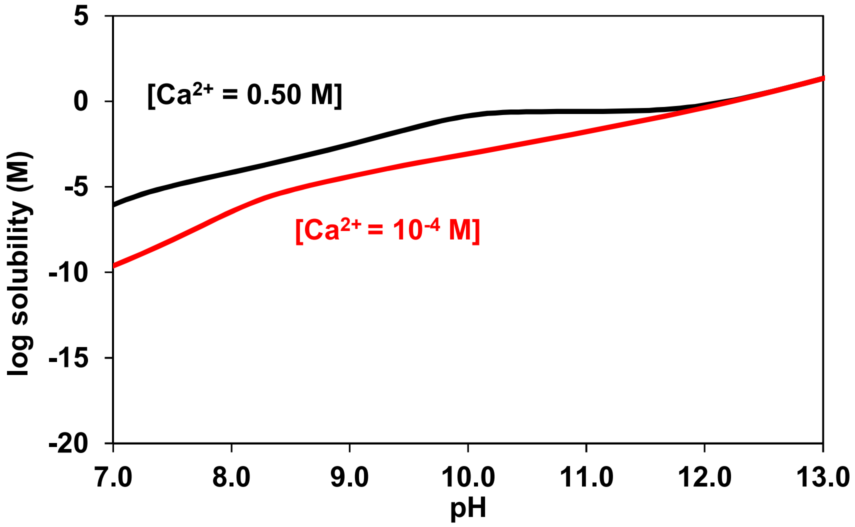

Figure 4-11. Solubility (red and black solid lines): a) $Zr(HPO_4)_2{\cdot}H_2O(cr)$ (top plot), and b) $Zr(HPO_4)_2$(alfa) (bottom plot). Red lines calculated at $[Ca]=10^{-4}$ M and black lines at [Ca]=0.5 M. In all cases $[P]_{TOT} = 10^{-5}$ M and $[CO_3]$ controlled through calcite equilibrium.

Based on those results, it is recommended to select $Zr(HPO_4)_2{\cdot}H_2O(cr)$ and $Zr(HPO_4)_2$(alfa) solid phases with thermodynamic data from NEA (Table 4-9) for being included in the Simple Functions Spreadsheet tool.

Table 4-9. Zr-PO_4 solid phases thermodynamic data selected in this work.

Species	Reaction	Log K^o_{eq}	Reference
$Zr(HPO_4)_2 \cdot H_2O(cr)$	$Zr^{4+} + 2H_2PO_4^- + H_2O \leftrightarrow 2H+ + Zr(HPO_4)_2 \cdot H_2O$	27.08 ± 3.93	Brown et al. (2005)
$Zr(HPO_4)_2$(alfa)	$Zr^{4+} + 2H_2PO_4^- \leftrightarrow 2H+ + Zr(HPO_4)_2$(alfa)	32.27 ± 4.28	Brown et al. (2005)

4.2.8 Niobium

To the authors’ knowledge, there are no available studies from which thermodynamic data for Nb-phosphate species and solid phases might be reasonably selected. Therefore, no data are selected for this chemical element.

4.2.9 Technetium

Rard (1983) performed a critical review of Tc chemistry. The author reported the existence of Tc(III/IV)-P species, but unfortunately the nature and stoichiometry of these complexes was unknown.

Later on, a NEA review on Tc chemical thermodynamics (Rard et al. 1999) included additional discussions for that system. Rard and co-workers reported that there are some indications on the formation of Tc(III) and Tc(IV) phosphate complexes, although no single species has been identified yet. This reflects that these type of complexes are not very strong.

To the authors’ knowledge, and in agreement with the NEA review findings, there are no available thermodynamic data for Tc-phosphate solid phases in the literature yet.

For these reasons, thermodynamic data for Tc complexation with phosphate have not been selected in this work.

4.2.10 Palladium

Very few reliable data are available for aqueous and solid palladium species (Baeyens and McKinley, 1989). In particular, there is a complete lack of data for the Pd phosphate system. Comprehensive compilations as the NIST thermodynamic database do not contain data for that system. Therefore, no thermodynamic data have been selected for the Pd-phosphate chemical system.

4.2.11 Silver

The NIST database (Martell and Smith, 2004) reported thermodynamic data for three different Ag-PO_4 aqueous species from a variety of potentiometric and solubility studies (Baldwin, 1969; Bottger, 1903; Ciavatta et al., 1996; Dash and Padhi, 1981; Zharovski, 1951). The stability constants reported by NIST are defined at high ionic strength (I = 3M). An estimation of these stability constants at infinite dilution has shown that these species are not relevant in the range of phosphate concentrations considered here. Therefore, they have not been included in the Simple Functions Spreadsheet.

Data for the solid phase $Ag_3PO_4(s)$ has been reported by Martell and Smith (2004), originally from the solubility study by Bottger (1903), see Table 4-10.

Table 4-10. Thermodynamic data for Ag-PO_4 as reported in the NIST database.

Solid phase	Reaction	Log K^o_{eq}	Reference
$Ag_3PO_4(s)$	$3Ag^+ + H_2(PO_4)^- \leftrightarrow 2H^+ + Ag_3PO_4(s)$	-1.98	Martell and Smith (2004) originally coming from Bottger (1903)

Calculations performed in this work indicate that, under the groundwater conditions detailed in the Appendix I, $Ag_3PO_4(s)$ will not be a solid phase that exerts a solubility control for this element. This is due to the formation of the stable aqueous silver-chloride complexes, even at low chloride levels as 10^{-4} M.

Based on these results, it is suggested not to include neither aqueous silver phosphate species nor silver phosphate solid phases in the Simple Functions Spreadsheet tool.

4.2.12 Tin

A tin data review was recently published by the NEA (Gamsjäger et al. 2012). The NEA review does not select any species for the system Sn(II/IV)-P due to the lack of experimental data. Nevertheless, the NEA team recommends the use of thermodynamic data based on the experimental work by Cilley (1968) and Ciavatta and Iuliano (2000), until new results about this system are published.

Cilley (1968) performed solubility measurements of the solid $SnHPO_4 \cdot 0.5H_2O$ as a function of phosphate concentration at constant pH. However, the authors did not provide information on the protonation state of the coordinated ligands, making it difficult to interpret the data.

Ciavatta and Iuliano (2000) investigated the formation of Sn(II)-phosphate complexes at different pHs in a 3 M $NaClO_4$ media through the use of potentiometric techniques. The authors reported several species, although only two of them, namely $SnHPO_4$(aq) and $SnPO_4^-$, seem relevant under the environmental conditions of interest. The NEA team extrapolated these data to I = 0 M using the SIT approach with estimated ion interaction coefficients. However, as the authors already mentioned, the validity of the estimated ion interaction coefficients is uncertain due to the difficulties in distinguishing between $Sn(HPO_4)$(aq) and $Sn(OH)H_2PO_4$(aq) by potentiometric measurements. For this reason, the NEA team did not select but recommended thermodynamic data for two Sn-P species, presented in Table 4-11.

Table 4-11. Thermodynamic data for the species Sn-P recommended by Gamsjäger et al. (2012).

Species	Reaction	Log K^o_{eq}	Reference
$SnHPO_4$(aq)	$Sn^{+2} + H_2(PO_4)^- \leftrightarrow H^+ + SnHPO_4(aq)$	2.29	Ciavatta and Iuliano (2000)
$SnPO_4^-$	$Sn^{+2} + H_2(PO_4)^- \leftrightarrow 2H^+ + SnPO_4^-$	-1.56	Ciavatta and Iuliano (2000)

A Sn predominance diagram is presented in Figure 4-12 that considers the formation of the Sn-P aqueous complexes, detailed in Table 4-11, at constant phosphate concentration (the upper limit phosphate aqueous concentration considered in the present work is 10^{-5} M). As seen in Figure 4-12 , the formation of these complexes is not relevant under the groundwater conditions of interest to SKB (see Appendix I).

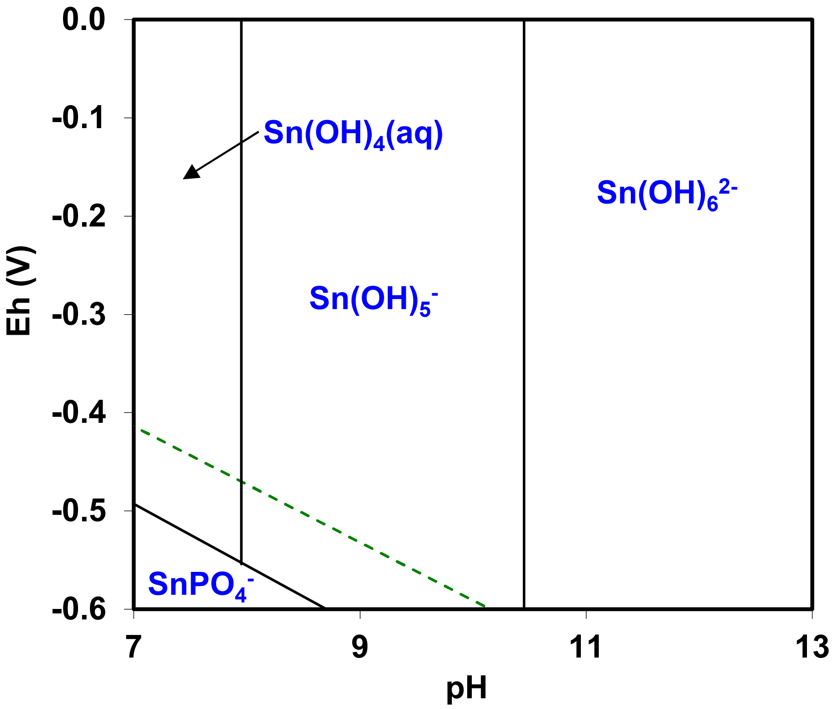

Figure 4-12. Predominance diagram Eh(V) vs pH showing the stability of Sn-P aqueous species ($[Sn]_{TOT}=5\cdot10^{-8}$ M, $[P]_{TOT}= 1\cdot10^{-5}$ M).

Moreover, if the presence of a competing cation, as Ca^{2+}, and a complementary anionic ligand as CO_3^{2-} (controlled through calcite equilibrium) is considered, it can be seen that Sn-phosphates species disappear from the diagram (Figure 4-13) due to the higher complexation capacity of Ca.

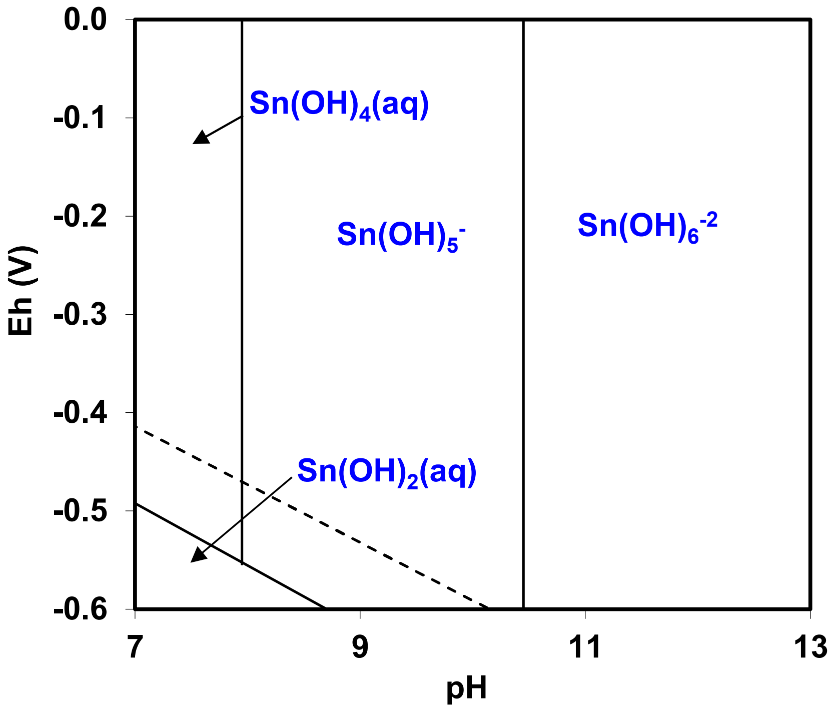

Figure 4-13. Predominance diagram Eh(V) vs pH showing the stability of Sn-P aqueous species ($[Sn]_{TOT}=5 \cdot 10^{-8}$ M, $[P]_{TOT}= 1 \cdot 10^{-5}$ M, $[Ca^{2+}]$ =0.50 M, carbonate controlled through calcite equilibrium).

The primary data reported by Cilley (1968), together with the aqueous species from Ciavatta and Iuliano (2000), was used by Gamsjäger and co-workers to determine the solubility constant of the solid $SnHPO_4 \cdot 0.5H_2O$ at low phosphate concentrations (0.3 to 2.5 mM), resulting in a log K = -12.21. The solubility of this solid phase as a function of pH is shown in Figure 4-14. As can be seen, the $SnHPO_4 \cdot 0.5H_2O$ results in too high tin aqueous concentrations, discarding the selection of this solid as a possible tin solubility limiting phase.

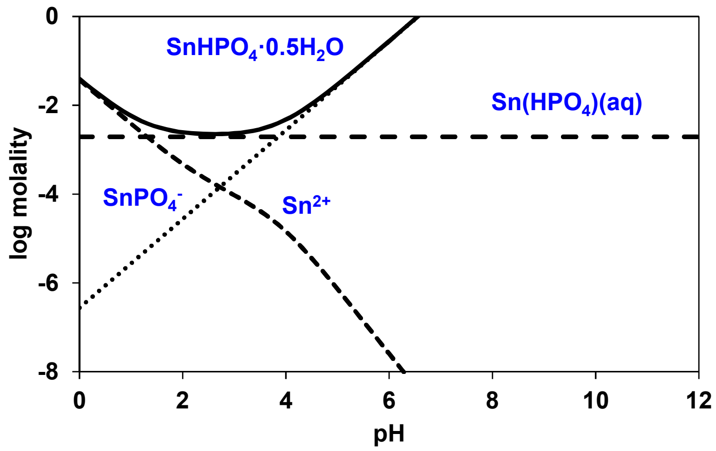

Figure 4-14. Solubility and speciation diagrams of $SnHPO_4 \cdot 0.5H_2O$ ($[P]_{TOT} = 1 \cdot 10^{-5}$ M).

Based on those results, it is recommended not to include neither the formation of Sn-P aqueous species nor any Sn-P solid phase in the Simple Functions Spreadsheet tool. Thus no thermodynamic data for that system is selected in the present work.

4.2.13 Lead

Several Pb-phosphate species, as well as solid phases, have been reported in the literature from solubility and potentiometric measurements (Nriagu, 1972, 1974; Ramamoorthy and Manning, 1974; Rao et al., 1986; Zharovskii, 1951).

In the comprehensive and extensive NIST database (Martell and Smith, 2004), two aqueous Pb phosphates, as well as two solid phases, have been selected for that system (Table 4-12). By using data in Table 4-12, we have calculated lead speciation in the pH range 6 - 13 at different phosphate aqueous concentrations (Figure 4-15). As can be seen, Pb complexation by phosphate seems to be relevant at phosphate concentrations higher than 10^{-3} M in the pH range ~4 - 9. This phosphate concentration is two orders of magnitude higher than the upper limit of phosphates established in the current work. Therefore, it may be concluded that Pb phosphates species will not affect the Pb solubility limits under the conditions studied here.

Table 4-12. Thermodynamic data for the Pb-P system as reported by Martell and Smith (2004).

Species	Reaction	Log K°$_{eq}$
$Pb(HPO_4)(aq)$	$Pb^{2+} + H_2(PO_4)^- \leftrightarrow H^+ + Pb(HPO_4)(aq)$	-4.11
$Pb(H_2PO_4)^+$	$Pb^{2+} + H_2(PO_4)^- \leftrightarrow Pb(H_2PO_4)^+$	1.50
Solid phase	**Reaction**	**Log K°$_{eq}$**
$Pb(HPO_4)(s)$	$Pb^{2+} + H_2(PO_4)^- \leftrightarrow H^+ + Pb(HPO_4)(s)$	4.22
$Pb_3(PO_4)_2(s)$	$3Pb^{2+} + 2H_2PO_4^- \leftrightarrow Pb_3(PO_4)_2(s) + 4H^+$	4.41

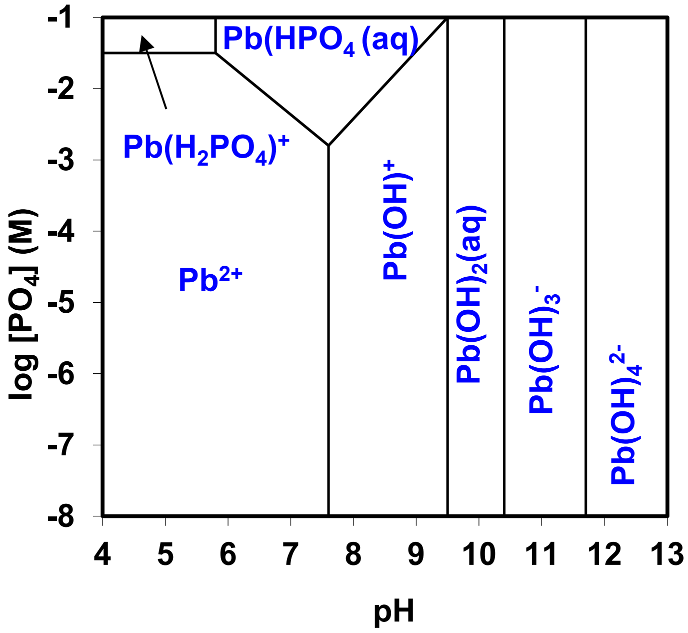

Figure 4-15. Predominance diagram log $[PO_4]$ vs pH showing the stability of Pb-P aqueous species. $[Pb]_{TOT}=1\cdot10^{-6}$ M.

Pb aqueous concentrations in equilibrium with the solid phases selected by NIST (Table 4-12) are shown in Figure 4-16. From this plot, it can be deduced that, at $[PO_4] = 10^{-5}$ M (upper limit in the studied groundwaters), both solid phases can be expected to exert solubility control for Pb in the pH range ~6 – 10. It is interesting to note again the non-relevance of phosphate complexation in that system, which cannot compete with the complexation of carbonate and hydroxyl towards lead.

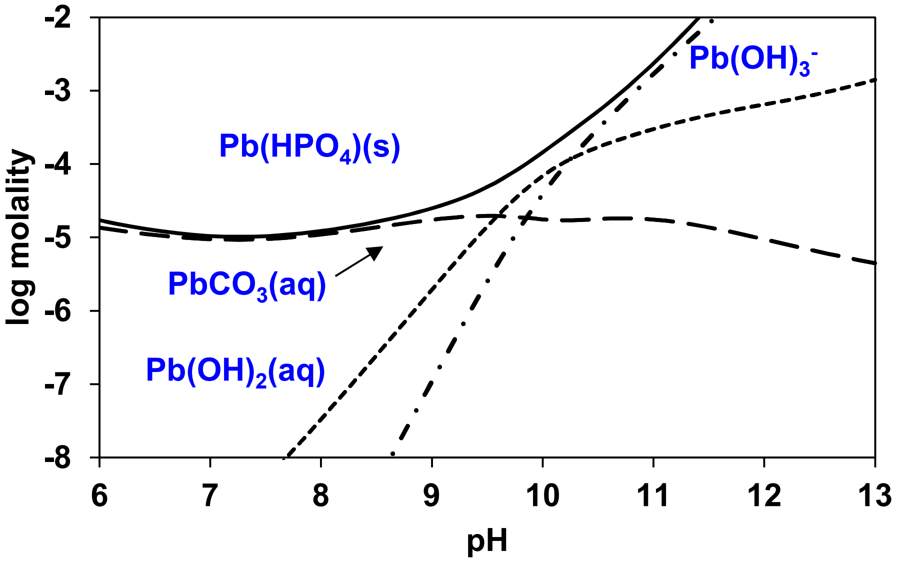

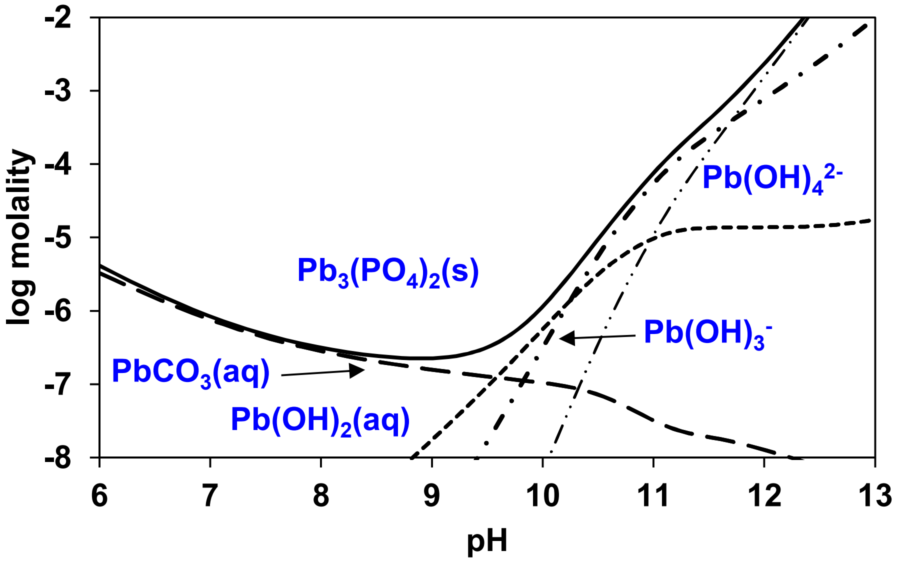

Figure 4-16. Lead molality and underlying speciation as a function of pH at a constant phosphate concentration (10^{-5} M) in equilibrium with: a) $Pb(HPO_4)(s)$ (top figure), and b) $Pb_3(PO_4)_2(s)$ (bottom figure). In both cases, [Ca] = $1 \cdot 10^{-4}$M and carbonate in equilibrium with calcite.

Based on those results, it is recommended not to consider the formation of Pb-P aqueous species in the Simple Functions Spreadsheet tool, but to include thermodynamic data for two solid phases ($Pb(HPO_4)(s)$ and $Pb_3(PO_4)_2(s)$) from the NIST compilation (Martell and Smith, 2004) as possible Pb solubility limiting phases (Table 4-13).

Table 4-13. Thermodynamic data for the Pb-P system as reported by Martell and Smith (2004).

Solid phase	Reaction	Log K^o_{eq}	Reference
$Pb(HPO_4)(s)$	$Pb^{2+} + H_2(PO_4)^- \leftrightarrow H^+ + Pb(HPO_4)(s)$	4.22 ± 0.5	Martell and Smith (2004)
$Pb_3(PO_4)_2(s)$	$3Pb^{2+} + 2H_2PO_4^- \leftrightarrow Pb_3(PO_4)_2(s) + 4H^+$	4.41 ± 0.5	Martell and Smith (2004)

4.2.14 Selenium

Thermodynamic data for selenium complexation with phosphate is scarce and uncertain. The NEA review on selenium thermodynamics (Olin et al., 2005) only reported one study, Glass et al. (1993), dealing with selenophosphate complexes. The author performed NMR analysis in a complex media (0.1 M Tricine + 0.02 M Dithiothreitol + 0.06 M Mg^{2+}) to discern the protonation constants of selenophosphate complexes. Nevertheless, Glass and co-workers did not provide information about the performance of pH measurements nor the temperature used. For this reason, the NEA team did not consider further this work.

In a study of selenophosphates interactions with enzymes, Kaminski et al. (1997) reported that this kind of complexes are thermodynamically unstable in aqueous solution and decomposes to $H_2PO_4^-$ and HSe^-.

No relevant thermodynamic data for Se-PO_4 solid phases have been found in the literature.

Based on those results, it is recommended not to consider neither the formation of Se-PO_4 species in the Simple Functions Spreadsheet tool nor any Se-PO_4 solid phase.

4.2.15 Lanthanides (Sm, Ho)

The thermodynamic database selection by Spahiu and Bruno (1995) has been considered for describing lanthanides complexation with phosphate. In that work the authors performed a detailed and concise review, including previous available thermodynamic databases (Hatches and EQ 3/6), as well as literature data (Afonin and Pechurova, 1987; Bingler and Byrne, 1989; Borisov et al., 1966; Byrne et al., 1991; Jonason et al., 1985; Millero, 1992; Rai et al., 1992; Rao et al., 1970; Wood, 1990), on REE data for being used in Performance Assessment exercises. Table 4-14 shows the datasets recommended in Spahiu and Bruno (1995). This thermodynamic data selection and their corresponding uncertainties are in fair agreement with data reported in other databases, such as the sit.dat database released with the PhreeqC code.

Table 4-14. Thermodynamic data for the Ln -P system (where Ln stand for Sm and Ho) as reported by Spahiu and Bruno (1995).

Species	Reaction	Log K^o_{eq}	
		Sm	**Ho**
$LnH_2PO_4^{2+}$	$Ln^{3+} + H_2(PO_4)^- \leftrightarrow LnH_2PO_4^{2+}$	2.35 ± 0.5	2.30 ± 0.5
$LnHPO_4^+$	$Ln^{3+} + H_2(PO_4)^- \leftrightarrow H^+ + LnHPO_4^+$	-1.61 ± 0.5	-1.41 ± 0.5
$Ln(HPO_4)_2^-$	$Ln^{3+} + 2H_2(PO_4)^- \leftrightarrow 2H^+ + Ln(HPO_4)^{2-}$	-5.02 ± 0.5	-4.52 ± 0.5
$LnPO_4(aq)$	$Ln^{3+} + H_2PO_4^- \leftrightarrow 2H^+ + LnPO_4(aq)$	-7.46 ± 0.5	-6.96 ± 0.5
$Ln(PO_4)_2^{3-}$	$Ln^{3+} + 2H_2PO_4^{3-} \leftrightarrow 4H^+ + Ln(PO_4)_2^{3-}$	-18.72 ± 0.5	-17.82 ± 0.5
Solid phase	**Reaction**	**Log K^o_{eq}**	
		Sm	**Ho**
$Ln(PO_4)\cdot xH_2O$	$Ln^{3+} + H_2PO_4^{3-} + xH_2O \leftrightarrow 2H^+ + Ln(PO_4)\cdot xH_2O$	4.94 ± 0.5	4.64 ± 0.5

Figure 4-17 shows $Ln(PO_4)\cdot xH_2O$ (where Ln = Ho or Sm) solubility and underlying lanthanide speciation as a function of pH obtained with data from Table 4-14. From this figure, it can be observed that only two species, $LnPO_4(aq)$ and $Ln(PO_4)_2^{3-}$, appears to be relevant in the pH range of groundwaters of interest to SKB (7 – 13, see Appendix I). It is also interesting to observe the low radionuclide aqueous concentration obtained when assuming $Ln(PO_4)\cdot xH_2O$ as a solubility limiting phase for Sm and Ho, up to pH ~10. Above this pH, the tendency to hydrolyse of both elements dominates, producing an increase of $Ln(PO_4)\cdot xH_2O$ solubility (Figure 4-17).

Based on those results, it is recommended to include in the Simple Functions Spreadsheet tool the whole set of thermodynamic data recommended by Spahiu and Bruno (1995) for Sm and Ho complexation with phosphate (Table 4-14). Moreover, it is also recommended to include Ln(PO$_4$)·xH$_2$O as a potential solubility limiting phase.

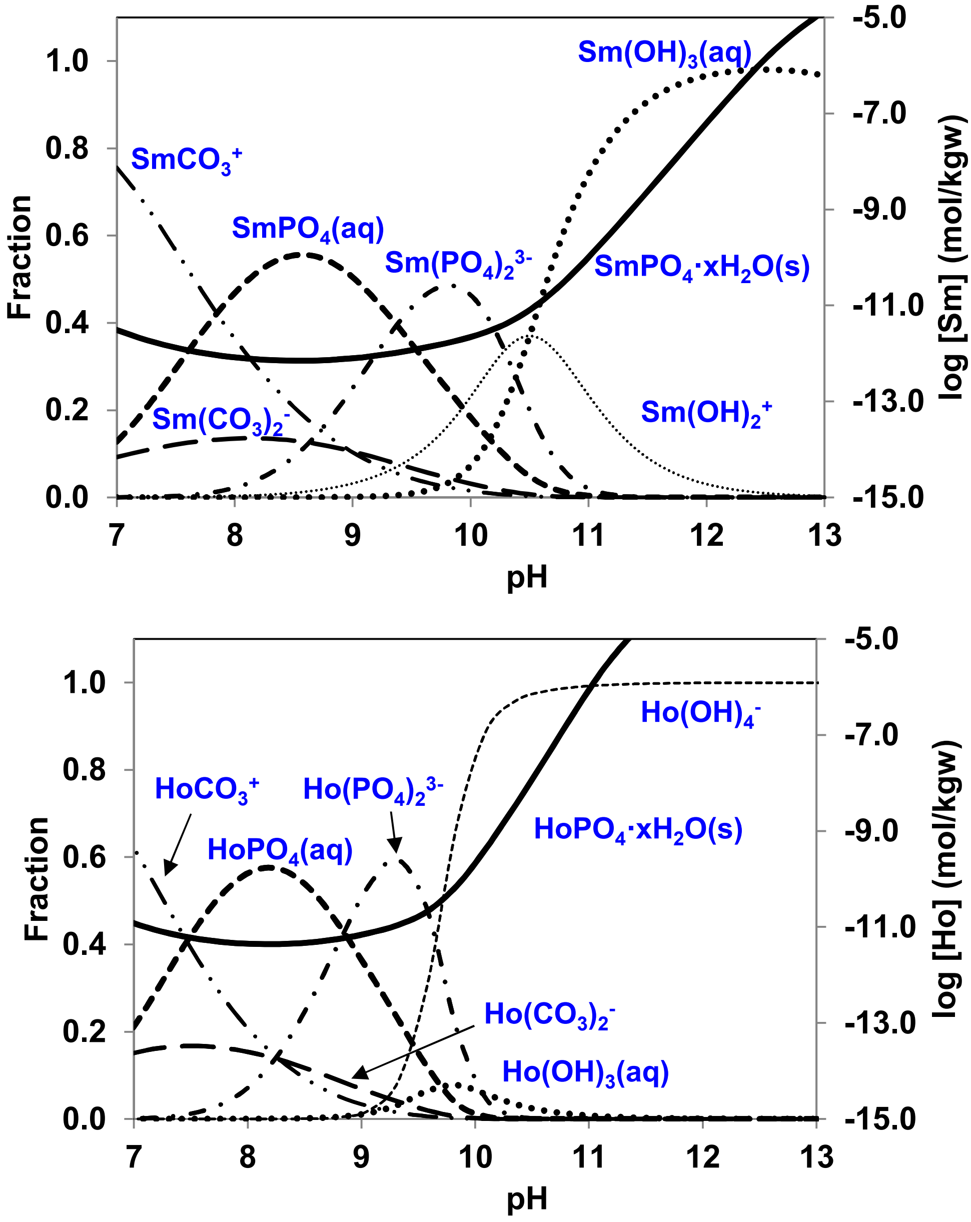

Figure 4-17. Ln(PO$_4$)·xH$_2$O solubility and underlying Ln speciation as a function of pH at a constant phosphate concentration (10^{-5} M). [Ca]= $1 \cdot 10^{-4}$ M and carbonate in equilibrium with calcite.

4.2.16 Actinides (Th, Pa, U, Np, Pu, Am, Cm)

4.2.16.1 Thorium

A comprehensive Th-phosphate data selection was recently performed by NEA (Rand et al., 2009). The data selected by Rand et al. (2009) was obtained mainly from liquid-liquid distribution and solubility studies, although also results from qualitative studies where used for justifying their selection. Rand et al. (2009) also reported the lack of relevant data regarding Th phosphate solid phases, being then difficult to perform a reliable thermodynamic data selection.

For this element it is recommended to include in the Simple Functions Spreadsheet tool the whole set of species selected by Rand et al. (2009) (Table 4-15). No thermodynamic data is selected in the present work for the formation of Th phosphate solid phases.

Table 4-15. Thermodynamic data for the Th -P system as reported by Rand et al. (2009).

Species	Reaction	Log K^o_{eq}
$Th(H_2PO_4)_2^{2+}$	$Th^{4+} + 2H_2(PO_4)^- \leftrightarrow Th(H_2PO_4)_2^{2+}$	10.48
$Th(H_2PO_4)^{3+}$	$Th^{4+} + H_2(PO_4)^- \leftrightarrow Th(H_2PO_4)^{3+}$	5.59
$Th(H_3PO_4)(H_2(PO_4)^{3+}$	$Th^{4+} + 2H_2(PO_4)^- + H^+ \leftrightarrow Th(H_3PO_4)(H_2(PO_4)^{3+}$	9.70
$Th(H_3PO_4)^{4+}$	$Th^{4+} + H_2(PO_4)^- + H^+ \leftrightarrow Th(H_3PO_4)^{4+}$	4.03

Figure 4-18 shows a Th predominance diagram obtained by using Rand et al. (2009) data selection.

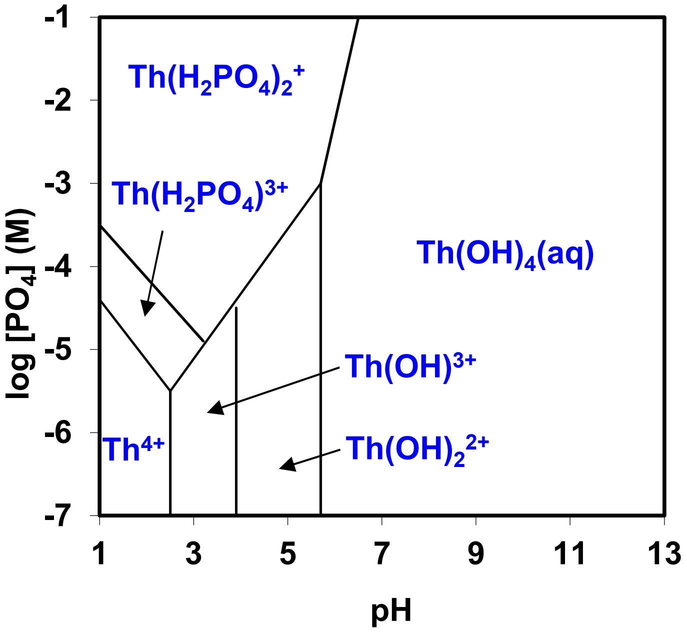

Figure 4-18. Predominance diagram log [PO_4] vs pH showing the stability of Th-P aqueous species. $[Th]_{TOT}=1\cdot10^{-8}$ M.

Table 4-16. Thermodynamic data for the Th -P system selected in the present work.

Species	**Reaction**	**Log K°$_{eq}$**	**Reference**
$Th(H_2PO_4)_2^{2+}$	$Th^{4+} + 2H_2(PO_4)^- \leftrightarrow Th(H_2PO_4)_2^{2+}$	10.48 ± 1.6	Rand et al .(2009)
$Th(H_2PO_4)^{3+}$	$Th^{4+} + H_2(PO_4)^- \leftrightarrow Th(H_2PO_4)^{3+}$	5.59 ± 1.4	Rand et al .(2009)
$Th(H_3PO_4)(H_2(PO_4)^{3+}$	$Th^{4+} + 2H_2(PO_4)^- + H^+ \leftrightarrow Th(H_3PO_4)(H_2(PO_4)^{3+}$	9.70 ± 1.6	Rand et al .(2009)
$Th(H_3PO_4)^{4+}$	$Th^{4+} + H_2(PO_4)^- + H^+ \leftrightarrow Th(H_3PO_4)^{4+}$	4.03 ± 1.4	Rand et al .(2009)

4.2.16.2 Protactinium

Although Pa-Phosphate interactions have been reported in the literature (Brandel and Dacheux, 2004; Le Cloarec and Cazaussus, 1978; Sergeyeva et al., 1994), no reliable thermodynamic data are currently available for this system.

Therefore thermodynamic data are not selected in the present work for Pa complexation with phosphates,.

4.2.16.3 *Uranium*

There are two NEA reviews (Grenthe et al., 1992; Guillaumont et al., 2003) reporting thermodynamic data for the uranium phosphate system. Guillaumont et al. (2003) reviewed the work performed after Grenthe et al. (1992), and found few additional data for U(VI)-phosphate complexation since 1992 (Brendler et al., 1996; Sandino and Bruno, 1992; Scapolan et al., 1998). Moreover those new data were in fair agreement with Grenthe et al. (1992) selection. Table 4-17 shows the set of data selected by Guillaumont et al. (2003).

Grenthe et al. (1992) and Guillaumont et al. (2003) indicated that qualitative studies (Baes, 1956; Louis and Bessière, 1987) have demonstrated strong interactions between U(IV) and phosphate. Nevertheless, no equilibrium constants can be selected for those species/solid phases based on the available studies.

A review of recent published literature has not provided any new or additional information.

Table 4-17. Thermodynamic data for the U -P system as reported by Guillaumont et al. (2003).

Species	**Reaction**	**Log K^o_{eq}**
$UO_2(PO_4)^-$	$UO_2^{2+} + H_2(PO_4)^- \leftrightarrow 2H^+ + UO_2(PO_4)^-$	-6.33 ± 0.6
$UO_2(HPO_4)(aq)$	$UO_2^{2+} + H_2(PO_4)^- \leftrightarrow H^+ + UO_2(HPO_4)(aq)$	0.03 ± 0.6
$UO_2(H_2PO_4)^+$	$UO_2^{2+} + H_2(PO_4)^- \leftrightarrow UO_2(H_2PO_4)^+$	3.26 ± 0.6
$UO_2(H_3PO_4)^{2+}$	$UO_2^{2+} + H_2(PO_4)^- \leftrightarrow H^+ + UO_2(H_3PO_4)^{2+}$	2.90 ± 0.6
$UO_2(H_2PO_4)_2(aq)$	$UO_2^{2+} + 2H_2(PO_4)^- \leftrightarrow UO_2(H_2PO_4)_2(aq)$	4.92 ± 0.9
$UO_2(H_2PO_4)(H_3PO_4)^+$	$UO_2^{2+} + 2H_2(PO_4)^- + H^+ \leftrightarrow UO_2(H_2PO_4)(H_3PO_4)^+$	5.93 ± 0.9
Solid phases	**Reaction**	**Log K^o_{eq}**
$UO_2(HPO_4)\cdot 4H_2O(cr)$	$UO_2^{2+} + H_2(PO_4)^- + 4H_2O \leftrightarrow H^+ + UO_2(HPO_4)\cdot 4H_2O(cr)$	4.64 ± 0.6
$U(HPO_4)_2\cdot 4H_2O(cr)$	$U^{4+} + 2H_2(PO_4)^- + 4H_2O \leftrightarrow 2H^+ + U(HPO_4)_2\cdot 4H_2O(cr)$	16.07 ± 0.9
$(UO_2)_3(PO_4)_2\cdot 4H_2O(cr)$	$3UO_2^{2+} + 2H_2(PO_4)^- + 4H_2O \leftrightarrow 4H^+ + (UO_2)_3(PO_4)_2\cdot 4H_2O(cr)$	10.24 ± 4.0

Figure 4-19 shows uranium speciation obtained with data from Table 4-17. As can be seen, phosphate concentrations about 10^{-5} M can exert an important control on uranium aqueous chemistry in a system without competing ligands (i.e. carbonate). In fact, as reported by Sandino and Bruno (1992), in the pH range of most natural waters, 6 - 9, U(VI) will only be associated with aqueous phosphate when the total concentration ratio $[PO_4]/[CO_3]$ is greater than 10^{-1}, which is rather difficult to encounter in groundwaters. In any case, given the relevance of uranium species, it is suggested to include the selection of U(VI)-phosphate species (Table 4-17) in the Simple Functions Spreadsheet tool.

In the case of the solid phases selected in Guillaumont et al. (2003), solubility calculations have shown that these solids presented higher solubilities than the solubility limits already reported in Grivé et al. (2010a) for uranium. This conclusion is in agreement with experimental results from Sandino and Bruno (1992), which reported thermodynamic data for a more crystalline $(UO_2)_3(PO_4)_2\cdot 4H_2O(cr)$ solid phase.

Therefore, it is recommended not to consider any uranium phosphate solid phase in the Simple Functions Spreadsheet tool.

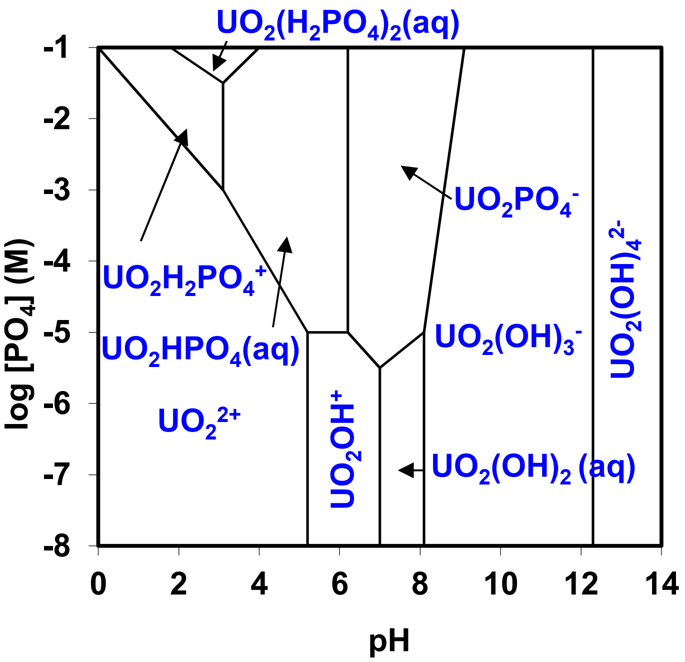

Figure 4-19. Predominance diagram log [PO_4] vs pH showing the stability of U-P aqueous species. $[U]_{TOT}=1\cdot10^{-8}$ M and Eh=0.5 V.

4.2.16.4 Neptunium

Lemire et al. (2001) reported thermodynamic data for the complexation of phosphate with several oxidation states of Np.

In the case of Np(IV) no experimental data was found by Lemire et al. (2001). Only estimations by Moskvin et al. (1967) based on results for the same Pu counterparts obtained by Denotkina et al. (1960) are available. However these estimations are not credited by Lemire and co-workers due to shortcomings with the methodology followed by the authors, mainly because the author neglected Pu^{4+} hydrolysis.

In the other hand, Lemire et al. (2001) selected few species for Np(V) and Np(VI) complexation with phosphate from a variety of experimental studies (spectrophotometric, ion-exchange solvent extraction and co-precipitation studies). Table 4-18 shows Lemire et al. (2001) data selection.

Any Np-phosphate solid phase is discussed by Lemire et al. (2001). Guillaumont et al. (2003) update the NEA thermodynamic data selection for Np, but no additional hints are provided in this work regarding Np-phosphate system.

A review of recent published literature for Np (IV, V and VI) conducted within the current work has not provided any new or additional valuable information for this system.

Table 4-18. Thermodynamic data for the Np -P system as reported by Lemire et al. (2001).

Species	**Reaction**	**Log K^o_{eq}**
$NpO_2(HPO_4)(aq)$	$NpO_2^{2+} + H_2(PO_4)^- \leftrightarrow H^+ + NpO_2(HPO_4)(aq)$	-1.01
$NpO_2HPO_4^-$	$NpO_2^+ + H_2(PO_4)^- \leftrightarrow H^+ + NpO_2HPO_4^-$	-4.26
$NpO_2(HPO_4)_2^{2-}$	$NpO_2^{2+} + 2H_2(PO_4)^- \leftrightarrow 2H+ + NpO(HPO_4)_2^{2-}$	-4.92
$NpO_2H_2PO_4^+$	$NpO_2^{2+} + H_2PO_4^- \leftrightarrow NpO_2H_2PO_4^+$	3.32

Neptunium predominance diagrams obtained with data from Table 4-18 are shown in Figure 4-20. As can be observed, Np complexation by phosphate is weak given that phosphate concentrations as high as 10^{-1} M would be required in order to stabilize Np-Phosphate species.

Based on those results, we would recommend to do not consider the formation of Np-PO_4 species in the Simple Functions Spreadsheet because of their low impact on Np chemistry in natural groundwater conditions.

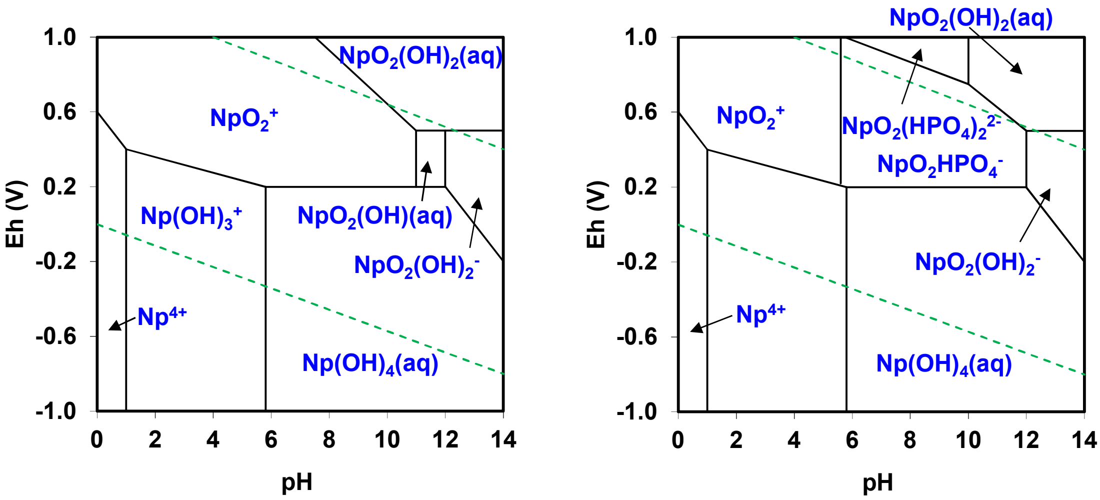

Figure 4-20. Predominance diagram Eh (V) vs pH showing the stability of Np-P aqueous species: a) $[PO_4] = 10^{-5}$ M, and b) $[PO_4] = 10^{-1}$ M. In both cases $[Np]_{TOT} = 1 \cdot 10^{-8}$ M.

4.2.16.5 Plutonium

As in the previous case, Lemire et al. (2001) and the subsequent NEA update (Guillaumont et al. 2003), discussed Pu interactions with phosphate.

Four different Pu oxidation states (III, IV, V, VI) are included in the Simple Functions. Nevertheless, NEA only recommended data for two Pu oxidation states (IV and V). In the case of Pu(III) phosphate species, only one experimental study reported thermodynamic data (Moskvin, 1971) but experimental shortcomings in that work does not allow a reliable data selection. As a rough estimation, and given the relevance of phosphates towards the trivalent lanthanides (section 4.2.15), we have estimated Pu(III) phosphate species thermodynamic data (Table 4-19) from ionic radii correlations with lanthanides data in Spahiu and Bruno (1995). This approach will help us to discern the role of phosphate over Pu(III).

Table 4-19. Thermodynamic data for the Pu(III)-P system estimated in this work with lanthanides data in Spahiu and Bruno (1995).

Species	**Reaction**	**Log K^o_{eq}**
$PuH_2PO_4^{2+}$	$Pu^{3+} + H_2(PO_4)^- \leftrightarrow PuH_2PO_4^{2+}$	2.43
$PuHPO_4^{+}$	$Pu^{3+} + H_2(PO_4)^- \leftrightarrow H^+ + PuHPO_4^{+}$	-1.86
$Pu(HPO_4)_2^{-}$	$Pu^{3+} + 2H_2(PO_4)^- \leftrightarrow 2H^+ + Pu(HPO_4)^{2-}$	-5.51
$PuPO_4(aq)$	$Pu^{3+} + H_2PO_4^- \leftrightarrow 2H^+ + PuPO_4(aq)$	-8.00
$Pu(PO_4)_2^{3-}$	$Pu^{3+} + 2H_2PO_4^{3-} \leftrightarrow 4H^+ + Pu(PO_4)_2^{3-}$	-19.94

For Pu(VI) phosphate species, Lemire et al. (2001) reported inconsistencies in the experimental results as well as in the interpretations made by the authors that dealt with this system. So that as reported by Lemire et al. (2001) a proper thermodynamic data selection cannot be done for the Pu(VI)-phosphate system.

Lemire et al. (2001) selected Pu(IV) phosphate species from the solubility study by King (1949). This selection was found to be in fair agreement with the reinterpretation of results from Denotkina et al. (1960). As cited before, Lemire et al. (2001) also discussed thermodynamic data for Pu(V) phosphate complexation. The authors only found one study dealing with this system (Moskvin and Poznyakov, 1979) based on sorption-coprecipitation of Pu(V) on Fe(III) hydroxide. Although the results by Moskvin and Poznyakov (1979) were better than for other systems, the NEA review only recommended but not selected this data while waiting for confirmation from other more conventional method.

Regarding Pu – phosphate solid phases, two different solids ($Pu(HPO_4)_2(am)$ and $PuPO_4(s)$) were selected by Lemire et al. (2001) from solubility studies. Thermodynamic selected by Lemire et al. (2001) for both solids and aqueous Pu phosphate species is shown in Table 4-20.

Table 4-20. Thermodynamic data for the Pu - P system as reported by Lemire et al. (2001).

Species	Reaction	Log K°$_{eq}$
$Pu(H_3PO_4)^{4+}$	$Pu^{4+} + H_2(PO_4)^- + H^+ \leftrightarrow Pu(H_3PO_4)^{4+}$	4.54
$PuO_2HPO_4^-$	$PuO^{2+} + H_2PO_4^- \leftrightarrow H^+ + PuO_2HPO_4^-$	-4.86
Solid phases	**Reaction**	**Log K°$_{eq}$**
$Pu(HPO_4)_2$(am)	$Pu^{4+} + 2H_2(PO_4)^- \leftrightarrow 2H^+ + Pu(HPO_4)_2$(am)	16.03
$Pu(PO_4)$(s)	$Pu^{3+} + H_2(PO_4)^- \leftrightarrow 2H^+ + PuPO_4$(s)	5.04

Figure 4-21 shows $PuPO_4$(s) solubility and its underlying speciation obtained with thermodynamic data from Table 4-19 and Table 4-20. From these results, we can conclude that in the pH range of the groundwaters detailed in Appendix I, even in the presence of carbonate as a competing ligand, phosphate can strongly complex Pu. Moreover, it can be also seen that in reducing conditions (Eh= -0.5V) $PuPO_4$(s) solubility below pH ~11 is lower than the solubility limits reported in Grivé et al. (2010a) for Pu. Thus in reducing environments, $PuPO_4$(s) can be considered as a possible Pu solubility limiting phase if phosphates are included in performance assessments calculations.

In redox conditions where Pu(IV) is favored, Pu aqueous concentrations in equilibrium with $Pu(HPO_4)_2$(am) are higher than solubility limits reported in Grivé et al. (2010a), and thus this solid phase is not relevant for the current work.

Based on those results, we would recommend including in the Simple Functions Spreadsheet tool the set of thermodynamic data detailed in Table 4-21.

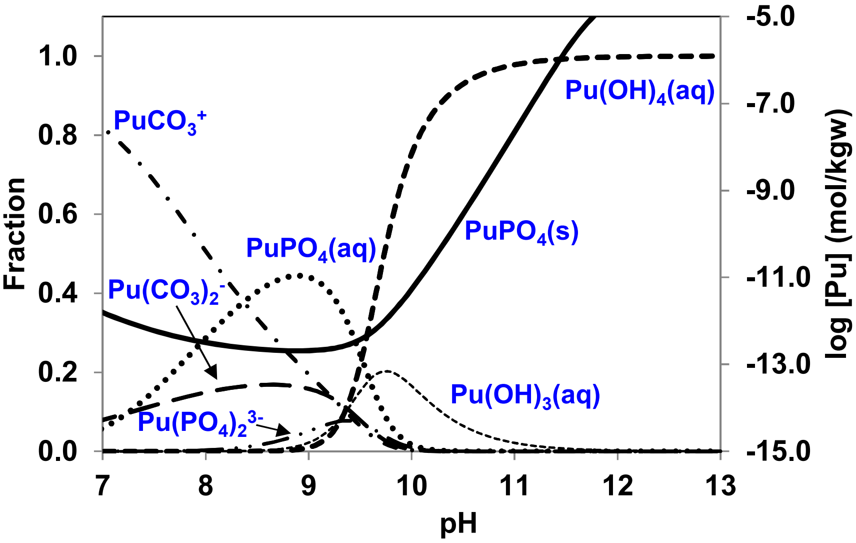

Figure 4-21. $Pu(PO_4)(s)$ solubility and underlying Pu speciation as a function of pH at a constant phosphate concentration (10^{-5} M). Eh=-0.5 (V), [Ca]= $1 \cdot 10^{-4}$ M and carbonate in equilibrium with calcite.

Table 4-21. Thermodynamic data for the Pu - P system selected in this work.

Species	Reaction	Log K^o_{eq}	Reference
$Pu(H_3PO_4)^{4+}$	$Pu^{4+} + H_2(PO_4)^- + H^+ \leftrightarrow Pu(H_3PO_4)^{4+}$	4.54 ± 1.0	Lemire et al. (2001)
$PuO_2HPO_4^-$	$PuO_2^+ + H_2PO_4^- \leftrightarrow H^+ + PuO_2HPO_4^-$	-4.86 ± 0.3	Lemire et al. (2001)
$PuH_2PO_4^{2+}$	$Pu^{3+} + H_2(PO_4)^- \leftrightarrow PuH_2PO_4^{2+}$	2.43 ± 0.5	This work
$PuHPO_4^+$	$Pu^{3+} + H_2(PO_4)^- \leftrightarrow H^+ + PuHPO_4^+$	-1.86 ± 0.5	This work
$Pu(HPO_4)_2^-$	$Pu^{3+} + 2H_2(PO_4)^- \leftrightarrow 2H^+ + Pu(HPO_4)^{2-}$	-5.51 ± 0.5	This work
$PuPO_4(aq)$	$Pu^{3+} + H_2PO_4^- \leftrightarrow 2H^+ + PuPO_4(aq)$	-8.00 ± 0.5	This work
$Pu(PO_4)_2^{3-}$	$Pu^{3+} + 2H_2PO_4^{3-} \leftrightarrow 4H^+ + Pu(PO_4)_2^{3-}$	-19.94 ± 0.5	This work
Solid phases	**Reaction**	**Log K^o_{eq}**	**Reference**
$Pu(PO_4)(s)$	$Pu^{3+} + H_2(PO_4)^- \leftrightarrow 2H^+ + PuPO_4(s)$	5.04 ± 1.1	Lemire et al. (2001)

4.2.16.6 Americium and curium

As reported in the NEA review on Am chemical thermodynamics (Silva et al., 1995), few reliable studies are available in the literature on americium complexation with phosphate. The same argument is valid for Cm phosphate complexation. In the case of Am, Silva et al. (1995) only selected $Am(H_2PO_4)^{2+}$ species and $Am(PO_4)(s)$ solid phase from cation exchange, solubility and spectrophotometric studies. Nevertheless the authors reported the existence of several Am phosphates species, but due to shortcomings in the works discussed by Silva et al. (1995), the NEA team decided to do not select additional data.

As previously we did for Pu(III), in present work Am and Cm interactions with phosphates has been studied through ionic radii correlations with the same counterparts of lanthanides (Figure 4-22 and Figure 4-23) reported by Spahiu and Bruno (1995).

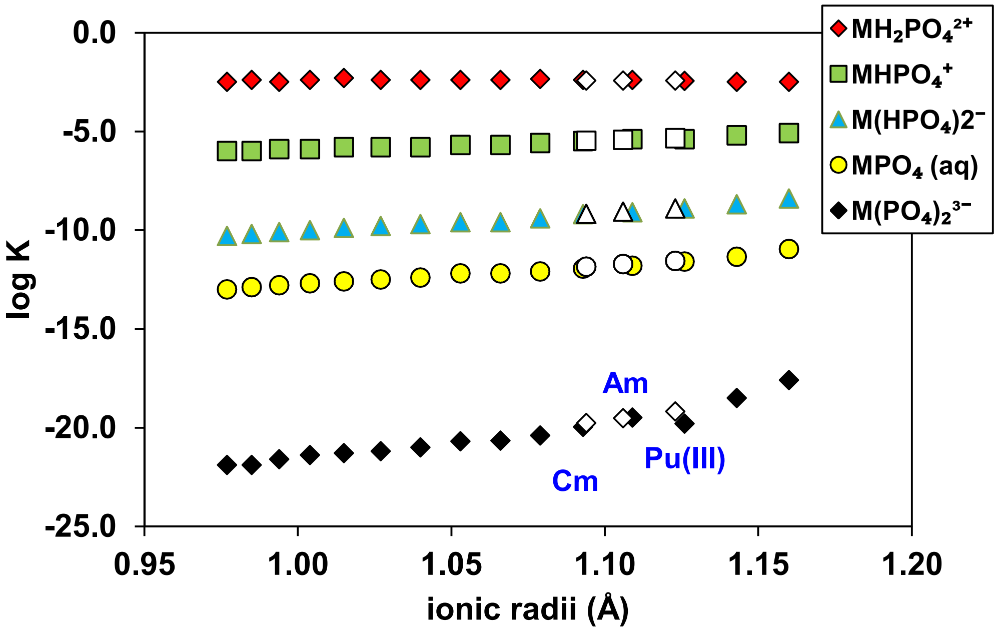

Figure 4-22. Formation constants from Spahiu and Bruno (1995) of the phosphate complexes for the trivalent lanthanides as a function of the ionic radii of the cations (filled symbols). Empty symbols stand for estimated data.

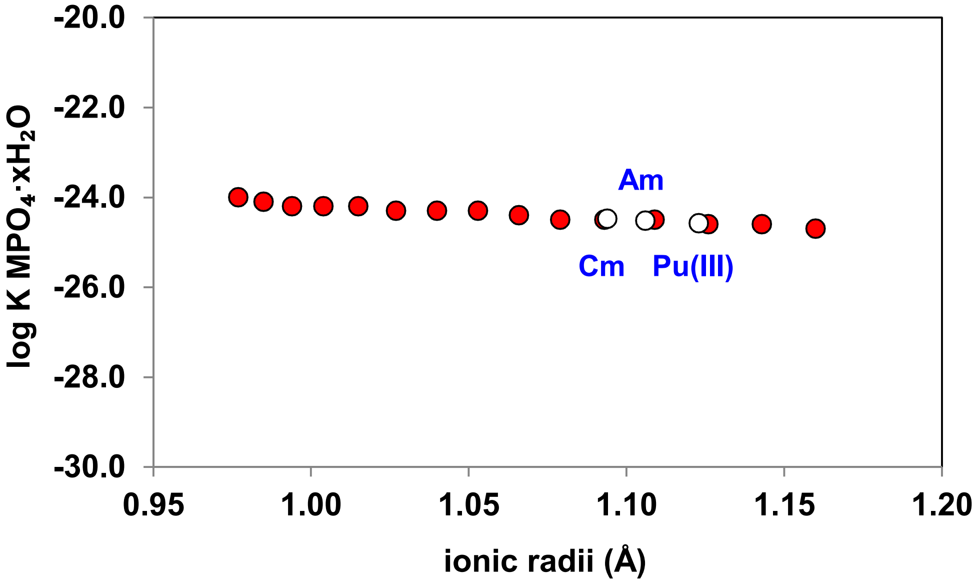

Figure 4-23. $MPO_4 \cdot xH_2O$ dissociation constant from Spahiu and Bruno (1995) for the trivalent lanthanides as a function of the ionic radii of the cations (filled symbols). Empty symbols stand for estimated data.

Thermodynamic data estimated by using this procedure, is in fair agreement with the ones selected for Am by NEA (Table 4-22). Additionally, the set of thermodynamic data recommended in the present work and their corresponding uncertainties are in fair agreement with data reported in other databases (i.e. sit.dat database released with the PhreeqC code).

Table 4-22. Thermodynamic data for the Am/Cm -P system estimated and selected in this work.

Species	**Reaction**	**Log K°$_{eq}$**	
		This work	**Silva et al. (1995)**
$AmH_2PO_4^{2+}$	$Am^{3+} + H_2(PO_4)^- \leftrightarrow AmH_2PO_4^{2+}$	2.43	3.00
Solid phase	**Reaction**	**Log K°$_{eq}$**	
		Am	**Cm**
$Am(PO_4) \cdot xH_2O$	$Am^{3+} + H_2PO_4^{3-} + xH_2O \leftrightarrow 2H^+ + Am(PO_4) \cdot xH_2O^-$	4.96	5.23

By using the estimated data we have calculated An(PO_4)·xH_2O solubility as a function of pH for both Am and Cm solid phases (Figure 4-24). As in the case of lanthanides, it can be clearly seen that phosphates can complex those lanthanides in the pH range of interest (~7-13, see appendix I). Moreover, the calculated solubilities are below the range of solubility limits reported for these radionuclides in Grivé et al. (2010a); and thus they can exert as a solubility limiting phase for those actinides.

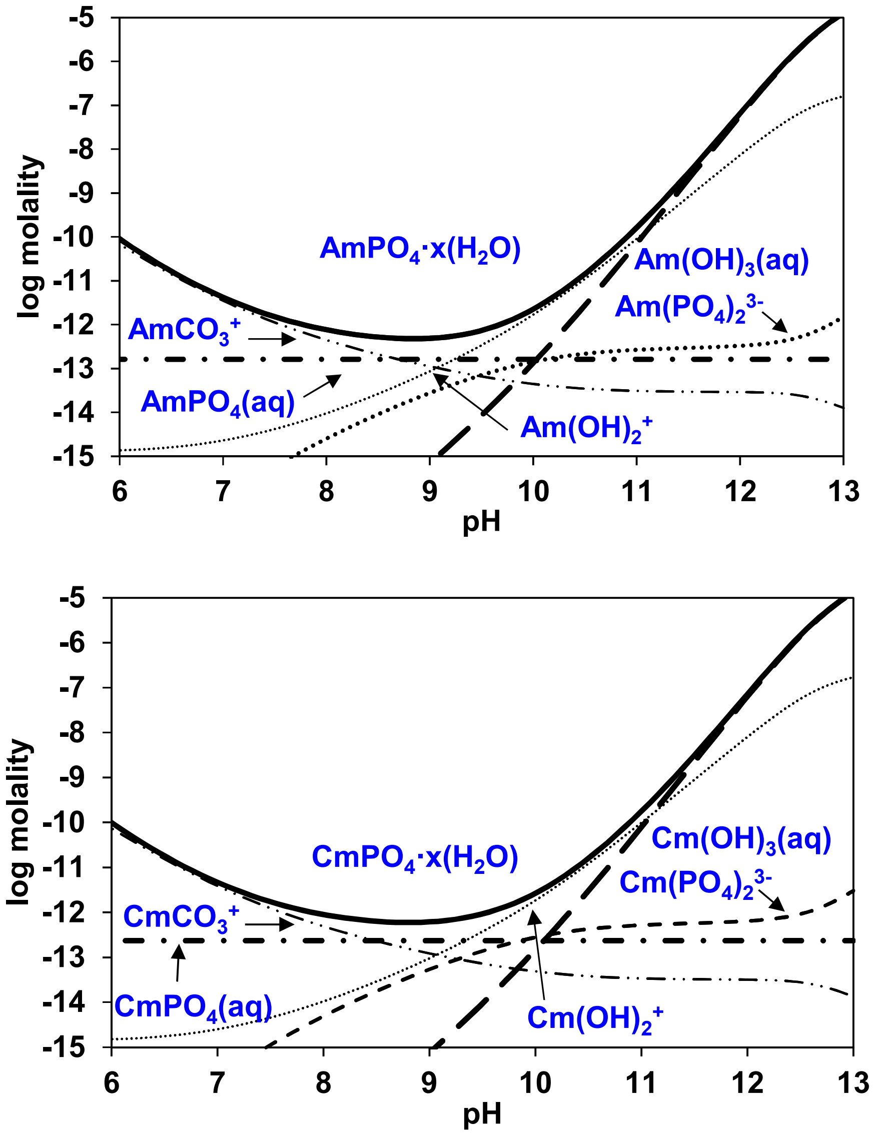

Figure 4-24. An(PO_4)·xH_2O solubility and underlying An speciation as a function of pH at a constant phosphate concentration (10^{-5} M). [Ca]= $1·10^{-4}$ M and carbonate in equilibrium with calcite.

Based on those results, we recommend including in the Simple Functions Spreadsheet tool the whole set of thermodynamic data detailed in Table 4-23.

Table 4-23. Thermodynamic data for the Am/Cm -P system estimated and selected in this work. An stands for Am and Cm.

Species	**Reaction**	**Log K^o_{eq}**	
		Am	**Cm**
$AnH_2PO_4^{2+}$	$An^{3+} + H_2(PO_4)^- \leftrightarrow AnH_2PO_4^{2+}$	2.43 ± 0.5	2.43 ± 0.5
$AnHPO_4^+$	$An^{3+} + H_2(PO_4)^- \leftrightarrow H^+ + AnHPO_4^+$	-1.78 ± 0.5	-1.72 ± 0.5
$An(HPO_4)_2^-$	$An^{3+} + 2H_2(PO_4)^- \leftrightarrow 2H^+ + An(HPO_4)^{2-}$	-5.35 ± 0.5	-5.24 ± 0.5
$AnPO_4(aq)$	$An^{3+} + H_2PO_4^- \leftrightarrow 2H^+ + AnPO_4(aq)$	-7.83 ± 0.5	-7.71 ± 0.5
$An(PO_4)_2^{3-}$	$An^{3+} + 2H_2PO_4^{3-} \leftrightarrow 4H^+ + An(PO_4)_2^{3-}$	-19.60 ± 0.5	-19.35 ± 0.5
Solid phase	**Reaction**	**Log K^o_{eq}**	
		Am	**Cm**
$An(PO_4){\cdot}xH_2O$	$An^{3+} + H_2PO_4^{3-} + xH_2O \leftrightarrow 2H^+ + An(PO_4){\cdot}xH_2O^-$	4.96 ± 0.5	4.92 ± 0.5

4.3 Simple Functions Spreadsheet Tool update

The aim of this section is to briefly summarize how the selected thermodynamic data from section 4.2 has been introduced in the Simple Functions Spreadsheet tool. It should be noticed that both versions of the spread sheet, VERSION A (designed to calculate radionuclide solubility limits in representative groundwater compositions supplied by the user) and VERSION B (designed for solubility assessments in a groundwater that has interacted with Fe-corrosion products), have been successfully updated.

4.3.1 DON’T TOUCH sheet

In this sheet, data for phosphate hydrolysis as well as calcium complexation and solid precipitation, have been introduced (Figure 4-25 and Figure 4-26). In addition, calculations for obtaining the Saturation Index of the solid phase hydroxyapatite ($Ca_5(PO_4)_3(OH)$) have also been introduced.

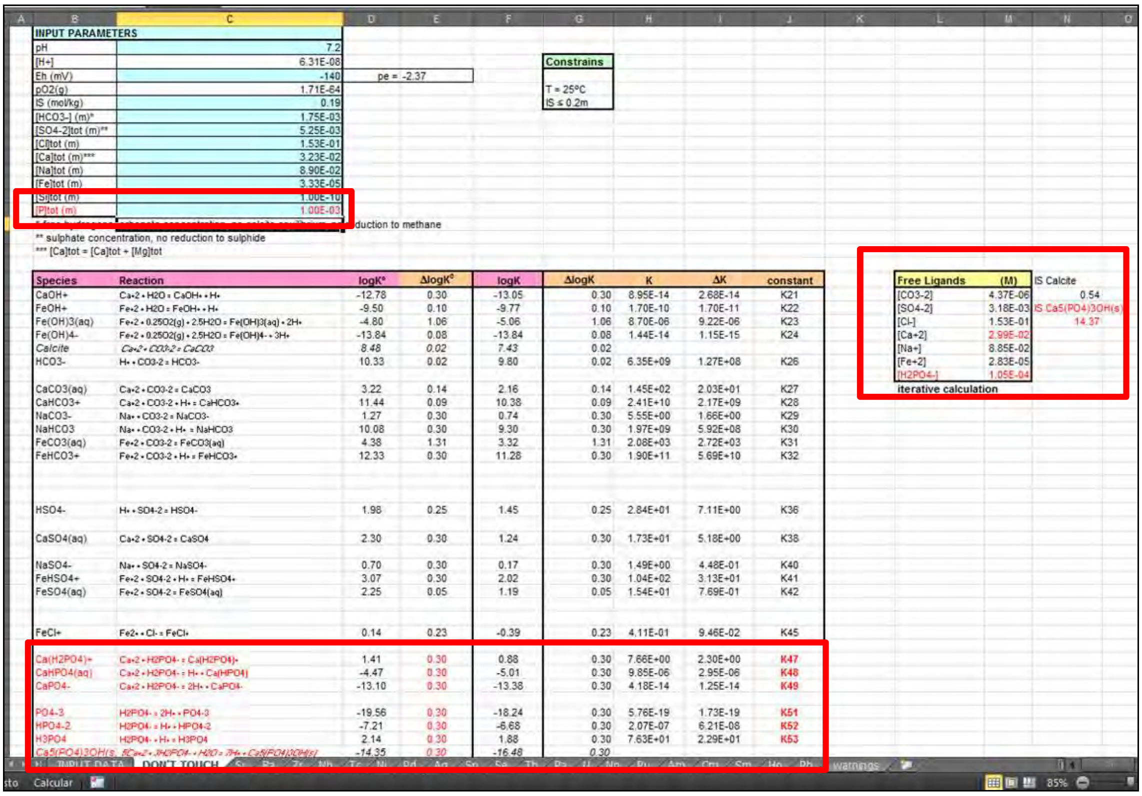

INPUT PARAMETERS	
pH	7.2
[H+]	6.31E-08
Eh (mV)	-140
pO2(g)	1.71E-64
IS (mol/kg)	0.19
[HCO3-] (m)*	1.75E-03
[SO4-2]tot (m)**	5.25E-03
[Cl]tot (m)	1.53E-01
[Ca]tot (m)***	3.23E-02
[Na]tot (m)	8.90E-02
[Fe]tot (m)	3.33E-05
[Si]tot (m)	1.00E-10
[P]tot (m)	1.00E-03

pe = -2.37

* free hydrogen [illegible] duction to methane
** sulphate concentration, no reduction to sulphide
*** [Ca]tot = [Ca]tot + [Mg]tot

Constrains
T = 25°C IS ≤ 0.2m

Species	Reaction	logK°	ΔlogK°	logK	ΔlogK	K	ΔK	constant
CaOH+	Ca+2 + H2O = CaOH+ + H+	-12.78	0.30	-13.05	0.30	8.95E-14	2.68E-14	K21
FeOH+	Fe+2 + H2O = FeOH+ + H+	-9.50	0.10	-9.77	0.10	1.70E-10	1.70E-11	K22
Fe(OH)3(aq)	Fe+2 + 0.25O2(g) + 2.5H2O = Fe(OH)3(aq) + 2H+	-4.80	1.06	-5.06	1.06	8.70E-06	9.22E-06	K23
Fe(OH)4-	Fe+2 + 0.25O2(g) + 2.5H2O = Fe(OH)4- + 3H+	-13.84	0.08	-13.84	0.08	1.44E-14	1.15E-15	K24
Calcite	*Ca+2 + CO3-2 = CaCO3*	*8.48*	*0.02*	*7.43*	0.02			
HCO3-	H+ + CO3-2 = HCO3-	10.33	0.02	9.80	0.02	6.35E+09	1.27E+08	K26
CaCO3(aq)	Ca+2 + CO3-2 = CaCO3	3.22	0.14	2.16	0.14	1.45E+02	2.03E+01	K27
CaHCO3+	Ca+2 + CO3-2 + H+ = CaHCO3+	11.44	0.09	10.38	0.09	2.41E+10	2.17E+09	K28
NaCO3-	Na+ + CO3-2 = NaCO3-	1.27	0.30	0.74	0.30	5.55E+00	1.66E+00	K29
NaHCO3	Na+ + CO3-2 + H+ = NaHCO3	10.08	0.30	9.30	0.30	1.97E+09	5.92E+08	K30
FeCO3(aq)	Fe+2 + CO3-2 = FeCO3(aq)	4.38	1.31	3.32	1.31	2.08E+03	2.72E+03	K31
FeHCO3+	Fe+2 + CO3-2 + H+ = FeHCO3+	12.33	0.30	11.28	0.30	1.90E+11	5.69E+10	K32
HSO4-	H+ + SO4-2 = HSO4-	1.98	0.25	1.45	0.25	2.84E+01	7.11E+00	K36
CaSO4(aq)	Ca+2 + SO4-2 = CaSO4	2.30	0.30	1.24	0.30	1.73E+01	5.18E+00	K38
NaSO4-	Na+ + SO4-2 = NaSO4-	0.70	0.30	0.17	0.30	1.49E+00	4.48E-01	K40
FeHSO4+	Fe+2 + SO4-2 + H+ = FeHSO4+	3.07	0.30	2.02	0.30	1.04E+02	3.13E+01	K41
FeSO4(aq)	Fe+2 + SO4-2 = FeSO4(aq)	2.25	0.05	1.19	0.05	1.54E+01	7.69E-01	K42
FeCl+	Fe2+ + Cl- = FeCl+	0.14	0.23	-0.39	0.23	4.11E-01	9.46E-02	K45
Ca(H2PO4)+	Ca+2 + H2PO4- = Ca(H2PO4)+	1.41	0.30	0.88	0.30	7.66E+00	2.30E+00	K47
CaHPO4(aq)	Ca+2 + H2PO4- = H+ + Ca(HPO4)	-4.47	0.30	-5.01	0.30	9.85E-06	2.95E-06	K48
CaPO4-	Ca+2 + H2PO4- = 2H+ + CaPO4-	-13.10	0.30	-13.38	0.30	4.18E-14	1.25E-14	K49
PO4-3	H2PO4- = 2H+ + PO4-3	-19.56	0.30	-18.24	0.30	5.76E-19	1.73E-19	K51
HPO4-2	H2PO4- = H+ + HPO4-2	-7.21	0.30	-6.68	0.30	2.07E-07	6.21E-08	K52
H3PO4	H2PO4- + H+ = H3PO4	2.14	0.30	1.88	0.30	7.63E+01	2.29E+01	K53
Ca5(PO4)3OH(s	*5Ca+2 + 3H2PO4- + H2O = 7H+ + Ca5(PO4)3OH(s)*	*-14.35*	*0.30*	*-16.48*	*0.30*			

Free Ligands	(M)	IS Calcite
[CO3-2]	4.37E-06	0.54
[SO4-2]	3.18E-03	IS Ca5(PO4)3OH(s)
[Cl-]	1.53E-01	14.37
[Ca+2]	2.99E-02	
[Na+]	8.85E-02	
[Fe+2]	2.83E-05	
[H2PO4-]	1.05E-04	

iterative calculation

Figure 4-25. Snapshot of the amended DON’T TOUCH sheet (VERSION A).

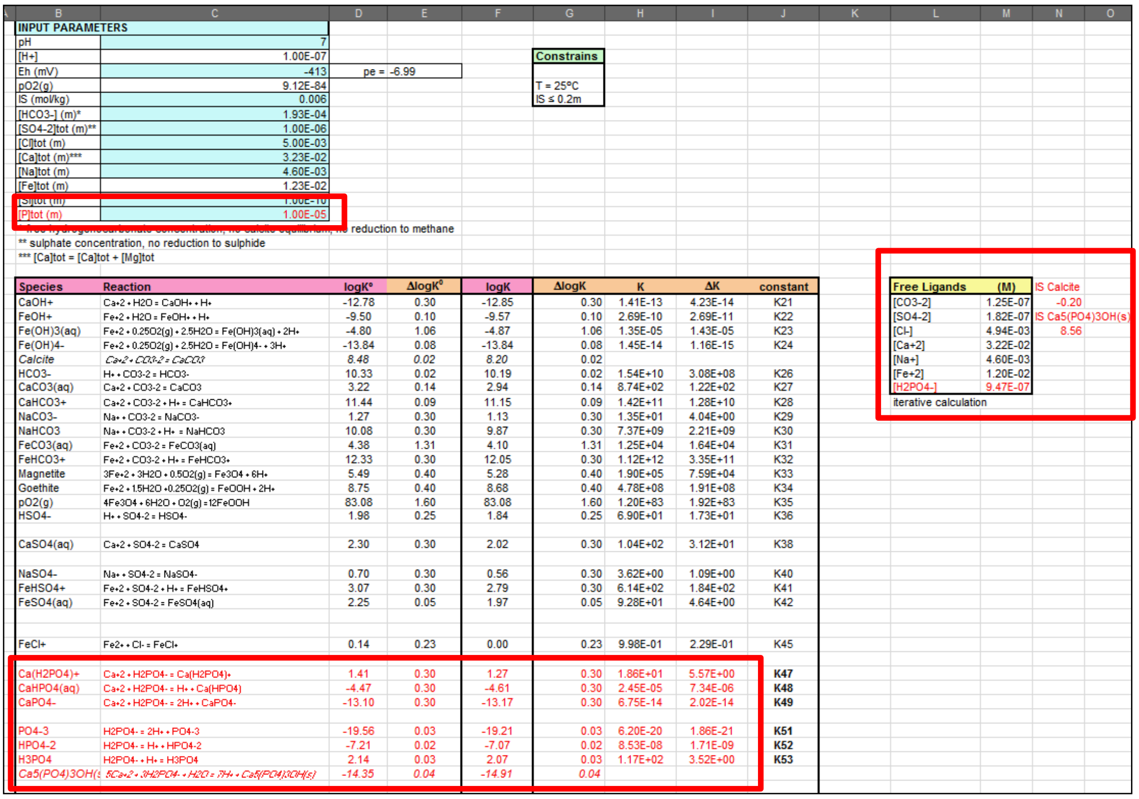

INPUT PARAMETERS	
pH	7
[H+]	1.00E-07
Eh (mV)	-413
pO2(g)	9.12E-84
IS (mol/kg)	0.006
[HCO3-] (m)*	1.93E-04
[SO4-2]tot (m)**	1.00E-06
[Cl]tot (m)	5.00E-03
[Ca]tot (m)***	3.23E-02
[Na]tot (m)	4.60E-03
[Fe]tot (m)	1.23E-02
[Si]tot (m)	1.00E-10
[P]tot (m)	1.00E-05

pe = -6.99

* free hydrogencarbonate concentration, no calcite equilibrium, no reduction to methane
** sulphate concentration, no reduction to sulphide
*** [Ca]tot = [Ca]tot + [Mg]tot

Constrains
T = 25ºC
IS ≤ 0.2m

Species	Reaction	logK°	ΔlogK°	logK	ΔlogK	K	ΔK	constant
CaOH+	Ca+2 + H2O = CaOH+ + H+	-12.78	0.30	-12.85	0.30	1.41E-13	4.23E-14	K21
FeOH+	Fe+2 + H2O = FeOH+ + H+	-9.50	0.10	-9.57	0.10	2.69E-10	2.69E-11	K22
Fe(OH)3(aq)	Fe+2 + 0.25O2(g) + 2.5H2O = Fe(OH)3(aq) + 2H+	-4.80	1.06	-4.87	1.06	1.35E-05	1.43E-05	K23
Fe(OH)4-	Fe+2 + 0.25O2(g) + 2.5H2O = Fe(OH)4- + 3H+	-13.84	0.08	-13.84	0.08	1.45E-14	1.16E-15	K24
Calcite	*Ca+2 + CO3-2 = CaCO3*	*8.48*	*0.02*	*8.20*	0.02			
HCO3-	H+ + CO3-2 = HCO3-	10.33	0.02	10.19	0.02	1.54E+10	3.08E+08	K26
CaCO3(aq)	Ca+2 + CO3-2 = CaCO3	3.22	0.14	2.94	0.14	8.74E+02	1.22E+02	K27
CaHCO3+	Ca+2 + CO3-2 + H+ = CaHCO3+	11.44	0.09	11.15	0.09	1.42E+11	1.28E+10	K28
NaCO3-	Na+ + CO3-2 = NaCO3-	1.27	0.30	1.13	0.30	1.35E+01	4.04E+00	K29
NaHCO3	Na+ + CO3-2 + H+ = NaHCO3	10.08	0.30	9.87	0.30	7.37E+09	2.21E+09	K30
FeCO3(aq)	Fe+2 + CO3-2 = FeCO3(aq)	4.38	1.31	4.10	1.31	1.25E+04	1.64E+04	K31
FeHCO3+	Fe+2 + CO3-2 + H+ = FeHCO3+	12.33	0.30	12.05	0.30	1.12E+12	3.35E+11	K32
Magnetite	3Fe+2 + 3H2O + 0.5O2(g) = Fe3O4 + 6H+	5.49	0.40	5.28	0.40	1.90E+05	7.59E+04	K33
Goethite	Fe+2 + 1.5H2O +0.25O2(g) = FeOOH + 2H+	8.75	0.40	8.68	0.40	4.78E+08	1.91E+08	K34
pO2(g)	4Fe3O4 + 6H2O + O2(g) =12FeOOH	83.08	1.60	83.08	1.60	1.20E+83	1.92E+83	K35
HSO4-	H+ + SO4-2 = HSO4-	1.98	0.25	1.84	0.25	6.90E+01	1.73E+01	K36
CaSO4(aq)	Ca+2 + SO4-2 = CaSO4	2.30	0.30	2.02	0.30	1.04E+02	3.12E+01	K38
NaSO4-	Na+ + SO4-2 = NaSO4-	0.70	0.30	0.56	0.30	3.62E+00	1.09E+00	K40
FeHSO4+	Fe+2 + SO4-2 + H+ = FeHSO4+	3.07	0.30	2.79	0.30	6.14E+02	1.84E+02	K41
FeSO4(aq)	Fe+2 + SO4-2 = FeSO4(aq)	2.25	0.05	1.97	0.05	9.28E+01	4.64E+00	K42
FeCl+	Fe2+ + Cl- = FeCl+	0.14	0.23	0.00	0.23	9.98E-01	2.29E-01	K45
Ca(H2PO4)+	Ca+2 + H2PO4- = Ca(H2PO4)+	1.41	0.30	1.27	0.30	1.86E+01	5.57E+00	**K47**
CaHPO4(aq)	Ca+2 + H2PO4- = H+ + Ca(HPO4)	-4.47	0.30	-4.61	0.30	2.45E-05	7.34E-06	**K48**
CaPO4-	Ca+2 + H2PO4- = 2H+ + CaPO4-	-13.10	0.30	-13.17	0.30	6.75E-14	2.02E-14	**K49**
PO4-3	H2PO4- = 2H+ + PO4-3	-19.56	0.03	-19.21	0.03	6.20E-20	1.86E-21	**K51**
HPO4-2	H2PO4- = H+ + HPO4-2	-7.21	0.02	-7.07	0.02	8.53E-08	1.71E-09	**K52**
H3PO4	H2PO4- + H+ = H3PO4	2.14	0.03	2.07	0.03	1.17E+02	3.52E+00	**K53**
Ca5(PO4)3OH(s	*5Ca+2 + 3H2PO4- + H2O = 7H+ + Ca5(PO4)3OH(s)*	*-14.35*	*0.04*	*-14.91*	*0.04*			

Free Ligands	(M)	
[CO3-2]	1.25E-07	IS Calcite
[SO4-2]	1.82E-07	-0.20
[Cl-]	4.94E-03	IS Ca5(PO4)3OH(s)
[Ca+2]	3.22E-02	8.56
[Na+]	4.60E-03	
[Fe+2]	1.20E-02	
[H2PO4-]	9.47E-07	

iterative calculation

Figure 4-26. Snapshot of the amended DON'T TOUCH sheet (VERSION B).

4.3.2 INPUT DATA sheet

The INPUT DATA sheet has been modified in two ways (Figure 4-27 and Figure 4-28). First, a cell has been added in the block "*GW composition*", where the user has to indicate groundwater phosphate concentration. Additionally, as already implemented for calcite ($CaCO_3$), if hydroxyapatite ($Ca_5(PO_4)_3(OH)$) solid phase becomes oversaturated, a warning alert will inform that this solid phase is oversaturated (Figure 4-27 and Figure 4-28).

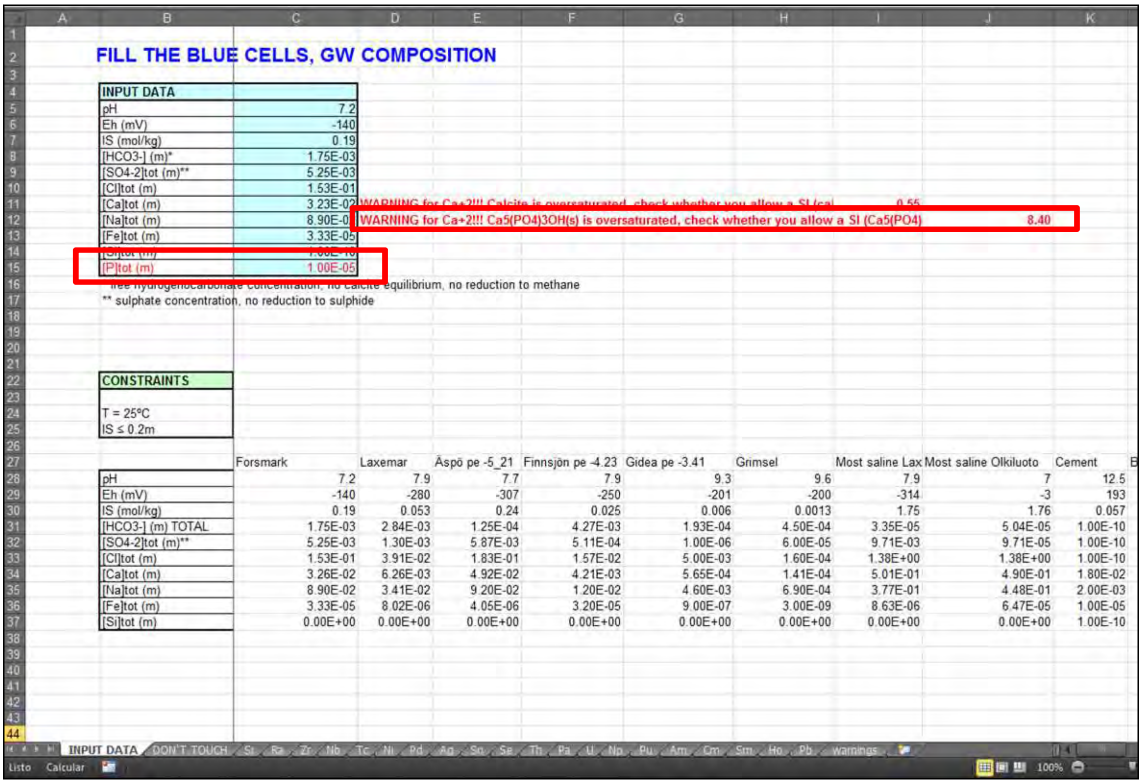

FILL THE BLUE CELLS, GW COMPOSITION

INPUT DATA	
pH	7.2
Eh (mV)	-140
IS (mol/kg)	0.19
[HCO3-] (m)*	1.75E-03
[SO4-2]tot (m)**	5.25E-03
[Cl]tot (m)	1.53E-01
[Ca]tot (m)	3.23E-02
[Na]tot (m)	8.90E-0
[Fe]tot (m)	3.33E-05
[Si]tot (m)	1.00E-10
[P]tot (m)	1.00E-05

WARNING for Ca+2!!! Calcite is oversaturated, check whether you allow a SI (ca 0.55

WARNING for Ca+2!!! Ca5(PO4)3OH(s) is oversaturated, check whether you allow a SI (Ca5(PO4) 8.40

* free hydrogenocarbonate concentration, no calcite equilibrium, no reduction to methane

** sulphate concentration, no reduction to sulphide

CONSTRAINTS

T = 25°C
IS ≤ 0.2m

	Forsmark	Laxemar	Äspö pe -5_21	Finnsjön pe -4.23	Gidea pe -3.41	Grimsel	Most saline Lax	Most saline Olkiluoto	Cement
pH	7.2	7.9	7.7	7.9	9.3	9.6	7.9	7	12.5
Eh (mV)	-140	-280	-307	-250	-201	-200	-314	-3	193
IS (mol/kg)	0.19	0.053	0.24	0.025	0.006	0.0013	1.75	1.76	0.057
[HCO3-] (m) TOTAL	1.75E-03	2.84E-03	1.25E-04	4.27E-03	1.93E-04	4.50E-04	3.35E-05	5.04E-05	1.00E-10
[SO4-2]tot (m)**	5.25E-03	1.30E-03	5.87E-03	5.11E-04	1.00E-06	6.00E-05	9.71E-03	9.71E-05	1.00E-10
[Cl]tot (m)	1.53E-01	3.91E-02	1.83E-01	1.57E-02	5.00E-03	1.60E-04	1.38E+00	1.38E+00	1.00E-10
[Ca]tot (m)	3.26E-02	6.26E-03	4.92E-02	4.21E-03	5.65E-04	1.41E-04	5.01E-01	4.90E-01	1.80E-02
[Na]tot (m)	8.90E-02	3.41E-02	9.20E-02	1.20E-02	4.60E-03	6.90E-04	3.77E-01	4.48E-01	2.00E-03
[Fe]tot (m)	3.33E-05	8.02E-06	4.05E-06	3.20E-05	9.00E-07	3.00E-09	8.63E-06	6.47E-05	1.00E-05
[Si]tot (m)	0.00E+00	0.00E+00	0.00E+00	0.00E+00	0.00E+00	0.00E+00	0.00E+00	0.00E+00	1.00E-10

Figure 4-27. Snapshot of the amended INPUT DATA sheet (VERSION A).

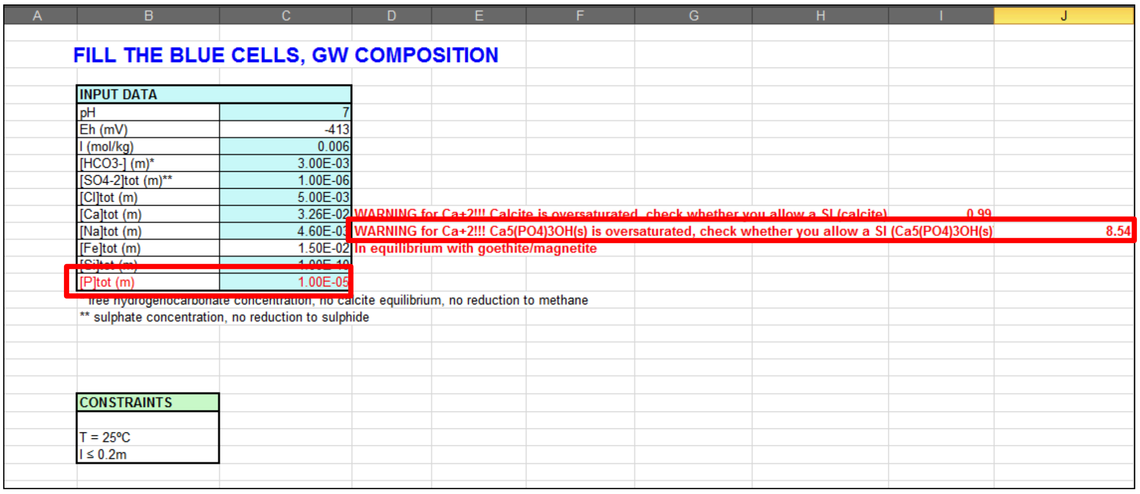

FILL THE BLUE CELLS, GW COMPOSITION

INPUT DATA	
pH	7
Eh (mV)	-413
I (mol/kg)	0.006
[HCO3-] (m)*	3.00E-03
[SO4-2]tot (m)**	1.00E-06
[Cl]tot (m)	5.00E-03
[Ca]tot (m)	3.26E-02
[Na]tot (m)	4.60E-03
[Fe]tot (m)	1.50E-02
[Si]tot (m)	1.00E-10
[P]tot (m)	1.00E-05

WARNING for Ca+2!!! Calcite is oversaturated, check whether you allow a SI (calcite) 0.99

WARNING for Ca+2!!! Ca5(PO4)3OH(s) is oversaturated, check whether you allow a SI (Ca5(PO4)3OH(s) 8.54

In equilibrium with goethite/magnetite

* free hydrogenocarbonate concentration, no calcite equilibrium, no reduction to methane

** sulphate concentration, no reduction to sulphide

CONSTRAINTS

T = 25°C
I ≤ 0.2m

Figure 4-28. Snapshot of the amended INPUT DATA sheet (VERSION B).

4.3.3 Radionuclides sheets

Thermodynamic data selected in section 4.2 of this report have been already implemented in both versions of the Simple Functions Spreadsheet tool. As an example, two radionuclide sheets (uranium and zirconium) are presented below.

Figure 4-29 shows the modified uranium data sheet, where six new uranium phosphates aqueous species have been added. Uncertainties have also been accordingly calculated (Grivé et al., 2010b).

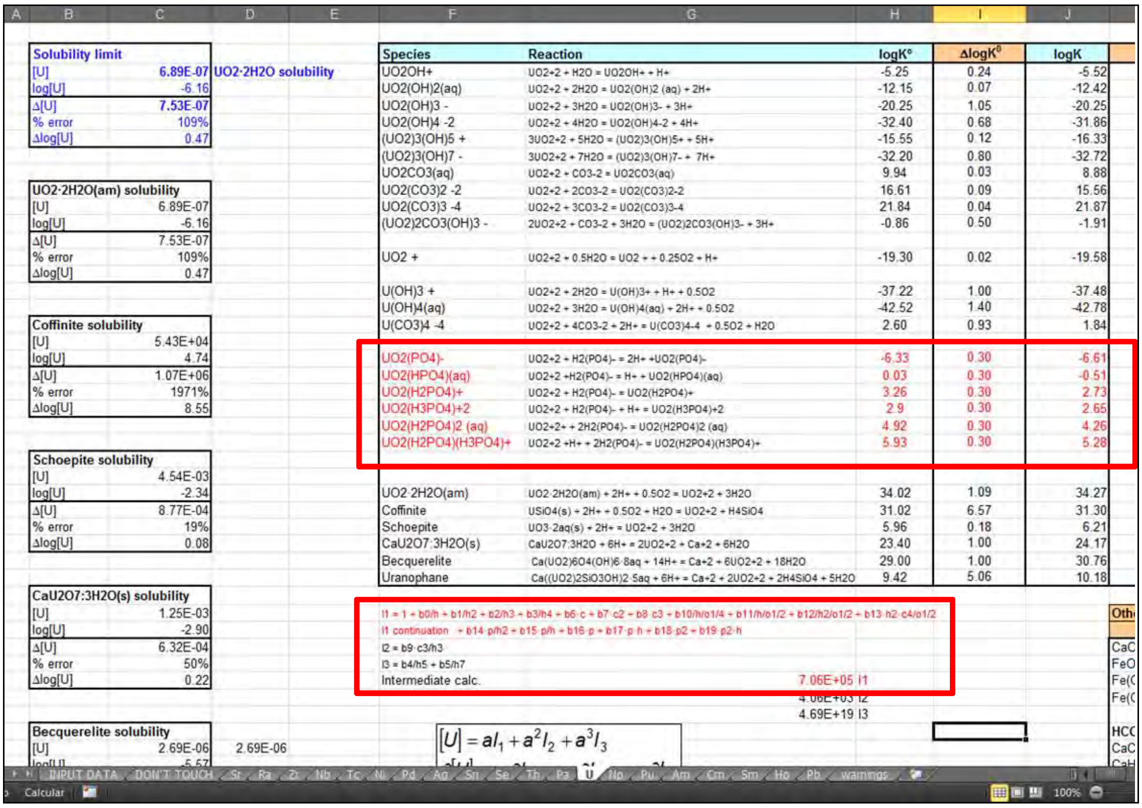

Solubility limit		
[U]	6.89E-07	UO2·2H2O solubility
log[U]	-6.16	
Δ[U]	7.53E-07	
% error	109%	
Δlog[U]	0.47	

UO2·2H2O(am) solubility	
[U]	6.89E-07
log[U]	-6.16
Δ[U]	7.53E-07
% error	109%
Δlog[U]	0.47

Coffinite solubility	
[U]	5.43E+04
log[U]	4.74
Δ[U]	1.07E+06
% error	1971%
Δlog[U]	8.55

Schoepite solubility	
[U]	4.54E-03
log[U]	-2.34
Δ[U]	8.77E-04
% error	19%
Δlog[U]	0.08

CaU2O7:3H2O(s) solubility	
[U]	1.25E-03
log[U]	-2.90
Δ[U]	6.32E-04
% error	50%
Δlog[U]	0.22

Becquerelite solubility		
[U]	2.69E-06	2.69E-06

Species	Reaction	logK°	ΔlogK⁰	logK
UO2OH+	UO2+2 + H2O = UO2OH+ + H+	-5.25	0.24	-5.52
UO2(OH)2(aq)	UO2+2 + 2H2O = UO2(OH)2 (aq) + 2H+	-12.15	0.07	-12.42
UO2(OH)3 -	UO2+2 + 3H2O = UO2(OH)3- + 3H+	-20.25	1.05	-20.25
UO2(OH)4 -2	UO2+2 + 4H2O = UO2(OH)4-2 + 4H+	-32.40	0.68	-31.86
(UO2)3(OH)5 +	3UO2+2 + 5H2O = (UO2)3(OH)5+ + 5H+	-15.55	0.12	-16.33
(UO2)3(OH)7 -	3UO2+2 + 7H2O = (UO2)3(OH)7- + 7H+	-32.20	0.80	-32.72
UO2CO3(aq)	UO2+2 + CO3-2 = UO2CO3(aq)	9.94	0.03	8.88
UO2(CO3)2 -2	UO2+2 + 2CO3-2 = UO2(CO3)2-2	16.61	0.09	15.56
UO2(CO3)3 -4	UO2+2 + 3CO3-2 = UO2(CO3)3-4	21.84	0.04	21.87
(UO2)2CO3(OH)3 -	2UO2+2 + CO3-2 + 3H2O = (UO2)2CO3(OH)3- + 3H+	-0.86	0.50	-1.91
UO2 +	UO2+2 + 0.5H2O = UO2 + + 0.25O2 + H+	-19.30	0.02	-19.58
U(OH)3 +	UO2+2 + 2H2O = U(OH)3+ + H+ + 0.5O2	-37.22	1.00	-37.48
U(OH)4(aq)	UO2+2 + 3H2O = U(OH)4(aq) + 2H+ + 0.5O2	-42.52	1.40	-42.78
U(CO3)4 -4	UO2+2 + 4CO3-2 + 2H+ = U(CO3)4-4 + 0.5O2 + H2O	2.60	0.93	1.84
UO2(PO4)-	UO2+2 + H2(PO4)- = 2H+ +UO2(PO4)-	-6.33	0.30	-6.61
UO2(HPO4)(aq)	UO2+2 +H2(PO4)- = H+ + UO2(HPO4)(aq)	0.03	0.30	-0.51
UO2(H2PO4)+	UO2+2 + H2(PO4)- = UO2(H2PO4)+	3.26	0.30	2.73
UO2(H3PO4)+2	UO2+2 + H2(PO4)- + H+ = UO2(H3PO4)+2	2.9	0.30	2.65
UO2(H2PO4)2 (aq)	UO2+2+ + 2H2(PO4)- = UO2(H2PO4)2 (aq)	4.92	0.30	4.26
UO2(H2PO4)(H3PO4)+	UO2+2 +H+ + 2H2(PO4)- = UO2(H2PO4)(H3PO4)+	5.93	0.30	5.28
UO2·2H2O(am)	UO2·2H2O(am) + 2H+ + 0.5O2 = UO2+2 + 3H2O	34.02	1.09	34.27
Coffinite	USiO4(s) + 2H+ + 0.5O2 + H2O = UO2+2 + H4SiO4	31.02	6.57	31.30
Schoepite	UO3·2aq(s) + 2H+ = UO2+2 + 3H2O	5.96	0.18	6.21
CaU2O7:3H2O(s)	CaU2O7:3H2O + 6H+ = 2UO2+2 + Ca+2 + 6H2O	23.40	1.00	24.17
Becquerelite	Ca(UO2)6O4(OH)6·8aq + 14H+ = Ca+2 + 6UO2+2 + 18H2O	29.00	1.00	30.76
Uranophane	Ca((UO2)2SiO3OH)2·5aq + 6H+ = Ca+2 + 2UO2+2 + 2H4SiO4 + 5H2O	9.42	5.06	10.18

I1 = 1 + b0/h + b1/h2 + b2/h3 + b3/h4 + b6·c + b7·c2 + b8·c3 + b10/h/o1/4 + b11/h/o1/2 + b12/h2/o1/2 + b13·h2·c4/o1/2
I1 continuation + b14·p/h2 + b15·p/h + b16·p + b17·p·h + b18·p2 + b19·p2·h
I2 = b9·c3/h3
I3 = b4/h5 + b5/h7
Intermediate calc. 7.06E+05 I1
4.06E+03 I2
4.69E+19 I3

$$[U] = aI_1 + a^2I_2 + a^3I_3$$

Figure 4-29. Snapshot of the amended uranium data sheet.

Figure 4-30 shows the modified zirconium data sheet including the two solid phases selected in this work. Additionally, the two new boxes on the left side of Figure 4-30 that accounts for the calculation of Zr phosphates solubility limits are shown.

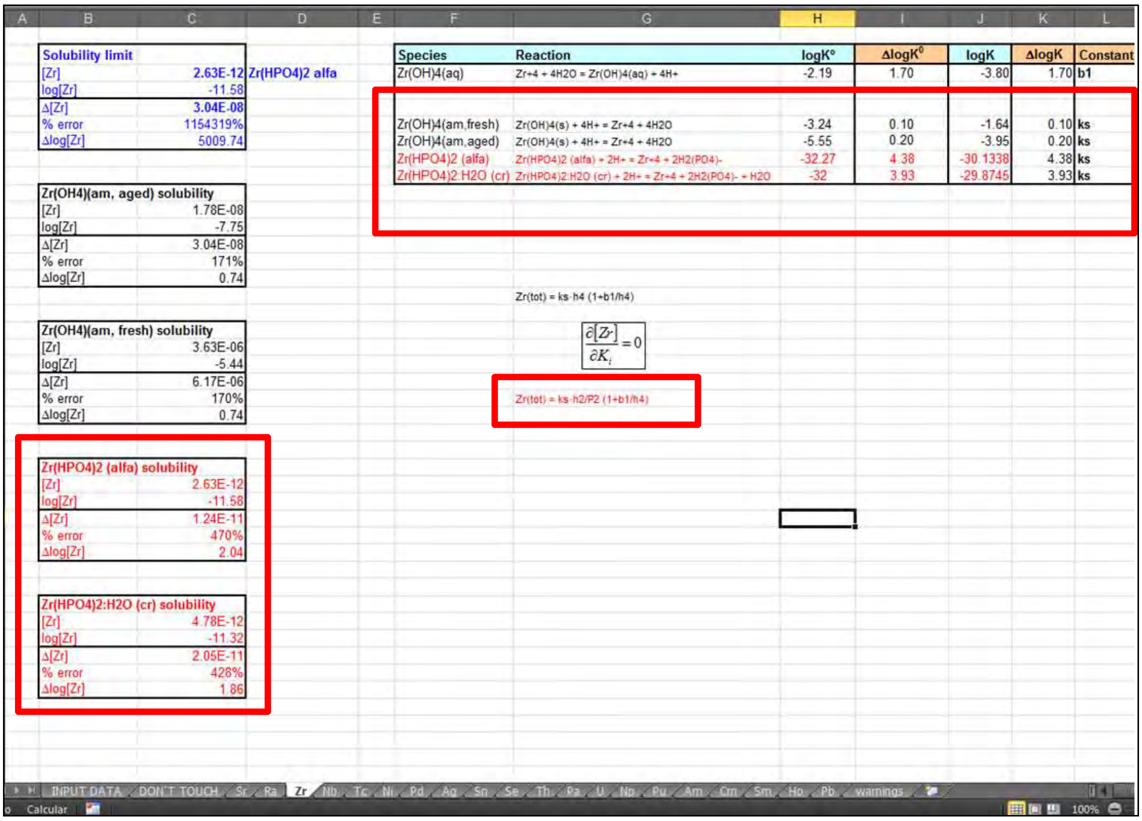

Solubility limit		
[Zr]	2.63E-12	Zr(HPO4)2 alfa
log[Zr]	-11.58	
Δ[Zr]	3.04E-08	
% error	1154319%	
Δlog[Zr]	5009.74	

Zr(OH4)(am, aged) solubility	
[Zr]	1.78E-08
log[Zr]	-7.75
Δ[Zr]	3.04E-08
% error	171%
Δlog[Zr]	0.74

Zr(OH4)(am, fresh) solubility	
[Zr]	3.63E-06
log[Zr]	-5.44
Δ[Zr]	6.17E-06
% error	170%
Δlog[Zr]	0.74

Zr(HPO4)2 (alfa) solubility	
[Zr]	2.63E-12
log[Zr]	-11.58
Δ[Zr]	1.24E-11
% error	470%
Δlog[Zr]	2.04

Zr(HPO4)2:H2O (cr) solubility	
[Zr]	4.78E-12
log[Zr]	-11.32
Δ[Zr]	2.05E-11
% error	428%
Δlog[Zr]	1.86

Species	Reaction	logK°	ΔlogK⁰	logK	ΔlogK	Constant
Zr(OH)4(aq)	Zr+4 + 4H2O = Zr(OH)4(aq) + 4H+	-2.19	1.70	-3.80	1.70	b1
Zr(OH)4(am,fresh)	Zr(OH)4(s) + 4H+ = Zr+4 + 4H2O	-3.24	0.10	-1.64	0.10	ks
Zr(OH)4(am,aged)	Zr(OH)4(s) + 4H+ = Zr+4 + 4H2O	-5.55	0.20	-3.95	0.20	ks
Zr(HPO4)2 (alfa)	Zr(HPO4)2 (alfa) + 2H+ = Zr+4 + 2H2(PO4)-	-32.27	4.38	-30.1338	4.38	ks
Zr(HPO4)2:H2O (cr)	Zr(HPO4)2:H2O (cr) + 2H+ = Zr+4 + 2H2(PO4)- + H2O	-32	3.93	-29.8745	3.93	ks

Zr(tot) = ks·h4 (1+b1/h4)

$$\boxed{\frac{\partial[Zr]}{\partial K_i}=0}$$

Zr(tot) = ks·h2/P2 (1+b1/h4)

Figure 4-30. Snapshot of the amended zirconium datasheet.

4.3.4 Simple Functions Spreadsheet Validation

In order to verify the implementation of the modifications in the Simple Functions Spreadsheet tool, solubility limits as well as Saturation Index calculated with the tool have been compared with results obtained for the same calculations performed with the geochemical code PhreeqC (Parkhurst and Appelo, 2013). Results of the comparison are shown in Figure 4-31, Figure 4-32, Figure 4-33, and Figure 4-34. The good agreement between the results obtained using the Simple Functions spreadsheet tool and the more sophisticated PhreeqC code is remarkable.

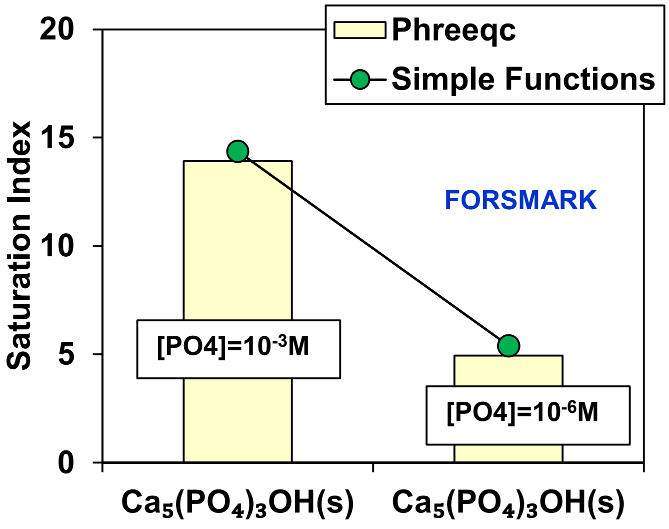

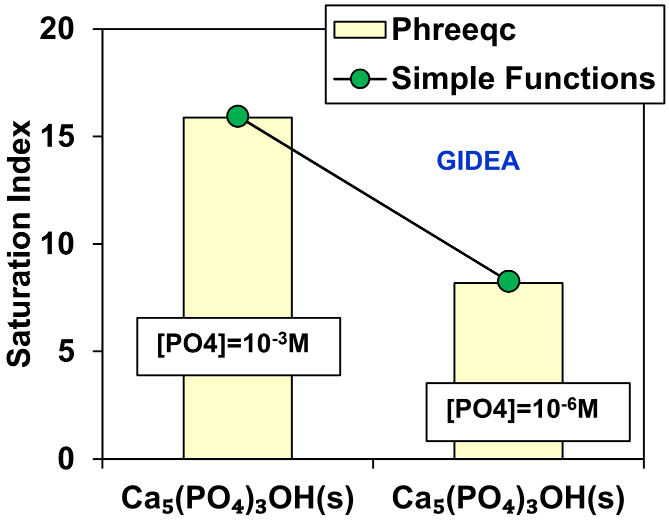

Figure 4-31. Comparison between hydroxyapatite ($Ca_5(PO_4)_3(OH)$) Saturation Index calculated with the Simple Functions (green dots) and PhreeqC (yellow bar) at two different phosphate aqueous concentrations (10^{-3} and 10^{-6}M) for Forsmark (left) and Gideå (right) conditions.

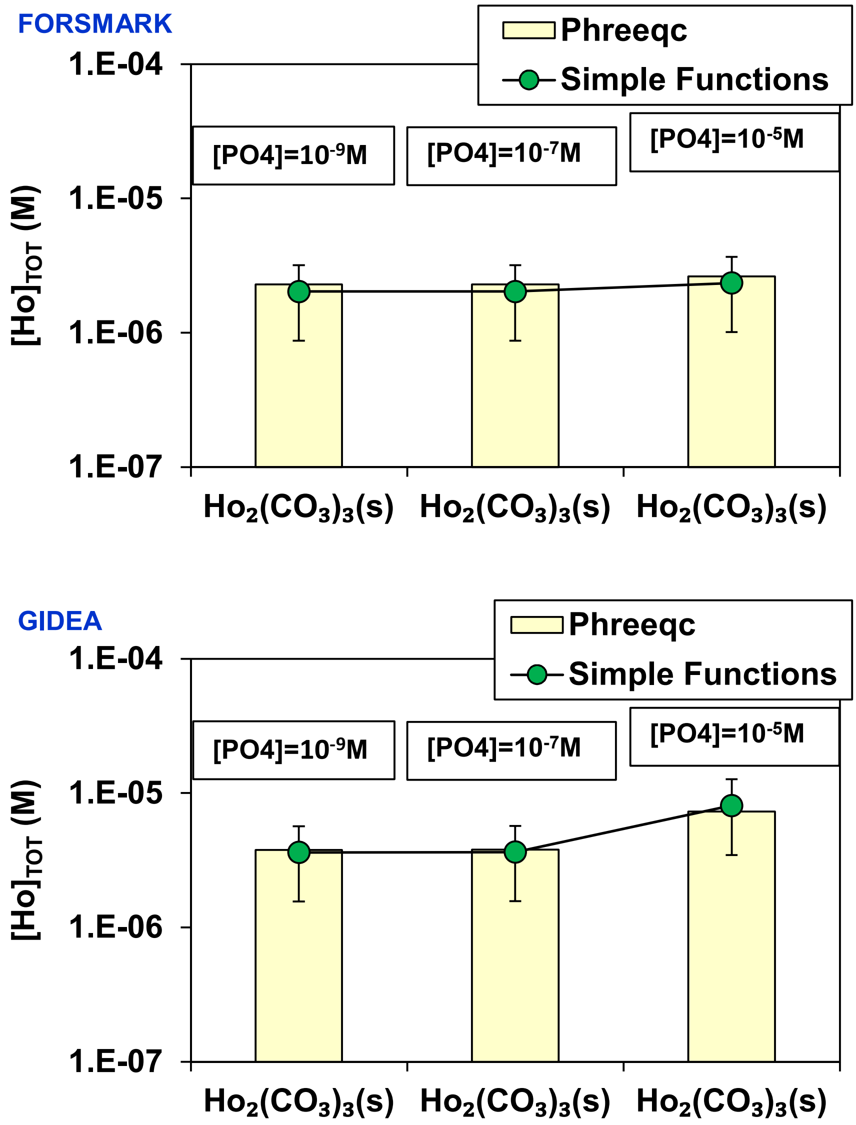

Figure 4-32. Comparison between $Ho_2(CO_3)(c)$ solubility limits calculated with the Simple Functions (green dots) and PhreeqC (yellow bar) at different phosphate aqueous concentrations (ranging from 0 to 10^{-3} M) for Forsmark (up) and Gideå (bottom) conditions.

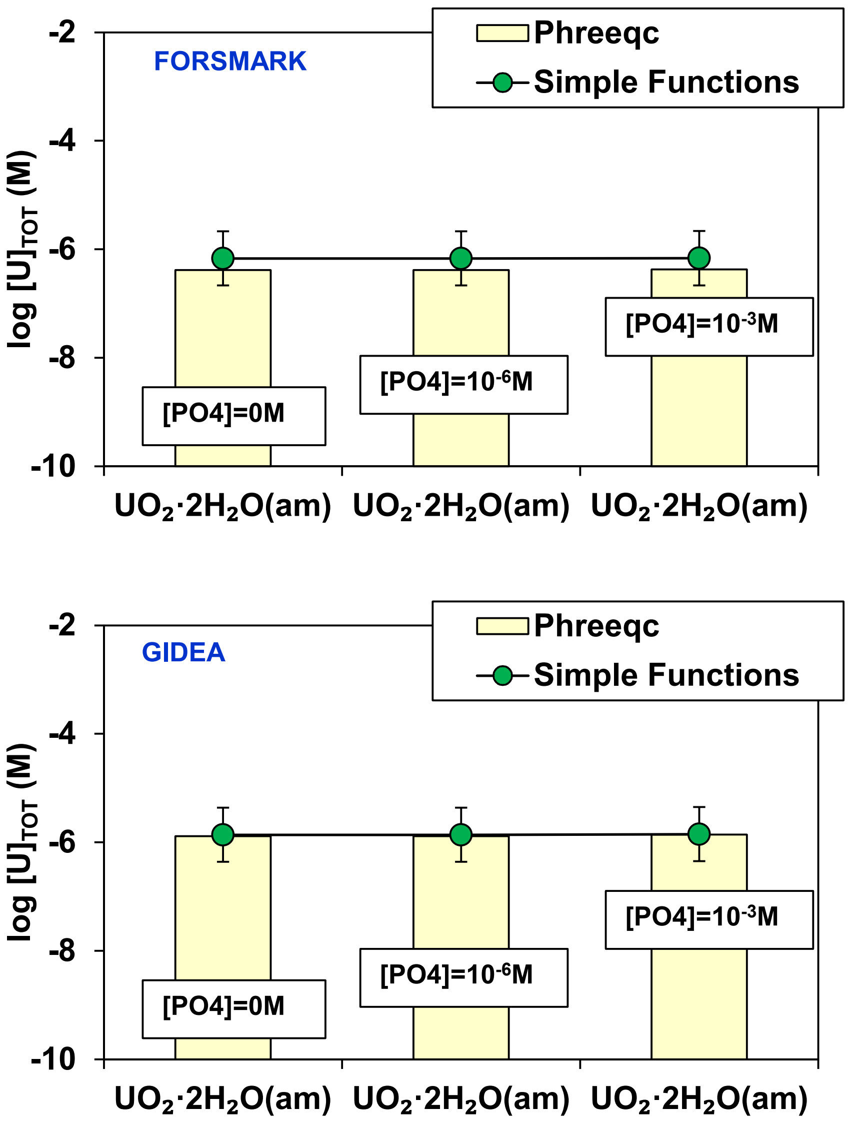

Figure 4-33. Comparison between $UO_2 \cdot 2H_2O$(am) solubility limits calculated with the Simple Functions (green dots) and PhreeqC (yellow bar) at different phosphate aqueous concentrations (ranging from 0 to 10^{-3} M) for Forsmark (up) and Gideå (bottom) conditions.

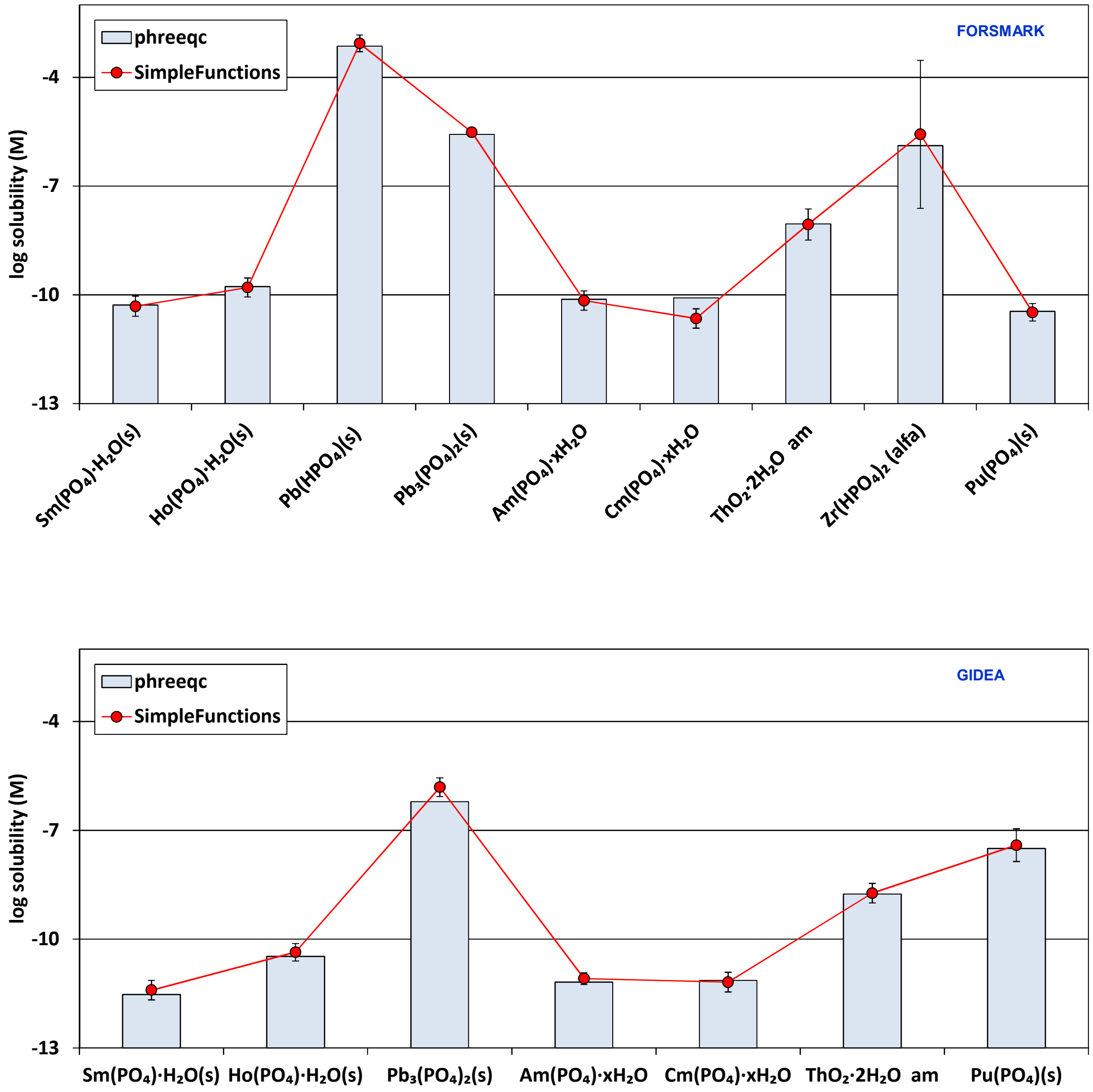

Figure 4-34. Comparison between $Sm(PO_4)\cdot H_2O(s)$, $Ho(PO_4)\cdot H_2O(s)$, $Pb(HPO_4)(s)$, $Pb_3PO_4(s)$, $Am(PO_4)\cdot xH_2O$, $Cm(PO_4)\cdot xH_2O$, $ThO_2\cdot 2H_2O(am)$, $Zr(HPO_4)_2(alfa)$ and $Pu(PO_4)(s)$ solubility limits calculated with the Simple Functions (red dots) and PhreeqC (blue bar) at different phosphate aqueous concentrations (ranging from 0 to 10^{-3} M) for Forsmark (up) and Gideå (bottom) conditions. Note that for Gideå groundwater conditions (see Appendix I), the solid phases $Pb(HPO_4)(s)$ and $Zr(HPO_4)_2(alfa)$ have not been included in the plot. This is because they cannot exert a solubility control over Pb and Zr aqueous concentrations under these conditions.

4.4 Phosphates effect over radionuclide solubility limits

From the information presented in the previous sections, it can be concluded that phosphates aqueous complexation will affect only slightly most of the radionuclide aqueous chemistry. Nevertheless, it has been shown that phosphate bearing phases could exert a solubility control over some radionuclides, namely the trivalent lanthanides and actinides under certain conditions (i.e. $[P]_{TOT}>10^{-5}$M, near-neutral pH). Figure 4-35 shows the solubility of An-Ln(III) phosphate bearing phases as a function of phosphate aqueous concentration. As expected, it is observed that phosphate bearing phases can exert radionuclide solubility control even at very low phosphate aqueous concentration. Therefore the consideration of phosphates in solubility limit calculations, from a PA perspective, will lead to a non-conservative scenario (i.e. lower solubilities).

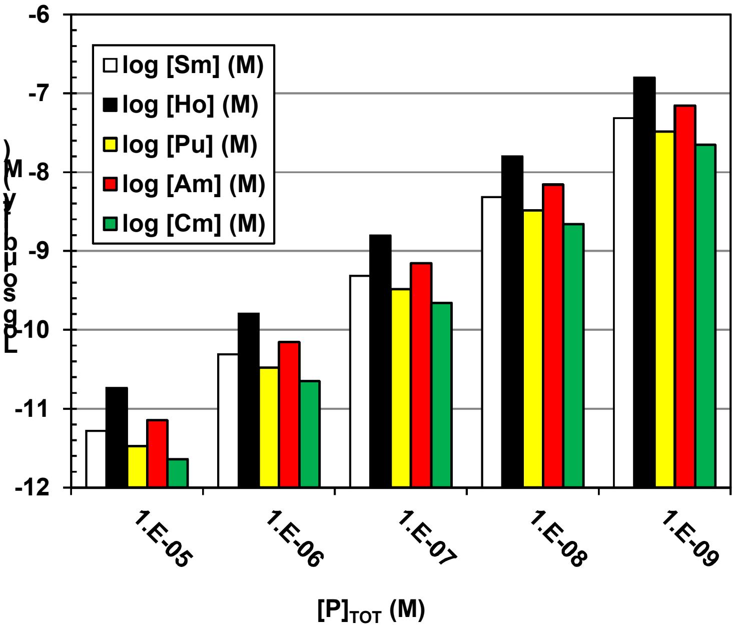

Figure 4-35. Solubility of An-Ln(III) phosphates ($SmPO_4·H_2O$, $HoPO_4·H_2O$, $PuPO_4$, $AmPO_4·xH_2O$, $CmPO_4·xH_2O$) as a function of phosphate aqueous concentration in Forsmark conditions.

On the other hand, Figure 4-36 shows the solubility of three different carbonate bearing phases of Ho, Am, and Cm as a function of phosphate aqueous concentration. The results presented in this figure illustrate that radionuclide-phosphate complexation appears to be not very relevant at phosphate concentrations higher than 10^{-5} M, which is the maximum expected phosphate aqueous concentration in natural groundwaters (see section 4.1). Therefore, it can be concluded that in the range of phosphate aqueous concentrations expected in natural groundwaters, phosphates will not affect the aqueous chemistry of the radionuclides studied in the present work to a significant extent.

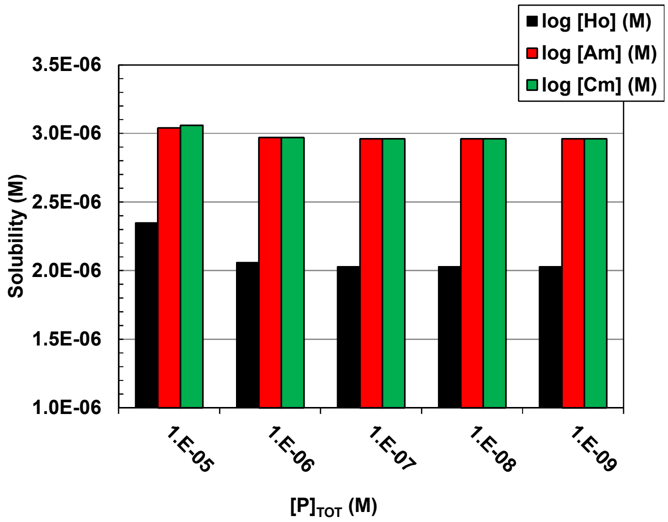

Figure 4-36. Solubility of $Ho_2(CO_3)_3$(s), $Am_2(CO_3)_3$(s), and $Cm_2(CO_3)_3$(s) as a function of phosphate aqueous concentration for Forsmark conditions.

5. Task 2: Influence of temperature on radionuclide solubility limits

5.1 Approaches to deal with temperature corrections

The evaluation of equations classically used to account for temperature variations in thermodynamic databases (r. 1 and r. 2) require the knowledge of the temperature dependence of heat capacities (C_p^o).

$$G^\circ_{T,P} - G^\circ_{T_r,P_r} = -S^\circ_{T_r,P_r}(T - T_r) + \int_{T_r}^{T} C^\circ_{P_r}\, dT - \int_{T_r}^{T} C^\circ_{P_r}\, d\ln T + \int_{P_r}^{P} V^\circ\, dP \qquad \text{r. 1}$$

$$K_{T,P} = e^{-\Delta G^\circ_r/RT} \qquad \text{r. 2}$$

In the absence of experimental information on the temperature and/or pressure dependence of the standard heat capacities (C_p^o) and volumes (V^o), and when changes in temperature (few tens of degrees Celsius) and pressure are not very important, the Van´t Hoff equation (r. 3) may be used to calculate equilibrium constants (log *K*) as a function of the temperature. In this approximation, it is assumed that the standard molar enthalpy of reaction does not vary with temperature.

$$\ln K_T = \ln K_{T_r} - \frac{\Delta H^\circ_r}{R}\left(\frac{1}{T} - \frac{1}{T_r}\right) \qquad \text{r. 3}$$

The performance of the Van´t Hoff equation over the temperature range of interest for this work (see below) can be evaluated by making comparisons between log *K* values computed using the Van´t Hoff approximation for reactions involving solid and aqueous species of major elements and radionuclides (including redox reactions), and either

- ✓ log *K* values estimated using the constant heat capacity approximation,
- ✓ or log *K* values calculated by taking into account the temperature dependence of heat capacities.

This information, although typically scarce, can be used as a direct evaluation of the validity of the Van´t Hoff equation to correctly explanation of solubility measurements reported in the literature for radionuclide-bearing solids using equilibrium constants generated with the Van´t Hoff equation.

In the present work, the stability constants already implemented in the Simple Functions Spreadsheet tool at 25ºC have been corrected by using the Van't Hoff equation to 0, 15, 40, 70, and 90ºC, which are the temperatures of interest for SKB (see Duro et al., 2006b for further information). The use of the Van't Hoff equation outside of this temperature range is not recommended given the freezing and the evaporation processes of water.

The necessary ΔH_f^o data have been obtained from the latest release of the SKB database (Grivé et al., 2008; Duro et al., 2006a). For a detailed description of the used enthalpy data and their corresponding references the reader is referred to Appendix II of this report.

5.2 Solubility limits variation with temperature

5.2.1 Geochemical conditions of the study

As mentioned above, a temperature range from 0 to 90ºC has been used in the present study. Additionally, the following constraints have been imposed in the calculations:

- Two pHs, 7 and 11, have been used;
- For redox sensitive radionuclide calculations, magnetite/goethite equilibrium has been assumed;
- Ca concentration is given by calcite equilibrium, while free carbonate has been varied between 10^{-2} and 10^{-4} M;
- Sulphate concentrations are those from Forsmark (see Appendix I);
- Neither sulphide nor phosphate have been considered in the calculations; and
- The potential competition/interaction between radionuclides has not been accounted for.

5.2.2 Radium

As reported in Grivé et al. (2010b), radium sulphate ($RaSO_4$) is the expected solubility limiting phase for this radionuclide under Forsmark groundwater conditions. The evolution of $RaSO_4$(cr) solubility with temperature is presented in Figure 5-1 at two different pH values (7 and 11) and at two different carbonate concentrations in equilibrium with calcite.

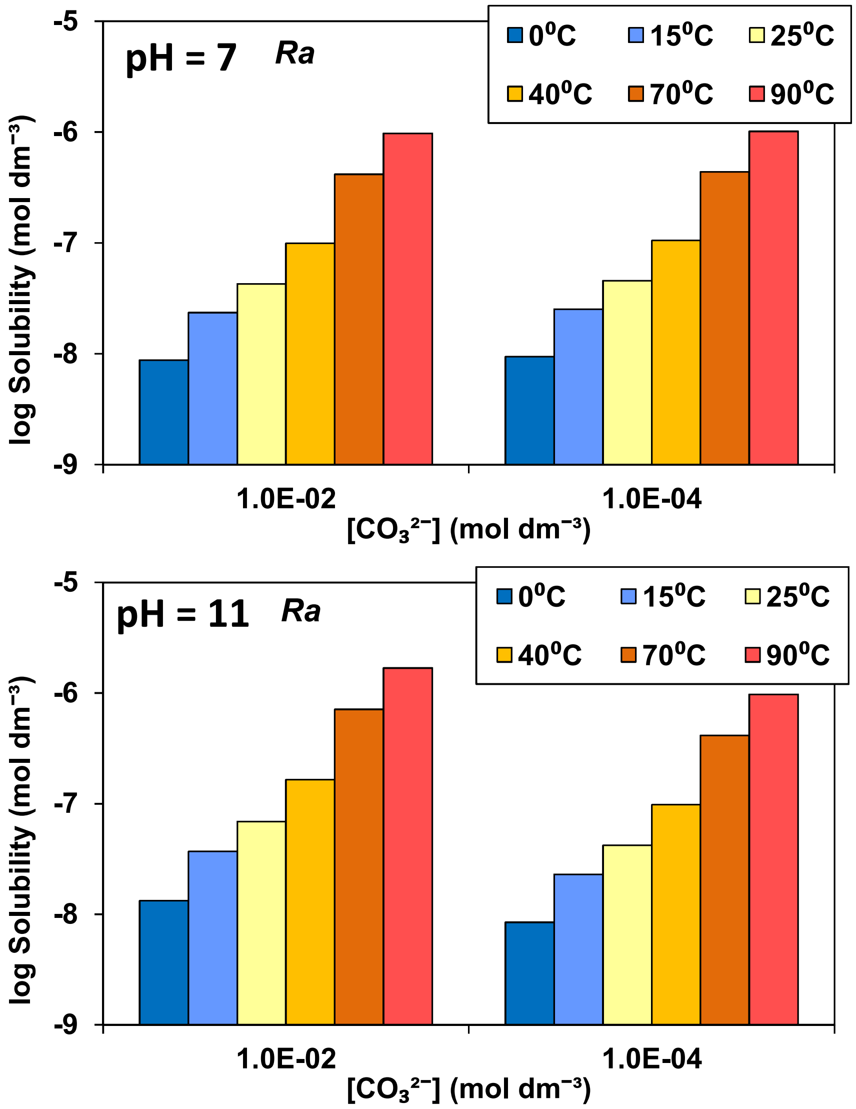

Figure 5-1. $RaSO_4$(cr) solubility evolution with temperature at two different pHs and two different concentrations of total carbonate. Ca concentration controlled through calcite equilibrium.

It can be observed in Figure 5-1 that, under the geochemical conditions of the present study, $RaSO_4$(cr) solubility is slightly affected (less than one order of magnitude of difference) by both pH and carbonate concentration changes. It is also shown that the increase of temperature from 0 to 90ºC produces a solubility increase of about two orders of magnitude. This observation is in agreement with Grivé et al. (2010b) results, which concluded that calculations at 25ºC might differ up to 2 log units from the expected solubilities in the studied range. It should be mentioned that for this radionuclide, the complete set of enthalpy values for both the aqueous and the solids was available.

In all cases, $RaSO_4$(aq) species controlled the aqueous speciation of this radionuclide, being $RaCO_3$(aq) only relevant at the highest carbonate aqueous concentration and at pH 11.

5.2.3 Nickel

Under the geochemical conditions studied in the present work, nickel hydroxide ($Ni(OH)_2$(s)) is the expected solubility limiting phase for Ni.

The evolution of $Ni(OH)_2$(s) solubility with temperature is presented in Figure 5-2 at two different pH values, 7 and 11, and at two different carbonate concentrations.

As can be observed in Figure 5-2, $Ni(OH)_2$(s) solubility is not influenced by the amount of carbonate in the system. On the other hand, Figure 5-2 also shows the important role that pH exerts over the solubility of this solid phase: higher pH values decrease the $Ni(OH)_2$(s) solubility.

The effects of temperature changes on the solubility of this radionuclide vary with pH due to the different chemical speciation of Ni. At near neutral pH (pH~7), Ni^{2+} governs the aqueous chemistry of this radionuclide in the whole range of temperatures studied. As reported in Grivé et al. (2010b), the main reaction in the system would be then $Ni(OH)_2(s) + 2H^+ = Ni^{2+} + 2H_2O$, which presents an exothermic character that produces the decrease of $Ni(OH)_2$(s) solubility with temperature. At higher pH (pH~11), the chemical speciation of Ni is controlled by $Ni(OH)_2$(aq) and $Ni(OH)_3^-$ species. The endothermic character of those species reactions produces the slight increase observed in $Ni(OH)_2$(s) solubility with temperature (Figure 5-2). It is noted that, as in the case of Ra, the complete set of enthalpy values for both the aqueous species and the solid phases was available for this radionuclide.

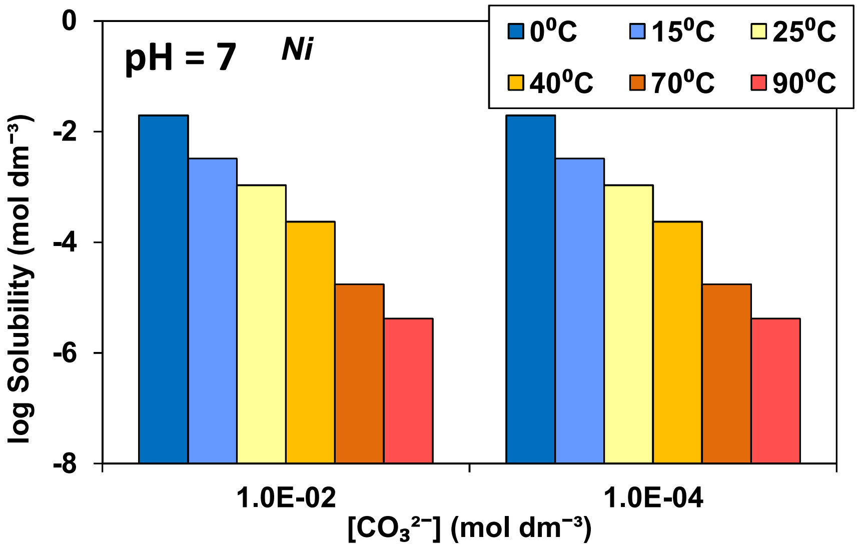

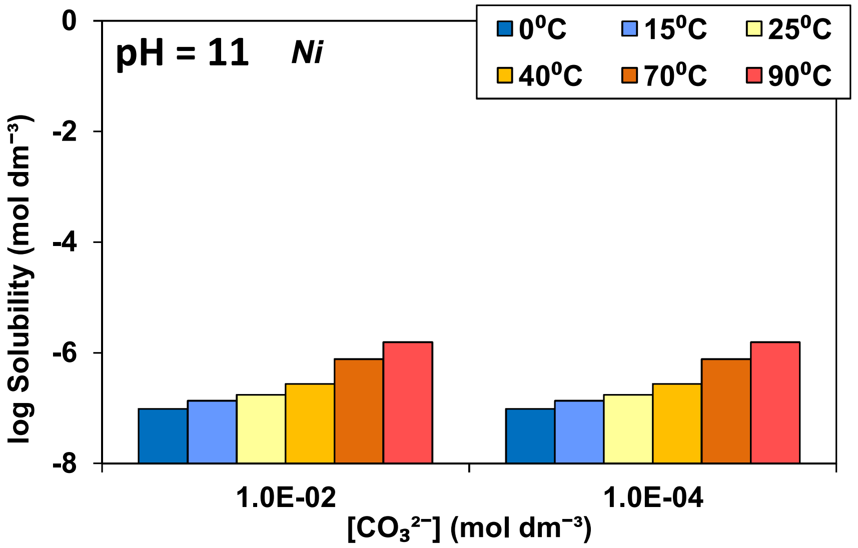

Figure 5-2. $Ni(OH)_2$(s) solubility evolution with temperature at two different pHs and two different concentrations of carbonate. Ca controlled through calcite equilibrium.

5.2.4 Selenium

Selenium, is a redox sensitive radionuclide that will be highly affected by both the Eh and the Fe concentration of the system, as well as temperature.

Under the geochemical conditions of the present work, $FeSe_2$(s) is the expected solubility limiting phase for this radionuclide. The evolution of $FeSe_2$(s) solubility with temperature is shown in Figure 5-3 at pH 7 and 11. The redox conditions of the system, as well as the iron aqueous concentration, are controlled through goethite/magnetite equilibrium. In turn, this produces a reducing environment that favours the formation of this solid phase in front of, for example, Se(s).

As can be seen in Figure 5-3, the solubility of $FeSe_2(s)$ is highly dependent on the system conditions. At pH=7, the goethite/magnetite equilibrium produces Eh and aqueous iron concentrations around -410 mV and 10^{-3} M, respectively; while at pH=11 the values are of -650 mV and 10^{-8} M. In all cases, the main Se aqueous species is HSe^-, independently of both the pH and Eh of the system (within the studied range). Based on the main reaction of the system ($FeSe_2(s) + 2H^+ + 2e^- = 2HSe^- + Fe^{2+}$), it can be concluded that the solubility increase observed from pH 7 to 11 is produced by the increase in pH: the higher the pH, the higher the solubility. A higher increase of solubility with temperature is observed for pH=11 compared with the results at pH=7. This is probably related to the different aqueous iron concentration fixed by the goethite/magnetite equilibrium in each case.

The increase of solubility with temperature is related with the fact that the main reaction ($FeSe_2(s) + 2H^+ + 2e^- = 2HSe^- + Fe^{2+}$) in the system is endothermic.

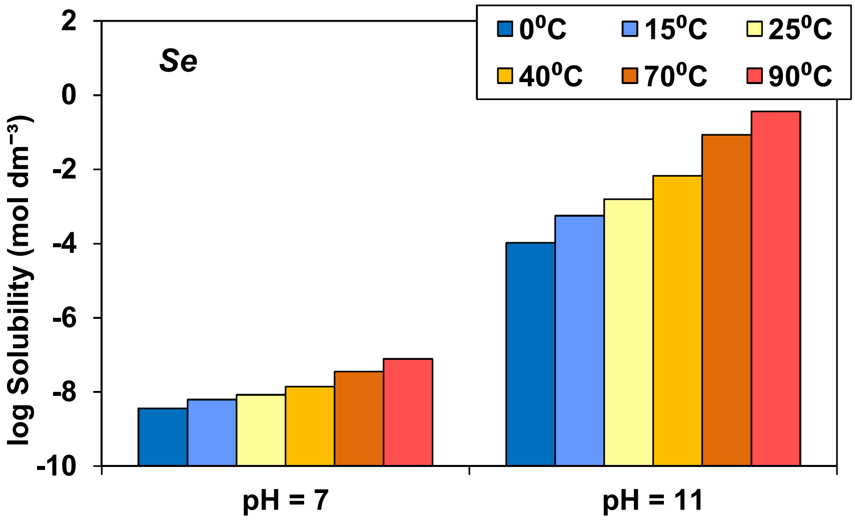

Figure 5-3. $FeSe_2(s)$ solubility evolution with temperature at two different pHs values, 7 and 11. Ca controlled through calcite equilibrium; Goethite/Magnetite equilibrium controls both Fe and Eh of the system.

5.2.5 Lanthanides (Sm and Ho)

Carbonate bearing phases, $SmOHCO_3$(s) and $Ho_2(CO_3)_3$(s), are the expected solubility limiting phases of Sm and Ho under the geochemical conditions studied here.

The solubility of both solids is shown in Figure 5-4 as a function of temperature and carbonate aqueous concentration at two different pHs. As can be observed, the trends of both solid phases are nearly equal. pH and aqueous carbonate variations slightly affect the solubility of those solid phases in the studied temperature range. On the other hand, the increase of temperature produces an increase in the solubility of both solid phases.

In the case of Sm, at neutral pH and temperatures below 25ºC, $SmCO_3^+$ and $Sm(CO_3)_2^-$ control the aqueous chemistry of this radionuclide with a small contribution by $SmSO_4^+$. When increasing the temperature above 25ºC $SmSO_4^+$ is negligible being $SmCO_3^+$ the most relevant Sm aqueous species. It should be considered here that there are no enthalpy data available for $SmCO_3^+$, $Sm(CO_3)_2^-$ and the solid phase $SmOHCO_3$(s) (data available only for $SmSO_4^+$). It is thus clear that the change in Sm speciation justifies the increases observed with increasing temperature. At low temperatures, the presence of $SmSO_4^+$ in the results justifies the slight increase of solubility from 0 to 25ºC. On the other hand, the inexistency of enthalpy data for Sm aqueous carbonates explains the increases observed in the solubility. At pH=11, the reasoning behind Sm behaviour is nearly the same, the sole difference being that instead of $SmSO_4^+$, the hydrolysed species $Sm(OH)_3$(aq) appears to be relatively more relevant at low temperatures.

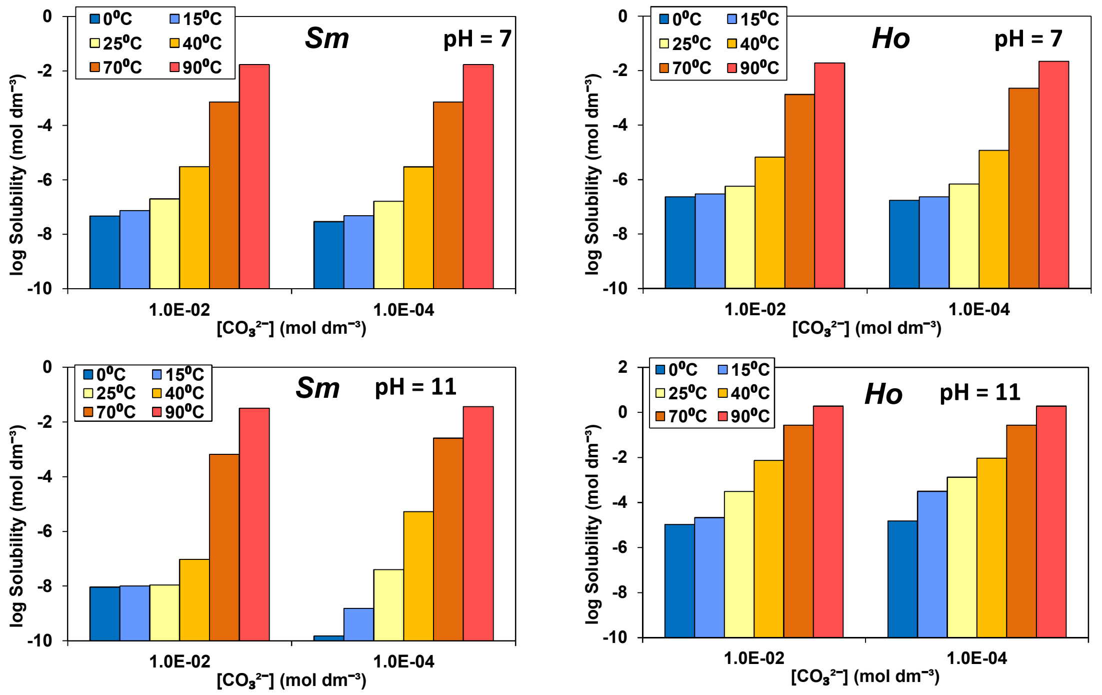

Figure 5-4. $SmOHCO_3$(s) (left plots) and $Ho_2(CO_3)_3$(s) (right plots) solubility evolution with temperature at two different pHs and two different concentrations of carbonate. Ca concentration controlled through calcite equilibrium.

It must be pointed out that, as for Sm, Ho aqueous carbonate species enthalpy data are not available. In addition, solid phase enthalpy is also not available. Only data for $HoSO_4^+$ have been considered in the calculations. Therefore, Ho aqueous chemistry behaves equal to Sm and so does their trends in solubility, as expected.

As a final remark, it is worth mentioning that the increase of $SmOHCO_3$(s) and $Ho_2(CO_3)_3$(s) solubility with temperature should be considered with caution given the scarcity of data for those solid phases. In addition, it is expected a transformation of the solid when increasing the temperature, which would favour a more crystalline phase, so that the calculated solubilities at higher T would presumably decrease. Giffaut and co-workers (Giffaut, 1994; Vercouter et al., 2005) studied Am(III)-carbonate systems with temperature and identified solid phase transformations when increasing the temperature, with a consequent decrease of the solubility.

At higher temperatures crystalline phases would prevail over amorphous phases and thus the expected radionuclide solubilities will be presumably lower than those calculated in Figure 5-4.

5.2.6 Actinides (U, Np, Pu, Am and Cm)

5.2.6.1 Uranium

Under the redox reducing conditions studied in the present work (i.e. goethite/magnetite equilibrium) uranium is mainly present as U(IV), and UO_2(am,hyd) is the solid phase expected to exert a solubility control over this radionuclide. The evolution of UO_2(am,hyd) solubility as a function of temperature is shown in Figure 5-5. As can be seen, under the geochemical conditions considered in the present study, neither the pH nor the carbonate concentration affect the solubility of UO_2(am,hyd) to a significant extent. However, temperature changes in the range 0-90ºC may produce solubility variations of more than 5 log units. It is worth to mention that under the whole set of studied conditions, $U(OH)_4$(aq) is the main uranium aqueous species formed. Regarding the availability of enthalpy data, there are enthalpy data available for the formation of $U(OH)_4$(aq), but not for the selected solid phase.

Thus, the important increase of UO_2(am,hyd) solubility as temperature increases should be considered with caution given the scarcity of data for the studied solid phase. In fact, as reported by Goodwin (1982), UO_2(am,hyd) solubility is only slightly dependent on temperature at reducing and near neutral conditions (~0.5 log units). Experimental data at higher temperatures than 25ºC (Parks and Pohl, 1988; Rai et al., 2003) have shown almost no increase in solubility with temperature. Thus, the results obtained for uranium are a clear example of erroneous solubility predictions due to the incompleteness of the used dataset.

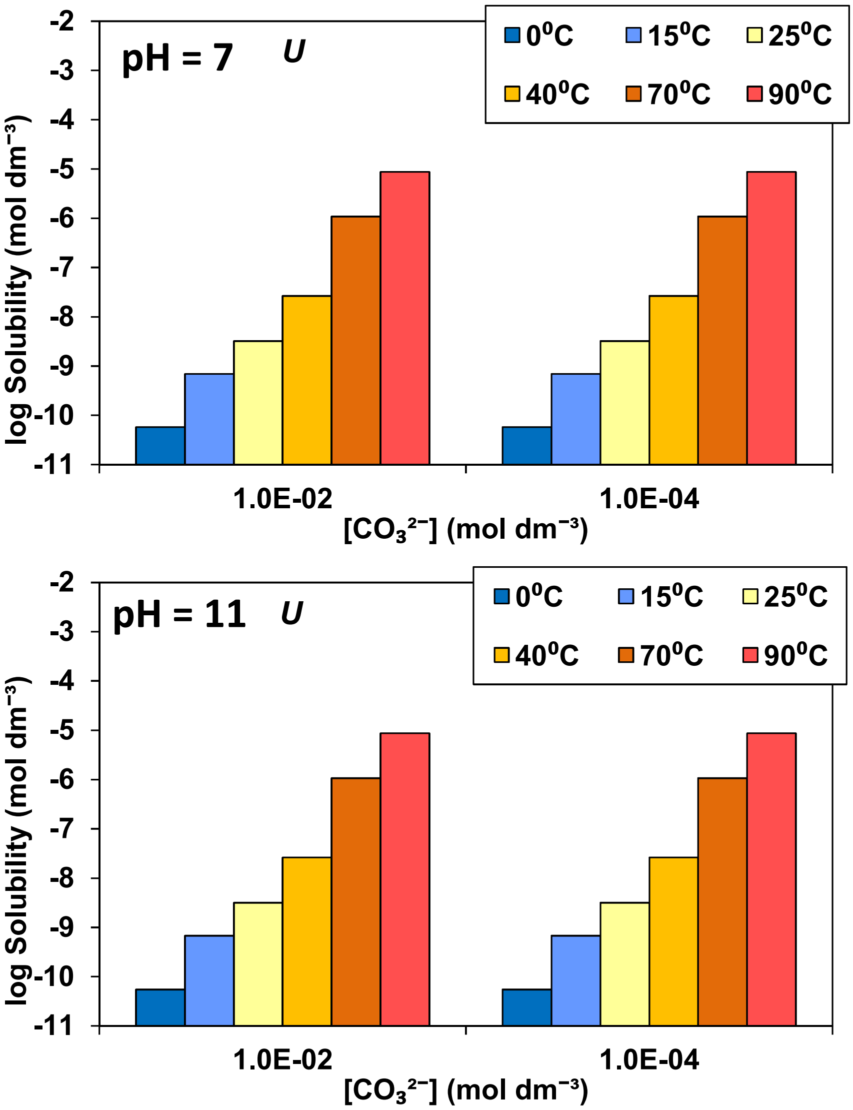

Figure 5-5. UO_2(am,hyd) solubility evolution with temperature at two different pHs and two different concentrations of carbonate. Ca concentration controlled through calcite equilibrium. Goethite/Magnetite equilibrium controls both Fe and Eh of the system.

5.2.6.2 Neptunium

As for uranium, the highly reducing conditions of the studied systems forces Np to be in +4 oxidation state. Under such conditions, the predicted solubility limiting phase is $NpO_2 \cdot xH_2O$(am). The solubility of this solid phase as a function of temperature is shown in Figure 5-6.

At the lowest pH studied here, the lowest $NpO_2 \cdot H_2O(am)$ solubility is obtained at 25ºC. Below and above 25ºC, the solubility of this solid phase increases due to the different chemical speciation of Np. At 25ºC and above, $Np(OH)_4(aq)$ (for which enthalpy data are available) is the main Np aqueous species in solution. When decreasing the temperature, $NpCO_3(OH)_3^-$ species (for which there are not enthalpy data) governs the aqueous chemistry of Np. It must be pointed out that $NpO_2 \cdot H_2O(am)$ enthalpy is available and has been considered in the calculations. Therefore, at 25ºC and above the main reaction occurring has an endothermic character that justifies the increase of solubility with temperature. On the other hand, below 25ºC, where the main reaction changes involves an aqueous species for which enthalpy data are not available, the trend of the results changed: the solubility of $NpO_2 \cdot H_2O(am)$ increases as temperature increases.

At pH 11, the same arguments used for explaining $NpO_2 \cdot H_2O(am)$ solubility at pH 7 are valid for calculations with the highest carbonate content in solution. The only difference is that, instead of $NpCO_3(OH)_3^-$ species, $Np(OH)_4(CO_3)^{2-}$ species is the one controlling the aqueous chemistry of Np below 25ºC. When dealing with low carbonate concentrations at pH 11, Np-carbonate aqueous species are not relevant anymore, and only $Np(OH)_4(aq)$ appears to control the aqueous chemistry of Np. That change justifies the increase of solubility when increasing the temperature at pH 11 and low amount of carbonate in the system (Figure 5-6).

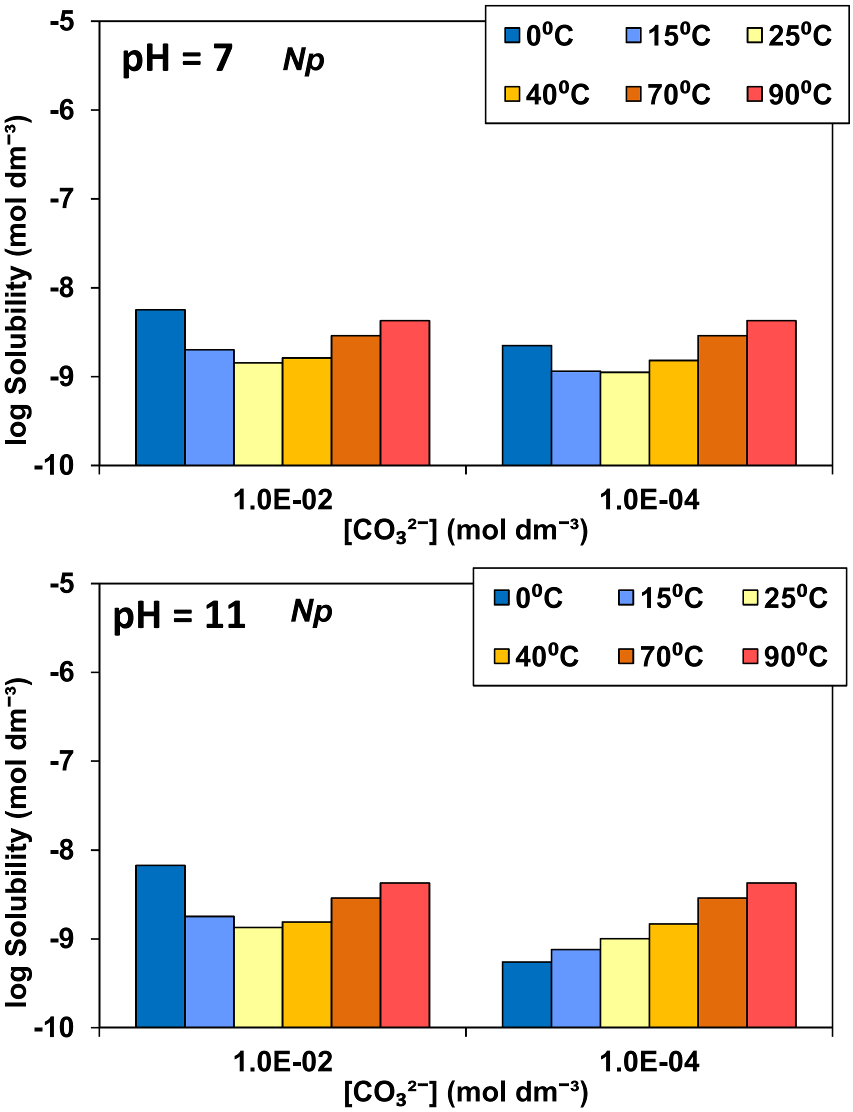

Figure 5-6. $NpO_2 \cdot H_2O(am)$ solubility evolution with temperature at two different pHs and two different concentrations of carbonate. Ca concentration controlled through calcite equilibrium. Goethite/Magnetite equilibrium controls both Fe and Eh of the system.

5.2.6.3 Plutonium

According to the Simple Functions Spreadsheet tool calculations, in the geochemical conditions framed in that work:

- at pH=7, $PuCO_3(OH)(s)$ is the expected solid governing the solubility of Pu. Thermodynamic data for this solid phase come from correlations with An(III)/Ln(III) counterparts (Duro et al., 2006a);
- at pH=11, $Pu(OH)_4(s)$ is the solid exerting a solubility control for Pu.

The evolution of $PuCO_3(OH)(s)$ and $Pu(OH)_4(s)$ solubility as a function of temperature at two different pHs and two different carbonate aqueous concentrations is shown in Figure 5-7.

At pH 7 and 25ºC the species $PuCO_3^+$ controls the aqueous chemistry of Pu with a small contribution by $PuSO_4^+$. Below that temperature, $PuSO_4^+$ becomes the main aqueous species of Pu. Enthalpy data for those species are available and have been considered in the calculations. Nevertheless there are not available enthalpy data for both solid phases, $PuCO_3(OH)(s)$ and $Pu(OH)_4(s)$. It is thus clear that the increase observed in their solubilities above 25ºC is directly related with the change of speciation. Notice that the reaction involving $PuCO_3^+$ has a higher endothermic character than that with $PuSO_4^+$. The results presented here at high temperature should be taken with caution, given the lack of both, enthalpy data for the studied system and thermodynamic stabilities for $PuCO_3(OH)(s)$. As explained in section 5.2.5, in this type of systems it is expected a transformation of the solid when increasing the temperature, prevailing the crystalline ones over the more hydrated solid phases, so that the calculated solubilities at higher T would presumably be lower.

At pH 11 and 25ºC, $Pu(OH)_3(aq)$ is the main Pu aqueous species at the lowest carbonate aqueous concentration while at high carbonate concentrations, $Pu(CO_3)_3^{3-}$ becomes the most relevant species. When increasing the temperature above 25ºC, $Pu(OH)_3(aq)$ becomes the main Pu aqueous species independently of the carbonate aqueous concentration in the system. Contrary to that, when decreasing the temperature $Pu(CO_3)_3^{3-}$ becomes the most relevant species at the highest carbonate concentrations. Given that there are not enthalpy data for the species $Pu(CO_3)_3^{3-}$ it is then obvious that the slight temperature dependency observed in the plots at pH=11 and $[CO_3^{2-}]=10^{-2}$M (Figure 5-7) is related with the lack of data for this species. Besides this lack of data, it should be mentioned that $Pu(OH)_3(aq)$ enthalpy data are available and have been taken into account. The increase of solubility observed when $Pu(OH)_3(aq)$ is the main aqueous species is due to the endothermic character of the main reaction occurring in the system.

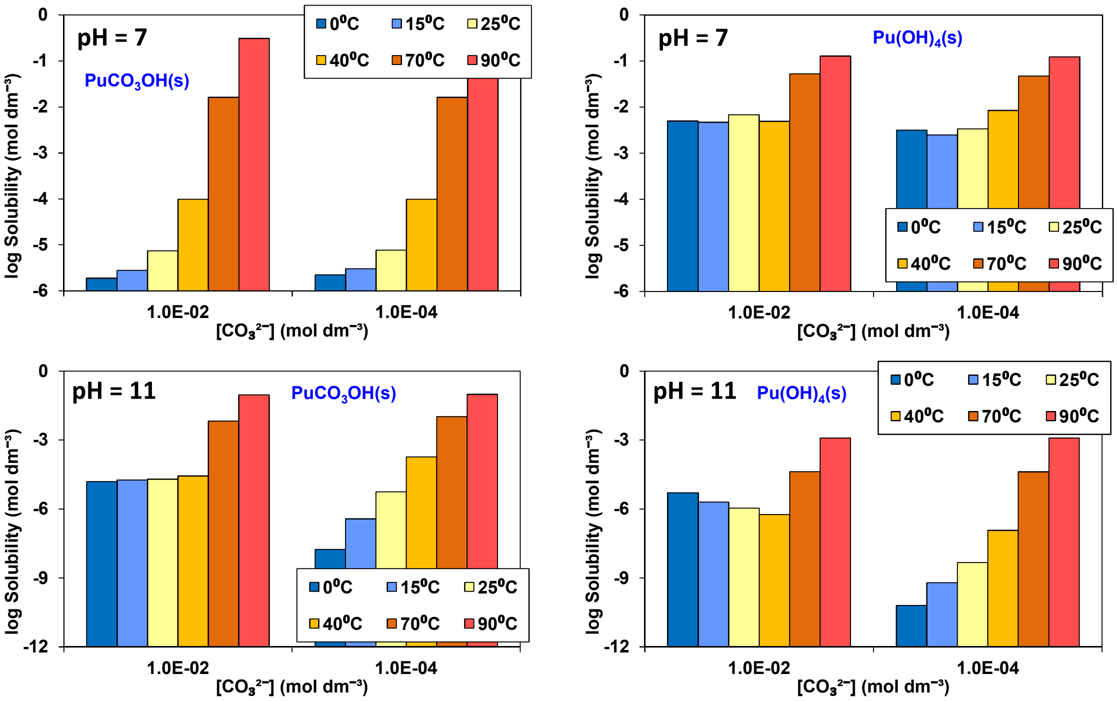

Figure 5-7. $PuCO_3(OH)(s)$ and $Pu(OH)_4(s)$ solubility evolution with temperature at two different pHs and two different concentrations of carbonate. Ca controlled through calcite equilibrium Goethite/Magnetite equilibrium controls both Fe and Eh of the system.

5.2.6.4 *Americium and Curium*

The actinides Am and Cm are expected to have a proxy behaviour due to their chemical similarities. Under the conditions of the present study, and according to the Simple Functions Spreadsheet tool, two solid phases (a carbonate bearing phase, $An_2(CO_3)_3(s)$, and a hydroxide solid phase, $An(OH)_3(s)$) are expected to be their solubility limiting phases depending on the system pH. At the lowest pH considered (pH=7) the carbonated phase will govern the solubility of both radionuclides while at pH=11 the hydroxide phase will control it.

Figure 5-8 shows the evolution of both the carbonated and the hydroxide Am/Cm solids solubilities as a function of temperature.

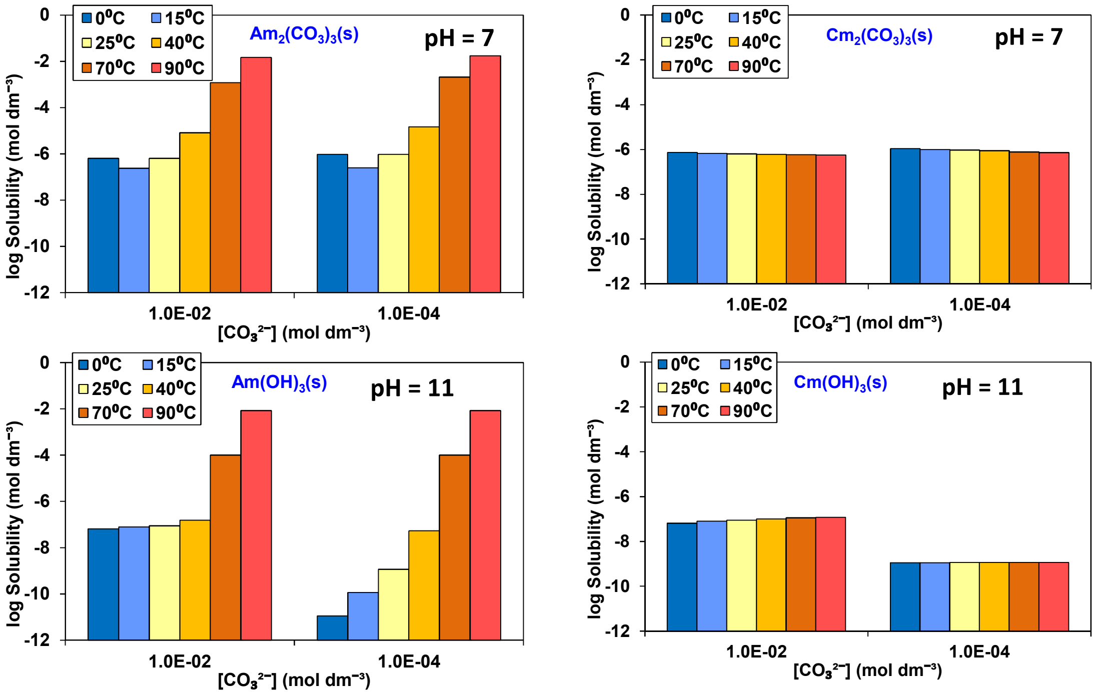

Figure 5-8. $Am_2(CO_3)_3(s)/Am(OH)_3(s)$ (left plots) and $Cm_2(CO_3)_3(s)/Cm(OH)_3(s)$ (right plots) solubility evolution with temperature at two different pHs and two different concentrations of carbonate. Ca concentration controlled through calcite equilibrium.

As can be observed, although the trends for both radionuclides were expected to be similar, the obtained results differ significantly. The differences observed are due to the lack of thermodynamic data in SKB database for the aqueous species and the solid phases. Thus, no temperature corrections have been applied for Cm in the current calculations.

The behaviour of Am can be explained taking into account its aqueous speciation and the availability of enthalpy data. At pH=7 and 25ºC (and above) $AmCO_3^+$ (for which enthalpy data are available) governs the aqueous chemistry of this radionuclide at any carbonate aqueous concentration. The endothermic character of the main reaction occurring explains the observed increase of solubility from 25 to 90ºC. Below 25ºC, $Am(CO_3)_2^-$ species becomes the main Am aqueous species. However, as there are no associated enthalpy for this species, the predicted solubility does not dramatically differ from that calculated at 25ºC.

The same occurs at pH=11, although instead of $AmCO_3^+$, in this case $Am(OH)_3(aq)$ (for which enthalpy data are available) governs the aqueous chemistry of this radionuclide. The different trend observed below 25ºC when assuming the lowest and highest carbonate aqueous concentrations is due to the role of $Am(CO_3)_2^-$ species. At the highest carbonate concentration, $Am(CO_3)_2^-$ species is the main Am species controlling the aqueous chemistry of this radionuclide, while at the lowest carbonate concentration the main species is $Am(OH)_3(aq)$. As already mentioned, the lack of enthalpy data for $Am(CO_3)_2^-$ species predicted solubilities below 25ºC nearly equals to that calculated at 25ºC.

6. Conclusions

A review of the existing thermodynamic data for phosphate complexation with radionuclides has been conducted and presented in this report. Based on this, a selection of thermodynamic data for assessing the impact of phosphate over the solubility limits of selected radionuclides (Sr, Ra, Ni, Zr, Nb, Tc, Pd, Ag, Sn, Pb, Se, Sm, Ho, Th, Pa, U, Np, Pu, Am and Cm) has been done. Phosphate basic hydrolysis species, as well as complexation with major cations (Fe and Ca), have been studied. Moreover, the effect that temperature variation may have on radionuclide solubilities has been addressed.

From the detailed analyses presented in this report, we can conclude that:

- Under the groundwater conditions for which the Simple Functions Spreadsheet tool is valid (Appendix I), phosphate complexation has no relevant effect on the solubility of Fe, Ra, Nb, Tc, Pd, Ag, Sn, Se, Pa, and Np.
- For some specific radionuclides (Sr, Zr, and Pb), although the aqueous phosphate complexation appears to be negligible under the conditions studied here, the role of their phosphate bearing solid phases as possible solubility limiting phases cannot be completely ruled out at this stage.
- In the case of Ca, Ni, Sm, Ho, Th, U, Pu, Am, and Cm, it has been shown that phosphates can exert an important control over their solubility and over their speciation scheme.
- The consideration of phosphates in solubility limit calculations, from a Performance Assessment perspective, will lead to a non-conservative scenario.
- In the range of temperatures studied in the present work, from 0 to 90ºC, radionuclide solubilities might differ up to 2 log units from that at 25ºC. An exception is U, which due to a lack of enthalpy data presents differences of up to 5 log units.
- For specific radionuclides as Ni, due to its chemical peculiarities (main system reaction is exothermic) solubility decreases when increasing temperature at neutral pH. At high pH, this tendency changes due to a change in their chemical speciation.
- In some cases (as for example for Sm, Ho, Pu, or Am) the lack of enthalpy data for some aqueous species lead to large variations in calculated solubilities.

- The total lack of enthalpy data for Cm does not allow a proper solubility limit estimation with temperature.
- The degree of confidence of solubility changes with temperature is subject to the availability of enthalpy data.

As a final remark, it is worth mentioning that the implementation of the whole set of phosphate selected thermodynamic data in the Simple Functions has been discussed and verified in the present work. The verification has been done by comparison between calculated results obtained with the Simple Functions Spreadsheet tool and obtained with the geochemical code PhreeqC.

7. References

Afonin, E.G. and Pechurova, N.I. (1987) Complex formation of Nd (III) with phosphoric acid. Zhur. Neorg. Khim., 33, 2141-2142.

Arcos, D. and Piqué, A. (2009): Update of the thermodynamic database used in SKB TR-06-32 and SKB TR-06-17. Amphos technical note to SKB.

Baes Jr, C.F. (1956) A spectrophotometric investigation of uranyl phosphate complex formation in perchloric acid solution. The Journal of Physical Chemistry, 60(7), 878-883.

Baeyens, B., and McKinley, I.G. (1989). A PHREEQE database for Pd, Ni and Se. NAGRA, NTB-88-28.

Baldwin, W.G. (1969) Phosphate equilibria. II. Studies on the silver phosphate electrodes. Arkiv Kemi, 31, 407-414.

Bingler, L.S. and Byrne, R.H. (1989) Phosphate complexation of Gd(III) in aqueous solutions. Polyhedron, 8, 1315-1320.

Borisov, M.S., Yelesin, A.A., Lebedev, I.A., Filimonov, V.T. and Yakoliev, G.I. (1966) Investigations of complex formation of trivalent actinides and lanthanides in phosphoric solutions. Radiokhimyia, 8, 42-48.

Bottger, W. (1903) Loslichkeitsstudien an schwer loslich en Stoffen (PhD. dissertation, Leipzig)

Brandel, V., and Dacheux, N. (2004) Chemistry of tetravalent actinide phosphates—Part I. Journal of Solid State Chemistry, 177(12), 4743-4754.

Brendler, V., Geipel, G., Bernhard, G., and Nitsche, H. (1996) Complexation in the system UO_2^{2+}/PO_4^{3-}/OH-(aq): Potentiometric and spectroscopic investigations at very low ionic strengths. Radiochimica Acta, 74, 75-80.

Brown, P., Curti, E. and Grambow, B. (2005) Chemical Thermodynamics 8. Chemical Thermodynamics of Zirconium. NEA Data bank, OECD. North Holland Elsevier Science Publishers B.V., Amsterdam, Netherlands

Bruno, J., Cera, E., de Pablo, J., Duro, L., Jordana, S. and Savage, D. (1997) Determination of radionuclide solubility limits to be used in SR 97. Uncertainties associated to calculated solubilities. SKB TR-97-33. Svensk Kärnbränslehantering AB.

Bruno, J., Duro, L. and Grivé, M. (2001) The applicability and limitations of the geochemical models and tools used in simulating radionuclide behaviour in natural waters. Lessons learned from the Blind Predictive Modelling exercises performed in conjunction with Natural Analogue studies. SKB TR-01-20. Stockholm, Swedish.

Byrne, R.H., Lee, J.H. and Bingler, L.S. (1991) Rare earth element complexation by PO_4^{3-} ions in aqueous solutions. Geochim. Cosmochim. Acta, 49, 2133-2139.

Chughtai, A., Marshall, R. and Nancollas, G.H. (1968) Complexes in Calcium Phosphate Solutions. The Journal of Physical Chemistry, 72, 1, 208-211.

Ciavatta, L. and Iuliano, M. (2000) Formation equilibria of tin(II) orthophosphate complexes. Polyhedron, 19, 2403-2407.

Ciavatta, L., Iuliano, M., and Porto, R. (1996) Complex formation equilibria between silver (I) and orthophosphate ions. Annali di chimica, 86(9-10), 411-427.

Cilley, A.W. (1968) The solubility of tin(II) orthophosphate and the phosphate complexes of tin(II). Inorganic Chemistry, 7, 612-614.

Cox, J.D., Wagman, D.D. and Medvedev, V.A. (1989) CODATA Key Values for Thermodynamics, New York; Hemisphere publishing corp.

Dash, U.N., and Padhi, M.C. (1981) Thermodynamics of the silver—silver tungstate, silver—silver phosphate and silver—silver arsenate electrodes in aqueous medium at different temperatures. Thermochimica Acta, 48(1), 241-250.

Denotkina, R.G., Moskvin, A.I. and Shevchenko, V.B. (1960) The composition and dissociation constants of phosphate complexes of plutonium(VI) determined by the solubility method. Russ. J. Inorg. Chem., 5, 731-734.

Duro, L., Grivé, M., Cera, E., Domènech, C., and Bruno, J. (2006a) Update of a thermodynamic database for radionuclides to assist solubility limits calculation for performance assessment. SKB TR-06-17.

Duro, L., Grivé, M., Cera, E., Gaona, X., Domènech, C., and Bruno, J. (2006b) Determination and assessment of the concentration limits to be used in SR-Can. SKB TR-06-32.

Duro, L., Grivé, M., Colàs, E., Gaona, X. and Richard, L. (2011) TDB for elevated temperatures conditions using entropy estimations. 1st International Workshop on high Temperature Aqueous Chemistry. KIT Technical Report, KIT-7625.

Duro, L., Montoya, V., Colàs, E. and García, D. (2010) Groundwater equilibration and radionuclide solubility calculations. NWMO TR-2010-02.

Ekberg, C., Knutsson, A., Albinsson, Y. and Brown, P.L. (2011) Complexation of thorium with phosphate. Radiochimica Acta, 99, 31-35.

Ekberg, C. Skarnemark, G., Emren, A.T. and Lundèn, I. (1995) Uncertainty and sensitivity analysis of solubility calculations at elevated temperatures. Material Research Society Symposium Proceedings, 412, 889-896.

Falck, W.E., Read, D., and Thomas, J.B. (1996) Chemval 2: Thermodynamic database. EUR 16897.

Gamsjäger, H., Bugajski, J., Gajda, T. Lemire, R. and Preis, W. (2005) Chemical Thermodynamics Vol. 6: Chemical Thermodynamics of Nickel, NEA North Holland Elsevier Science Publishers B. V., Amsterdam, The Netherlands.

Gamsjäger, H., Gajda, T., Sangster, J., Saxena, S. K. and Voigt, W. (2012) Chemical Thermodynamics 12: Chemical thermodynamics of tin. NEA OECD, Elsevier.

Giffaut E (1994). Influence des ions chlorure sur la chimie des actinides. Effets de la radiolyse et de la température. PhD. Thesis, Universite de Paris-Sud, U.F.R. Scientifique D´Orsay.

Glass, R.S., Singh, W.P., Jung, W., Veres, Z., Scholz, T.D. and Stadtman, T. (1993) Monoselenophosphate: synthesis, characterization, and identity with the prokaryotic biological selenium donor, compound SePX. Biochemistry, 32(47), 12555-12559.

Goodwin, B. (1982) Calculated uranium solubility in groundwater: implications for nuclear fuel waste disposal. J . Chem. 60, 1759.

Grenthe, I., Fuger, J., Konings, R.J.M., Lemire, R.J., Muller, A.B., Nguyen-Trung, C. and Wanner, H. (1992) Chemical Thermodynamics 1; Chemical Thermodynamics of Uranium (Wanner H. and Forest I. eds.). NEA OECD, Elsevier.

Grivé, M., Domènech, C., Montoya, V. and Duro, L. (2008) Update of the thermodynamic database of sulphur aqueous species and solid phases. Project S-TDB Final Report. Amphos Report.

Grivé, M., Domènech, C., Montoya, V., García, D., and Duro, L. (2010a) Determination and assessment of the concentration limits to be used in SR-Can. Supplement to TR-06-32. SKB R-10-50.

Grivé, M., Domènech, C., Montoya, V., Garcia, D., and Duro, L. (2010b) Simple Functions Spreadsheet tool presentation. SKB TR-10-61.

Guillaumont, R., Fanghänel, J., Neck, V., Fuger, J., Palmer, D.A., Grenthe, I. and Rand, M.H. (2003) Chemical Thermodynamics 5. Update on the Chemical Thermodynamics of Uranium, Neptunium, Plutonium, Americium and Technetium. NEA OECD, Elsevier.

Hummel W. and Berner U. (2001) Application of the Nagra/PSI Thermochemical Data Base 01/01: Solubility and sorption of Th, U, Np and Pu. PSI Internal Report TM-44-01-04, Paul Scherrer Institut, Villigen, Switzerland.

Jonasson, R.G., Bancroft, G.M. and Nesbit, H.W. (1985) Solubilities of some hydrous REE phosphates with implications for diagenesis and sea water concentrations. Geochim. Cosmochim. Acta., 49, 2133-2139.

Kamiński, R., Glass, R.S., Schroeder, T.B., Michalski, J. and Skowrońska, A. (1997) Monoselenophosphate: Its hydrolysis and its ability to phosphorylate alcohols and amines. Bioorganic Chemistry, 25(4), 247-259.

Kaszuba, J. and Runde, W.H. (1999) The aqueous geochemistry of neptunium: Dynamic control of soluble concentrations with applications to nuclear waste disposal. Environ. Sci. Technol, 33, 4427-4433.

King, E.L. (1949) The solubility of plutonium(IV) phosphates and the phosphate complexes of plutonium(IV), in: The transuranium elements, New York, USA. McGraw-Hill, 638-665.

Kitamura, A. and Yoshida, Y. (2010) Preparation of Text Files of JAEA-TDB for geochemical calculation programs. JAEA 2010-011

Laaksoharju, M., Smellie, J., Nilsson, A.-C. and Skarman, C. (1995) Groundwater sampling and chemical characterisation of the Laxemar deep borehole KLX02. SKB TR-95-05

Laaksoharju, M., Smellie, J.,Tullborg, E.-L., Gimeno, M, Hallbeck, L., Molinero, J. and Waber, N. (2008) Bedrock hydrogeochemistry Forsmark. Site descriptive modelling SDM-Site Forsmark. SKB R-08-47

Laaksoharju, M., Smellie, J.,Tullborg, E.-L., Wallin, B., Drake, H., Gascoyne, M., Gimeno, M, Gurban, I., Hallbeck, L., Molinero, J., Nilsson, A.-C. and Waber, N. (2009) Bedrock hydrogeochemistry Laxemar. Site descriptive modelling SDM-Site Laxemar. SKB R-08-93

Langmuir, D. (1978) Uranium solution-mineral equilibria at low temperatures with applications to sedimentary ore deposits. Geochimica et Cosmochimica Acta, 42(6), 547-569.

Le Cloarec, M. F., and Cazaussus, A. (1978) Preparation and properties of tetravalent protactinium phosphates. Journal of Inorganic and Nuclear Chemistry, 40(9), 1680-1681.

Lemire, R. J. (1984) An assessment of the thermodynamic behaviour of Neptunium in water and model groundwaters from 25 to 150ºC. Whiteshell Nuclear Research Establishment, 7817.

Lemire, R.J. (1995) The solubility of nickel and copper (II) oxides in water and aqueous phosphate solutions at high temperatures: a reanalysis of the data of Ziemniak, Jones and Combs. AECL, Report RC-1330.

Lemire, R.J., Fuger, J., Nitsche, H., Potter, P., Rand, M.H., Rydberg, J., Spahiu, K., Sullivan, J.C., Ullman, W.J., Vitorge, P. and Wanner, H. (2001) Chemical Thermodynamics 4. Chemical thermodynamics of Neptunium and Plutonium. NEA OECD, Elsevier.

Louis, C. and Bessiere, J. (1987) Diagrammes potentiel—niveau d'acidité dans les milieux H_2O - H_3PO_4—II: Systemes électrochimiques faisant intervenir le proton. Talanta, 34(9), 771-777.

Martell, A. and Smith, R. (2004) NIST critically selected stability constants of metal complexes. NIST standard reference database 46, version 8.0, Technical report, NIST.

Mathur, J. (1991) Complexation and thermodynamics of the uranyl ion with phosphate. Polyhedron, 10, 1.

McDowell, H., Gregory, T. M. and Brown, W.E. (1977) Solubility of $Ca_5(PO_4)_3OH$ in the system $Ca(OH)_2$-H_3PO_4-H_2O at 5, 15, 25 and 37ºC. Journal of research of the National Bureau of Standards – A. Physics and Chemistry, 81A, 2-3, 273-281.

Millero, F.J. (1992) Stability constants for the formation of rare earth inorganic complexes as a function of ionic strength. Geochim. Cosmochim. Acta, 56, 3123-3132.

Montes Hernández, G. (2002) Etude expérimentale de la sorption d'eau et du gonflement des argiles par microscopie électronique à balayage environnementale (ESEM) et l'analyse digitale d'images. PhD Thesis, Université Louis Pasteur de Strasbourg, France (in French)

Moskvin, A.I. (1971) Investigation of the complex formation of trivalent plutonium, americium, and curium in phosphate solutions. Sov. Radiochem., 13, 688-693.

Moskvin, A.I., Essen, L.N. and Bukhtiyarova, T.N. (1967) The formation of Thorium(IV) and uranium (IV) complexes in phosphate solutions. Russ. J. Inorg. Chem., 12, 1794-1795.

Moskvin, A.I. and Poznyakov, A.N. (1979) Coprecipitation study of complex formation by neptunium(V), plutonium(V), and americium(V) with the anions of various inorganic acids. Russ. J. Inorg. Chem., 24, 1357-1362.

Nancollas, G.H. (1984). The nucleation and growth of phosphate minerals. In: Phosphate Minerals; Nriagu J.O., Moore P.B. Eds., Springer-Verlag, Berlin, 137-154.

Nessa, S.A., Idemitsu, K., Yamazaki, S., Ikeuchi, H., Inagaki, Y. and Arima, T, (2008) Experimental Study on the pH of Pore water in Compacted Bentonite under Reducing Conditions with Electromigration. In WM2008 Conference, Phoenix, AZ, USA, Abstract 8213.

Nriagu, J. O. (1972) Lead orthophosphates. I. Solubility and hydrolysis of secondary lead orthophosphate. Inorganic Chemistry, 11(10), 2499-2503.

Nriagu, J. O. (1974) Lead orthophosphates—IV Formation and stability in the environment. Geochimica et Cosmochimica Acta, 38(6), 887-898.

Nriagu J.O. and Moore, P.B. (1984) Phosphate Minerals. Springer-Verlag, Berlin.

Olin, A., Noläng, B., Osadchii, E.G., Öhman, L.O. and Rosén, E. (2005) Chemical Thermodynamics 7: Chemical Thermodynamics of Selenium. NEA OECD, Elsevier

Parkhurst, D.L. and Appelo, C.A.J. (2013) Description of Input and Examples for PHREEQC Version 3 – A computer program for speciation, batch-reaction, one-dimensional transport, and inverse geochemical calculations. Chapter 43 of Section A. Groundwater Book 6, Modelling Techniques.

Parks, G.A., Pohl, D.C. (1988) Hydrothermal solubility of uraninite. Geochimica et Cosmochimica Acta 52, 863-875.

Pitkänen, P., Luukkonen, A., Ruotsalainen, P., Leino-Forsman, H., Vuorinen, U. (1999) Geochemical modelling of groundwater evolution and residence time at the Olkiluoto site. POSIVA 98-10, Posiva Oy, Helsinki, Finland.

Plyasunova, N. V., Zhang, Y. and Muhammed, M. (1998) Critical evaluation of thermodynamics of complex formation of metal ions in aqueous solution. IV. Hydrolysis and hydroxo-complexes of Ni^{2+} at 298.15 K. Hydrometallurgy, 48, 43-63.

Rai, D., Felmy, A.R., Fulton, R.W. and Ryan, J.L. (1992) Aqueous chemistry of Nd in borosilicate-glass / water systems. Radiochimica Acta, 58/59, 9-16.

Rai, D., Yui, M. and Moore, D.A. (2003) Solubility product at 22ºC of UO_2(c) precipitated from aqueous U(VI) solutions. Journal of Solution Chemistry 32, 1-17.

Ramamoorthy, S. and Manning, P.G. (1974) Equilibrium studies of solutions containing Pb^{2+} or Zn^{2+}, and cysteine, orthophosphate and a carboxylic acid. Journal of Inorganic and Nuclear Chemistry, 36(7), 1671-1674.

Rand, M., Fuger, J., Grenthe, I., Neck, V. and Rai, D. (2009) Chemical Thermodynamics 11: Chemical Thermodynamics of Thorium, NEA North Holland Elsevier Science Publishers B. V., Amsterdam, The Netherlands.

Rao, P.V.R., Gupta, S.K. and Narasaraju, T.S.B. (1986) Determination of solubility products of phosphate and vanadate apatites of lead and their solid solutions in 0.165 M sodium chloride solution. Canadian journal of chemistry, 64(3), 484-487.

Rao., V.K., Shahani, C.J. and Rao, C.L. (1970) Studies on the phosphate complexes of actinium and lanthanum. Radiochimica Acta, 14, 32-34.

Rard, J.A. (1983) Critical review of the chemistry and thermodynamics of technetium and some of its inorganic compounds and aqueous species (No. UCRL-53440). Lawrence Livermore National Lab., CA (USA).

Rard J.A., Rand M.H., Anderegg G. and Wanner H. (1999) Chemical Thermodynamics 3. Chemical thermodynamics of technetium (A. Sandino and E. Östhols eds.) NEA OECD, Elsevier.

Salas, J., Gimeno, M.J., Auqué, L., Molinero, J., Goméz, J. and Juárez, I. (2010) SR-Site – hydrogeochemical evolution of the Forsmark site. SKB TR-10-58.

Sandino, A. and Bruno, J. (1992) The solubility of $(UO_2)_3(PO_4)_2 \cdot 4H_2O$ (s) and the formation of U(VI) phosphate complexes: Their influence in uranium speciation in natural waters, Geochim. et Cosmochim. Acta, 56, 4, 4135-4145.

Scapolan, S., Ansoborlo, E., Moulin, C. and Madic, C. (1998) Investigations by time-resolved laser-induced fluorescence and capillary electrophoresis of the uranyl–phosphate species: application to blood serum. Journal of alloys and compounds, 271, 106-111.

Sergeyeva, E.I., Devina, O.A. and Khodakovsky, I.L. (1994) Thermodynamic database for actinide aqueous inorganic complexes. Journal of alloys and compounds, 213, 125-131.

Shock, E.L. and Helgeson, H.C. (1988) Calculation of the thermodynamic an transport properties of aqueous species at high pressures and temperatures: Correlation algorithms for ionic species and equation of state predictions to 5 kb and 1000ºC. Geochimica et Cosmochimica Acta, 52, 2009-2036.

Shock, E. L., Sassani, D. C., Willis, M. and Sverjensky, D. A. (1998) Inorganic species in geologic fluids: correlations among standard molal thermodynamic properties of aqueous ions and hydroxide complexes. Geochimica et cosmochimica acta, 61, 907-950.

Silva, R.J., Bidoglio, G., Rand, M.H., Robouch, P.B., Wanner, H. and Puigdomenech, I. (1995) Chemical Thermodynamics 2; Chemical Thermodynamics of Americium . NEA OECD, Elsevier.

SKB (2005) Hydrogeochemical evaluation. Preliminary site description Forsmark area – version 1.2. SKB report R-05-17. Svensk Kärnbränslehantering AB.

SKB (2006) Hydrogeochemical evaluation. Preliminary site description Laxemar subarea – version 1.2. SKB report R-06-12. Svensk Kärnbränslehantering AB.

Spahiu, K. and Bruno, J. (1995) A selected thermodynamic database for REE to be used in HLNW performance assessment exercises. SKB Technical Report 95-35.

Stille, P. Gauthier-Lafaye, F., Jensen, K.A., Salah, S., Bracke, G., Ewing, R.C., Louvat, D. and Million, D. (2003) REE mobility in groundwater proximate to the natural fission reactor at Bangombé (Gabon). Chemical Geology, 198, 289-304.

Sverjensky, D. A., Shock, E. L. and Helgeson, H. C (1997) Prediction of the thermodynamic properties of aqueous metal complexes to 1000ºC and 5 kb. Geochimica et cosmochimica acta, 61, 1359-1412.

Tardy, Y. and Vieillard, P. (1977) Relationships among Gibbs free energies and enthalpies of formation of phosphates, oxides and aqueous ions. Contributions to Mineralogy and Petrology, 63(1), 75-88.

Vercouter, T., Vitorge, P., Amekraz, B., Giffaut, E., Hubert, S. and Moulin, C. (2005) Stabilities of the aqueous complexes $Cm(CO_3)_3^{3-}$ and $Am(CO_3)_3^{3-}$ in the temperature range 10-70ºC. Inorganic Chemistry, 44, 5833-5843.

Vuorinen, U. and Snellman, M., (1998) Finnish reference waters for solubility, sorption and diffusion studies. POSIVA WR 98-61.

Wagman, D.D., Evans, W.H., Parker, V.B., Schumm, R.H. Halow. I. Bailey, S.M. Churney, K.L. and Nuttal, R.L. (1982) The NBS tables of chemical thermodynamic properties, selected values for inorganic and c1 and c2 organic substances in SI units. Journal of Physical Chemistry Reference Data, 11, 392.

Wanner, H. (1996) Modelling interaction of deep groundwaters with bentonite and radionuclide speciation. EIR-Bericht Nr. 589.

Wilhelmy, R.B., Patel, R.C. and Matijevic, E. (1985) Thermodynamics and kinetics of aqueous ferric phosphate complex formation. Inorganic Chemistry, 24(20), 3290-3297.

Wood, S.A. (1990) The aqueous geochemistry of the rare-earth elements and yttrium. 1 Review of available low temperature data for inorganic complexes and the inorganic REE speciation of natural waters. Chem. Geol., 82, 159-186.

Xia, Y., Friese, J.I., Bachelor, P.P., Moore, D.A. and Rao, L. (2009) Thermodynamics of Neptunium(V) complexes with phosphate at elevated temperatures. Journal of Radioanalytical and Nuclear Chemistry, 280, 599-605.

Yanase, N., Payne, T. and Sekine, K. (1995) Groundwater geochemistry in the Koongarra ore deposit, Australia (I): Implications for uranium migration. Geochemical Journal, 29 (1), 1995.

Zharovskii, F.G. (1951) Trudy Kowissii Analit. Khim. Akad. Nau k. SSSR, 101.

Ziemniak, S.E., Jones, M.E. and Combs, K.E.S. (1989) Solubility and phase behaviour of nickel oxide in aqueous sodium phosphate solutions at elevated temperatures. Journal of solution chemistry, 18(12), 1133-1152.

Appendix I: SKB Groundwater compositions

Table A1. Groundwater compositions used in the calculations (from SKB, 2006). Shadowed cells: redox data for groundwater compositions used in this work (original data in bold).

	Forsmark	Laxemar	Äspö	Finnsjön	Gideå	Grimsel: interacted glacial meltwater	"Most Saline" groungwater at Laxemar	"Most Saline" groungwater at Olkiluoto	Cement pore water	Baltic seawater	Ocean water	Maximun salinity from glacial upcoming
pH	7.2	7.9	7.7	7.9	9.3	9.6	7.9	7	12.5	7.9	8.15	7.9
Na	0.089	0.034	0.091	0.012	0.0046	0.00069	0.349	0.415	0.002	0.089	0.469	0.25
Ca	0.023	0.0058	0.047	0.0035	0.00052	0.00014	0.464	0.449	0.018	0.0024	0.0103	0.27
Mg	0.0093	0.00044	0.0017	0.0007	0.000045	0.0000006	0.0001	0.0053	≤ 0.0001	0.010	0.053	0.0001
K	0.0009	0.00014	0.0002	0.00005	0.00005	0.000005	0.0007	0.0007	0.0057	0.002	0.01	0.0005
Fe	33×10^{-6}	8×10^{-6}	4×10^{-6}	32×10^{-6}	9×10^{-7}	3×10^{-9}	8×10^{-6}	6×10^{-5}	$\leq 10\times10^{-6}$	3×10^{-7}	4×10^{-8}	2×10^{-6}
HCO_3^-	0.0022	0.0031	0.00016	0.0046	0.00023	0.00045	0.00010	0.00014	≈ 0	0.0016	0.0021	0.00015
Cl^-	0.153	0.039	0.181	0.0157	0.0050	0.00016	1.283	1.275	≈ 0	0.106	0.546	0.82
SO_4^{2-}	0.0052	0.0013	0.0058	0.00051	0.000001	0.00006	0.009	0.00009	≈ 0	0.0051	0.0282	0.01
HS^-	≈ 0	3×10^{-7}	5×10^{-6}	-	$\leq 3\times10^{-7}$	-	$\leq 3\times10^{-7}$	$\leq 1.6\times10^{-7}$	≈ 0	-	-	$\leq 3\times10^{-7}$
Ionic Strength (kmol/m^3)	0.19	0.053	0.24	0.025	0.006	0.0013	1.75	1.76	0.057	0.13	0.65	1.09
Eh (mV)	***-140***	***-280***	*-307/-73*	*-250/-68*	*-201/-60*	***-200***	***-314***	***-3***				***-400***
pe	*-2.37*	*-4.75*	***-5.21/-1.24***	***-4.23/-1.16***	***-3.41/-1.01***	*-3.39*	*-5.32*	*-0.05*				*-6.78*
Ref.Eh/pe	*1*	*2*	*3*	*3*	*3*	*4*	*4*	*5*				*2*

1) SKB (2005). 2) SKB (2006). 3) Bruno et al. (1997) 4). Duro et al. (2006b) 5). Pitkänen et al. (1999)

Appendix II: Enthalpy data used in the calculations

Table A2. Enthalpy data used for the Ra chemical system.

Radium (Ra)		
Aqueous Species	**ΔH_r (KJ/mol)**	**Reference**
$RaSO_4$ (aq)	5.400	Hummel and Berner (2001)
$RaCO_3$ (aq)	4.480	Hummel and Berner (2001)
Solid Phase	**ΔH_r (KJ/mol)**	**Reference**
$RaSO_4$ (s)	39.300	Hummel and Berner (2001)

Table A3. Enthalpy data used for the Ni chemical system.

Nickel (Ni)		
Aqueous Species	**ΔH_r (KJ/mol)**	**Reference**
Ni^{2+}	Basic specie	-
$Ni(OH)_2$ (aq)	85.760	Plyasunova et al. (1998)
$Ni(OH)_3^-$	120.590	Plyasunova et al. (1998)
Solid Phase	**ΔH_r (KJ/mol)**	**Reference**
$Ni(OH)_2$ (s)	-78.837	Plyasunova et al. (1998)

Table A4. Enthalpy data used for the Se chemical system.

	Selenium (Se)	
Aqueous Species	**ΔH_r (KJ/mol)**	**Reference**
HSe^-	-528.272	Shock and Helgeson (1988)
Solid Phase	**ΔH_r (KJ/mol)**	**Reference**
$FeSe_2$ (s)	50.500	Arcos and Piqué (2009)

Table A5. Enthalpy data used for the Sm chemical system.

	Samarium (Sm)	
Aqueous Species	**ΔH_r (KJ/mol)**	**Reference**
$Sm(OH)_3$ (aq)	226.683	Shock et al. (1997)
$Sm(OH)_4^-$	276.904	Spahiu and Bruno (1995)
$Sm(CO_3)_2^-$	-	-
$Sm(CO_3)^+$	163.392	Spahiu and Bruno (1995)
$Sm(SO_4)^+$	16.575	Wagman et al. (1982)
Solid Phase	**ΔH_r (KJ/mol)**	**Reference**
$SmOHCO_3$ (s)	-	-

Table A6. Enthalpy data used for the Ho chemical system.

Holmium (Ho)		
Aqueous Species	**ΔH_r (KJ/mol)**	**Reference**
$Ho(OH)_4^-$	254.153	Shock et al. (1997)
$Ho(CO_3)_2^-$	-	-
$Ho(CO_3)^+$	168.562	Sverjensky et al. (1997)
$Ho(SO_4)^+$	15.387	Wagman et al. (1982)
Solid Phase	**ΔH_r (KJ/mol)**	**Reference**
$Ho_2(CO_3)_3(s)$	-	-

Table A7. Enthalpy data used for the U chemical system.

Uranium (U)		
Aqueous Species	**ΔH_r (KJ/mol)**	**Reference**
$U(OH)_4$ (aq)	109.881	Grenthe et al. (1992)
Solid Phase	**ΔH_r (KJ/mol)**	**Reference**
UO_2 (am,hyd)	-	-

Table A8. Enthalpy data used for the Np chemical system.

Neptunium (Np)		
Aqueous Species	**ΔH_r (KJ/mol)**	**Reference**
$Np(OH)_4$ (am)	101.442	Langmuir (1978)
$NpCO_3(OH)_3^-$	-	-
$Np(OH)_4(CO_3)^{2-}$	-	-
Solid Phase	**ΔH_r (KJ/mol)**	**Reference**
$NpO_2 \cdot H_2O$ (am)	-81.156	Lemire (1984)

Table A9. Enthalpy data used for the Pu chemical system.

Plutonium (Pu)		
Aqueous Species	**ΔH_r (KJ/mol)**	**Reference**
$Pu(OH)_3$ (aq)	227.540	Shock et al. (1997)
$Pu(OH)_4$ (aq)	99.049	Langmuir (1978)
$Pu(CO_3)_3^{3-}$	-	-
$Pu(CO_3)^+$	152.754	Sverjensky et al. (1997)
$Pu(CO_3)_2^-$	-	-
$Pu(SO_4)^+$	17.240	Lemire et al. (2001)
Solid Phase	**ΔH_r (KJ/mol)**	**Reference**
$PuCO_3OH(s)$	-	-
$Pu(OH)_4(s)$	-	-

Table A10. Enthalpy data used for the Am chemical system.

Americium (Am)		
Aqueous Species	**ΔH_r (KJ/mol)**	**Reference**
$Am(OH)_3$ (am)	230.125	Shock et al. (1997)
$Am(OH)_2^+$	143.704	Shock et al. (1997)
$Am(CO_3)_3^{3-}$	-	-
$Am(CO_3)^+$	157.585	Sverjensky et al. (1997)
$Am(CO_3)_2^-$	-	-
$Am(SO_4)^+$	15.493	Estimated from lanthanides
Solid Phase	**ΔH_r (KJ/mol)**	**Reference**
$Am(OH)_3$ (am)	-	-
$Am_2(CO_3)_3$ (s)	-	-

Table A11. Enthalpy data used for the Cm chemical system.

Curium (Cm)		
Aqueous Species	**ΔH_r (KJ/mol)**	**Reference**
$Cm(OH)_3$ (am)	-	-
$Cm(OH)_2^+$	-	-
$Cm(CO_3)_3^{3-}$	-	-
$Cm(CO_3)^+$	-	-
$Cm(CO_3)_2^-$	-	-
$Cm(SO_4)^+$	-	-
Solid Phase	**ΔH_r (KJ/mol)**	**Reference**
$Cm(OH)_3$ (am)	-	-
$Cm_2(CO_3)_3$ (s)	-	-